DISSERTATION

Überprüfung neuer therapeutische Strategien in Zellen des kutanen T-Zell-Lymphoms und deren Wirkung auf die Apoptoseregulation

Novel Therapeutic Strategies for Cutaneous T-Cell-Lymphoma and Its Effect on Apoptosis Regulation

zur Erlangung des akademischen Grades
Doctor rerum medicinalium (Dr. rer. medic.)

vorgelegt der Medizinischen Fakultät
Charité – Universitätsmedizin Berlin

von

Uly Sumarni

Erstbetreuung: PD. Dr. Jürgen Eberle

Datum der Promotion: 30.06.2024

Inhaltsverzeichnis

Tabellenverzeichnis

Abbildungsverzeichnis

Abkürzungsverzeichnis

AICD	aktivierungsinduzierter Zelltod
AML	akute myeloische Leukämie
Apaf-1	apoptotic protease activating factor-1
APS	Amonium Persulfat
BCA	Bicinchoninsäure
BIR	Baculoviral IAP repeat
BRUCE	Ubiquitin-konjugierendes BIR-Domänen-Enzym
BSA	bovine serum albumin
CARD	Caspase-Rekrutierungs-Domäne
CD95L	CD95-Ligand
CTCL	Kutane T-Zell-Lymphome
c-FLIP$_{L/S}$	cellular FLICE inhibitory protein, long/short isoform
c-IAP1	zelluläres IAP1
c-IAP2	zelluläres IAP2
DD	Todesdomäne
DED	Todeseffektordomäne
DISC	death inducing signaling complex
DLBCL	diffus großzelliges B-Zelllymphom
DR	Todesrezeptoren
EDTA	Ethylendiamintetraessigsäure
FADD	Fas-associating protein with death domain
GAPDH	Glycerinaldehyd-3-phosphat-Dehydrogenase
h	Stunde(n)
H$_2$DCFDA	2-, 7-Dichlorodihydrofluoresceindiacetat
IAP	Inhibitors of apoptosis protein
ILP2	IAP-ähnliches Protein 2
kDa	Kilodalton
Min	Minute(n)
ML-IAP	Melanom-IAP
MMP	mitochondriales Membranpotential
NAC	N-Acetylcystein
NIAP	neuronales IAP
nM	Nanomolar

PAGE	Polyacrylamidgelelektrophorese
PBMC	mononukleäre Zellen des peripheren Blutes
PBS	Phosphate-buffered saline
PI	Propidium Iodid
PKC	Protein Kinase C
ROS	reaktives Sauerstoffspezies
rpm	Revolution pro Minute
RPMI	Roswell Park Memorial Institute
RT	Raumtemperatur
SDS	Natriumdodecylsulfat
SMAC	second mitochondria-derived activator of caspase
SS	Sézary-Syndrom
TMRM$^+$	Tetramethylrhodamin Methylester-Perchlorate
TNF-α	Tumor-Nekrose-Faktor alpha
TRAIL	TNF-related apoptosis-inducing ligand
Tris-HCl	Tris-(hydroxymethyl)-aminomethanhydrochloridn
TZR	T-Zell-Rezeptor
XIAP	X-Chromosom-gebundenes IAP
µl	Mikroliter
µM	Mikromolar

Zusammenfassung

Die kutanen T-Zell-Lymphome (CTCL) sind mit geschätzten 3-4 Neuerkrankungen pro Jahr und einer Million Einwohner in Europa eine relativ seltene Erkrankung, die jedoch aufgrund der lebenslangen Morbidität und dauerhaft nachhaltigen Beeinträchtigung der Lebensqualität als schwerwiegend eingestuft wurde. Aktuelle Therapien sind häufig unzureichend oder haben keine dauerhafte Wirksamkeit. Signalwege, die den Zelltod induzieren, sind sowohl für die Unterdrückung der Tumorentstehung als auch für die erfolgreiche Umsetzung einer Antitumortherapie wichtig. Jedoch sind die Prozesse, die zum Zelltod beim CTCL führen, derzeit noch unzureichend verstanden.

Ziel der Arbeit war es, neue Therapieansätze zur Apoptoseinduktion in CTCL-Zellen zu identifizieren und die apoptotischen Signalwege in CTCL-Zellen auf molekularer Ebene zu untersuchen. Vier CTCL-Zelllinien (HH, HuT-78, MyLa, SeAx) wurden mit verschiedenen Effektoren behandelt und anschließend mittels Durchflusszytometrie zur Quantifizierung von Apoptose, ROS Produktion sowie Verlust des mitochondrialen Membranpotentials sowie mittels Westernblot die Regulation der apoptotischen Signalwege untersucht.

In dieser Arbeit konnten drei therapeutische Strategien indentifiziert werden. Eine proapoptotische Wirkung des Ingenolmebutats PEP005 wurde in zwei von vier CTCL-Zelllinien nachgewiesen. Der Mechanismus war mit der Aktivierung der PKCδ (Protein Kinase C-delta) sowie der darauffolgenden Aktivierung der proapoptotischen Caspase-3 verbunden. Die resistenten Zelllinien zeichneten sich durch bestimmte molekulare Merkmale wie die Expression von p53 und p21 sowie durch eine verstärkte Expression der antiapoptotischen Faktoren c-FLIP und XIAP aus, die somit als Kandidaten für eine Stratifizierung von Patienten dienen könnten.

Die zweite untersuchte Substanzgruppe stellten BH3-Mimetika dar. Dies sind Inhibitoren für antiapoptotische Bcl-2-Proteine, die strukturelle Ähnlichkeit zur BH3-Domäne (Bcl-2 homology domain 3) besitzen. Die Untersuchung des Mcl-1-Inhibitors S63845 zeigte, dass zwei von vier CTCL-Zelllinien hohe Sensitivität besaßen, während die zwei Zelllinien mit geringer Sensitivität für S63845 andererseits durch eine hohe Sensitivität gegenüber den für Bcl-2, Bcl-w und Bcl-x_L spezifischen Inhibitoren ABT-263 und ABT-737 charakterisiert waren. Die Sensitivität gegenüber S63845 korrelierte mit einer verminderten Expression von Bcl-2 und Bcl-x_L sowie einer fehlenden Bcl-w-Expression.

Bcl-w könnte daher als Biomarker für die S63845-Sensitivität des CTCLs eingesetzt werden.

Die dritte Strategie beruhte auf dem Indirubin-Derivat DKP-071, die Apoptose in Abhängigkeit der ROS Produktion induzierte. Diese drei untersuchten Effektoren könnten als neue therapeutische Strategien für das CTCL genutzt werden. Weitere Untersuchungen sind erforderlich, um die aktuellen Ergebnisse zu validieren.

Abstract

Cutaneous T-cell lymphomas (CTCL) are a relatively rare disease with an estimated 3-4 new cases per year per million population in Europe and yet have been classified as serious due to lifelong morbidity and permanent sustained impairment of quality of life. Current therapies are often inadequate or lacking durable efficacy. Signaling pathways that inducing cell death are important for both suppression of tumorigenesis and efficacy of the antitumor therapy. However, the mechanisms leading to cell death in CTCL are currently poorly understood.

The aim of this study was to identify new therapeutic strategies to induce apoptosis in CTCL cells and to investigate the apoptotic signaling pathways in CTCL cells at the molecular level. Four CTCL cell lines (HH, HuT-78, MyLa, SeAx) were treated with different effectors and subsequently analyzed by flow cytometry to quantify apoptosis, ROS production as well as loss of mitochondrial membrane potential and for regulation of the apoptotic signaling pathways by Westernblot.

In this study, three therapeutic strategies were identified. A proapoptotic effect of ingenol mebutate PEP005 was demonstrated in two of four CTCL cell lines. The mechanism was associated with PKCδ (protein kinase C-delta) activation and subsequent activation of proapoptotic caspase-3. The resistant cell lines were characterized by certain molecular characteristics such as expression of p53 and p21, as well as increased expression of the antiapoptotic proteins c-FLIP and XIAP, which could thus serve as candidates for stratification of patients. BH3 (Bcl-2 homology domain 3) mimetics represented the second group of compounds studied. The investigation on Mcl-1 inhibitor S63845 showed that two out of four CTCL cell lines were highly sensitive. The two cell lines with only low sensitivity to S63845, on the other hand, were characterized by high sensitivity to ABT-263 and ABT-737, which are known as specific inhibitors of Bcl-2, Bcl-w, and Bcl-x_L. The sensitivity to S63845 was found to be correlated with the decreased expression of Bcl-2 and Bcl-x_L and most importantly, with the absence of Bcl-w expression. Bcl-w could therefore be used as a biomarker for sensitivity of CTCL to S63845. The third strategy was based on the indirubin derivative DKP-071, which induced apoptosis depending on ROS induction. These three studied effectors could potentially be used as new therapeutic strategies for CTCL. Further analyses are required to validate the current findings.

1 Einleitung

1.1 Kutane T-Zell-Lymphome

Kutane T-Zell-Lymphome (CTCL) umfassen eine Gruppe von Krankheiten mit der Ansammlung von bösartigen T-Zellen unter der Haut. Die häufigsten Entitäten sind die Mycosis Fungoides (MF) mit einem Anteil von ca. 60%, das primäre kutane CD30-positive anaplastische, großzellige T-Zell-Lymphom mit einem Anteil von ca. 25% sowie das Sézary-Syndrom (SS) (Willemze et al., 2019). Das CTCL zählt mit 3-4 Neuerkrankungen pro Million Einwohner pro Jahr in Europa zu den eher seltenen Erkrankungen (Dobos et al., 2020). Die Möglichkeit einer Unterschätzung der Fallzahlen durch Diagnoseverzug ist jedoch nicht auszuschließen (Scarisbrick et al., 2019).

1.1.1 Ätiologie und Pathophysiologie

Beim CTCL wurden Dysregulationen von Genen und Signalwegen gefunden, deren genaue Rolle bei der Krankheitsentstehung jedoch bisher unbekannt ist. Eine Reihe von externen Faktoren wie chronische Hautentzündungen, mikrobielle Besiedlung und Virusinfektionen werden ebenfalls als begünstigende Faktoren für die Entstehung von CTCL berichtet (Bagherani & Smoller, 2016).

1.1.2 Klinisches Bild

Die klinischen Erscheinungsbilder von CTCL unterscheiden sich je nach Entität. Bei 70% der Patienten mit klassischer MF zeigen sich erythematöse schuppige Flecken. Neben den Hautläsionen und der körperlichen Entstellung leiden MF-Patienten unter Juckreiz und Schmerzen. Im Spätstadium können sich dann Tumore oder Erythrodermie entwickeln, die auf Lymphknoten oder innere Organe übergreifen.

Bei Patienten mit SS wird in der Haut, den Lymphknoten und dem peripheren Blut meistens eine Trias aus generalisierter Erythrodermie, Lymphadenopathie und neoplastischen, aus T-Zellen stammenden Sezary-Zellen beobachtet. Diese Patienten leiden unter extremem Juckreiz und häufig unter einer Infektion mit atypischer Lymphozyteninfiltration im Gesicht. Durch die hohe Aggressivität vom SS beträgt die mediane Überlebenszeit von SS Patienten 3 Jahre (Willemze et al., 2005).

Allgemein wird bei etwa 30% der CTCL-Patienten innerhalb von 10 Jahren eine progressive Tumorentwicklung oder Metastasierung mit einer reduzierten 5-Jahres-Überlebensrate beobachtet (Agar et al., 2010).

1.1.3 Diagnose

Die Diagnose von CTCL umfassen die histologischen, die immunhistochemischen und die molekularbiologischen Untersuchungen, die vor allem bei unklarer Differentialdiagnose miteinbezogen werden. Bei SS sind bösartige T-Zellen mit Serpentinenkernen im peripheren Blut durch Wright-gefärbten Abstrich oder mittels Durchflusszytometrie nachzuweisen.

1.1.4 Behandlungsschema

Für das Behandlungsschema für MF und SS finden sich Leitlinien von verschiedenen Gruppen. Die Erkenntnisse über die Pathogenese des CTCL haben die Liste der therapeutische Zielmoleküle zwar erweitert, aber eine langfristige und kurative Behandlung bleibt weiterhin die große Herausforderung (Dummer et al., 2021). Die Untersuchungen des aktivierungsinduzierten Zelltods (AICD) zeigte, dass beim CTCL nach Stimulation des T-Zell-Rezeptors (TZR) keine Apoptose mehr ausgelöst werden kann (Klemke et al., 2009). Der gezielte Eingriff in die gestörten Apoptose-Signalwege stellt somit einen vielversprechenden Therapieangriffspunkt für CTCL dar.

1.1.5 Apoptoseinduktion als therapeutisches Ziel

Bei der Apoptose handelte es sich um ein durch genetische Programme kontrolliertes Absterben der Zellen. Dieser Zelltodmechanismus wurde zum ersten Mal in 1972 beschrieben (Kerr, et al., 1972). Die Merkmale einer Initialphase der Apoptose sind Schrumpfung der Zellen, Kondensation des Chromatins sowie Bildung von Aggregaten im Zellkern. In der nachfolgenden Phase wird die DNA zwischen den Nukleosomen mithilfe von Endonukleasen fragmentiert. Parallel kommt es zu einem Verlust der Zellmembranstabilität. Es bilden sich Ausstülpungen der Zellmembran, die sich nach Abschnürung zu apoptotischen Körperchen entwickeln. Der Verlust der Membran-Asymmetrie führt zur Exposition von Phosphatidylserin auf der Zelloberfläche.

Es werden zwischen extrinsischen und intrinsischen proapoptotischen Signalwegen unterschieden. Die extrinsischen Signalwege werden durch Bindung von Todesliganden an Todesrezeptoren (DR) initiiert. Zu den bekanntesten Todesliganden gehören Tumor-Nekrose-Faktor alpha (TNF-α), CD95-Ligand (CD95L; auch bekannt als FASL) und TNF-related apoptosis-inducing ligand (TRAIL). Diese Liganden sind homotrimere Proteine, die durch Bindung an die Rezeptoren deren Oligomerisierung induzieren und dadurch Apoptose-Signalwege aktivieren. Bislang wurden sechs Mitglieder der

Todesrezeptorfamilie identifiziert: TNF-R1, CD95 (Fas, APO-1), TRAIL-R1 (DR4), TRAIL-R2 (DR5), DR6 und TRAMP (Schulze-Osthoff et al., 1998). Ihre typischen Bestandteile umfassen extrazelluläre Domänen, eine Transmembranregion sowie eine zytoplasmatische Todesdomäne (DD).

Bei der Regulierung der Initialphase von Todesrezeptor-vermittelter Apoptose spielen sowohl proapoptotische wie Procaspase-8 und -10 als auch antiapoptotische Proteine wie c-FLIP$_{L/S}$ (cellular FLICE inhibitory protein, long/short isoform) eine Rolle.

Die CD95-vermittelte Apoptose ist einer der am besten untersuchten Apoptosesignalwege. Bei diesem Signalweg erfolgt nach der Bindung von CD95L die Trimerisierung des Rezeptors CD95. Durch die darauffolgende Rekrutierung des Adapterproteins (Fas-associating protein with death domain, FADD) über die homophile Interaktion der Todesdomänen aus Rezeptor und Adapterprotein wird ein Mutiprotein-Komplex (death inducing signaling complex, DISC) gebildet. In diesem Komplex können sowohl proapoptotische DED-Proteine wie Pro-Caspase-8 als auch antiapoptotische DED-Proteine wie c-FLIP$_{L/S}$–rekrutiert werden. Je nach Mengenverhältnis dieser DED-Proteine zueinander wird die Apoptose initiiert oder blockiert. Ein Überschuss von Pro-Caspase-8 führt zu deren autokatalytischen Aktivierung. Die aktive, aus dem Todesrezeptorkomplex freigesetzte Caspase-8 spaltet durch Proteolyse anschließend Effektorcaspasen, wie die Caspase-3.

Der intrinsische apoptotische Signalweg wird unter anderem durch Zellschäden induziert. Typische Merkmale des intrinsischen Signalwegs sind der Verlust des mitochondrialen Membranpotentials (MMP), die Permeabilisierung der mitochondrialen Außenmembran sowie die Freisetzung proapoptotischer Proteine wie Cytochrom c aus dem Intermembranraum der Mitochondrien in das Zytoplasma (Hossini & Eberle, 2008) (Tait & Green, 2010). Die Aktivierung der mitochondrialer proapoptotischen Signalwege kann außerdem von einer ROS-Bildung begleitet werden (Redza-Dutordoir & Averill-Bates, 2016). Desweiteren induziert das Cytochrom c eine Konformationsänderung des Adapterproteins apoptotic protease activating factor-1 (Apaf-1), wodurch dessen Caspase-Rekrutierungs-Domäne (CARD) freigelegt wird. Anschließend kommt es zu einer Oligomerisierung von Apaf-1 und zur Bildung des hochmolekularen Apoptosom-Komplexes. Dies ermöglicht die Anlagerung der Pro-Caspase-9 an das Apoptosom und die daranschließende autokatalytische Aktivierung von Caspase-9. Caspase-9, ihrerseits, prozessiert und aktiviert wiederum die Effektor-Caspase-3.

Caspasen gehören zu einer hoch konservierten Familie von Cystein-Proteasen. Die proteolytische Aktivierung führt zur Spaltung der 30-55 kDa großen Proform in eine große (ca. 20 kDa) und eine kleine Untereinheit (ca. 10 kDa) sowie zur Entfernung der N-terminalen Prodomäne. Neben proteolytischer Prozessierung führt auch die nahe Anlagerung der Proformen in Komplexen, wie im Apoptosom oder im DISC zu einer Aktivierung der Procaspasen (induced proximity) und zur darauffolgenden autokatalytischen Prozessierung.

Die Bcl-2 Proteinfamilie spielt in den intrinsischen proapoptotischen Signalwegen eine Rolle. Bcl-2 Proteine mit vier BH-3 Domänen wie Bcl-2, Mcl-1, Bcl-w, Bcl-x$_L$ und A1 sind antiapoptotisch, während die Proteine mit weniger als vier Domänen proapoptotische Funktion haben. Die proapoptotischen Bcl-2 Proteine werden in Multidomänen-Proteine wie Bak und Bax sowie in BH3-only-Proteine mit ausschließlich der BH3-Domäne wie Bid, Bad, Noxa, Puma, Bim u.a unterschieden. Bax und Bak lassen sich durch die Bindung der antiapoptotischen Bcl-2 Proteinen hemmen, während die antiapoptotischen Bcl-2 Proteine wiederum durch die BH3-only-Proteine inhibiert werden können (Tait & Green, 2010).

Bei Apoptoseinhibitoren (IAPs) handelt es sich um Proteine mit einer variablen Anzahl von sogenannten Baculoviral IAP repeat (BIR)-Domänen. Bisher wurden acht Mitglieder der IAP-Familie bei Säugetieren identifiziert: neuronales IAP (NIAP), zelluläres IAP1 (c-IAP1), zelluläres IAP2 (c-IAP2), X-Chromosom-gebundenes IAP (XIAP), Survivin, Ubiquitin-konjugierendes BIR-Domänen-Enzym (BRUCE), Melanom-IAP (ML-IAP) und IAP-ähnliches Protein 2 (ILP2). Vor allem c-IAP1, c-IAP2 und XIAP binden an aktivierte Caspasen, hemmen diese und tragen so zu einer Apoptoseresistenz bei. Die Aktivität von IAP kann durch second mitochondria-derived activator of caspase (SMAC) gehemmt werden, wodurch die Aktivierung der Caspase-3/7/9 sowie Apoptose ausgelöst wird (Cong et al., 2019).

Auch Protein-Phosphorylierungen spielen in der Apoptose eine bedeutende Rolle. Die Rolle von Serin-Threonin-Kinase namens Protein Kinase C (PKC) fand sich in der Regulierung vieler zellulärer Prozesse wie Zell-Proliferation, Differenzierung und Apoptose (Zhang, et al., 2004). Basierend auf ihren Domänenstrukturen und Regulationsmechanismen wird die PKC-Familie in klassische (α, βI, βII und γ), neue (δ, ε, η und Θ) und atypische (λ und ζ) PKCs unterteilt. PKCδ dient je nach Zelltyp als positiver oder negativer Wachstumsregulator. So kann es die Induktion der Expression

und Funktion proapoptotischer Proteine bewirken, und ist selbst ebenfalls ein Ziel für Caspasen (Kaltoft et al., 1992).

1.2 PEP005

PEP005 oder Ingenolmebutat ist ein hydrophober Diterpenester aus der Pflanze *Euphorbia peplus.* Der Substanz wurde 2012 von der FDA für aktinische Keratose zugelassen (Kaltoft et al., 1987). In Zelllinien der humanen myeloischen Leukämie zeigte PEP005 eine PKCδ aktivierende Wirkung und die darauffolgende Apoptoseinduktion (Gootenberg, et al., 1981). Der Substanz scheint selektiv für die Wachstumshemmung von Krebszellen zu sein, da dieser das Wachstum menschlicher neonataler Fibroblasten nicht hemmte und bei normalen $CD34^+$-Myeloblasten keine Apoptose induzierte (Gootenberg et al., 1981).

Ausgehend von den Erkenntnissen über die antiproliferative Wirkung von PEP005 bei soliden und hämatologischen Malignomen (Netchiporouk et al., 2017) wurde in dieser Arbeit die Wirkung von PEP005 in vier CTCL-Zelllinien HH, HuT-78, MyLa und SeAx untersucht und der Wirkmechanismus entschlüsselt.

1.3 S63845

Die Substanz S63845 ist ein selektiver Inhibitor des antiapoptotischen Bcl-2 Proteins Mcl-1. Das Protein ist ein Schlüsselfaktor für das Überleben von multiplen Myelomzellen (Gong et al., 2016); seine Deregulation in aktiviertem, B-Zell-ähnlichem diffus großzelligem B-Zelllymphom wurde mit Therapieresistenz (Wenzel et al., 2013) und seine Überexpression wurde mit Strahlen- und Chemotherapieresistenz in Leukämie-Zelllinien in Verbindung gebracht (Kaufmann et al., 1998). Da eine Dysregulation und Überexpression von Mcl-1 auch in CTCL-Zellen festgestellt wurde (Spinner et al., 2016) (Koch et al., 2019), scheint der Einsatz selektiver Mcl-1-Inhibitoren als eine vielversprechende therapeutische Strategie zu sein. In dieser Arbeit wurde die Wirkung von S63845 im Vergleich zu zwei spezifischen Inhibitoren für Bcl-2, Bcl-x$_L$ und Bcl-w (ABT-263 und ABT-737) in vier CTCL-Zelllinien und die Mechanismen untersucht.

1.4 DKP-071

Bei DKP-071 handelt es sich um ein Indirubin-Derivat. Indirubin wurde als aktiver Bestandteil eines traditionellen chinesischen Heilmittels. In klinischen Studien zeigte Indirubin eine signifikante Antitumoraktivität bei chronisch-myeloischer und chronisch-granulozytärer Leukämie (Xiao, et al., 2002) (Blažević et al., 2015). Eine Aktivierung

sowohl extrinsischer als auch intrinsischer Apoptose-Signalwege durch Indirubinderivate wurde ebenfalls in Melanomzellen berichtet (Berger et al., 2011) (Zhivkova, et al., 2019). In dieser Arbeit wurde die Wirkung des Indirubin-Derivats DKP-071 in drei CTCL-Zelllinien MyLa, HH und HuT-78 mit Bezug auf die Apoptoseinduktion, Zellviabilität und die Proliferationsrate untersucht.

1.5 Fragestellung

Trotz zahlreicher wissenschaftlicher neuer Befunde sind die therapeutischen Möglichkeiten für CTCL noch begrenzt. Dies macht die Suche nach neuen therapeutischen Strategien dringend erforderlich.

Die Resistenz gegen den apoptotischen Zelltod hat sich als ein grundlegender Faktor für die Malignität des CTCLs herausgestellt. In der vorliegenden Arbeit wurden daher Strategien untersucht, die auf die molekularen Regulatoren der Apoptose zugreifen. Damit sollte deren Potenzial als neue Therapieansätze durch Überwindung von Apoptose-Defizienz in CTCL-Zellen belegt werden. Folgende Fragen wurden insbesondere bearbeitet:

1) Kann durch neue therapeutische Optionen wie dem PKCδ-Aktivator PEP005, dem Mcl-1-Inhibitor S63845 oder dem Indirubin-Derivat DKP-071 effizient Apoptose in CTCL-Zellen induziert werden?

2) Wie wird die Apoptoseinduktion in CTCL-Zellen auf molekularer Ebene reguliert?

2   Methodik

2.1   Verwendete Materialien

Roswell Park Memorial Institute (RPMI) 1640 (Life Technologies, Darmstadt, Deutschland)

Fetal Bovine Serum (FBS, S0615, Biochrom, Deutschland)

Penicillin/Streptomycin (A2213, Biochrom, Deutschland)

L-Glutamin (K0282, Biochrom, Deutschland)

PEP005 (AdipoGen Life Sciences, Switzerland)

S63845 (CAS# 1799633-27-4, Hölzel Diagnostika Handels GmbH, Deutschland)

ABT-263 (CAS# 923564-51-6, Biozol, Deutschland)

ABT-737 (CAS# 852808-04-9, Biozol, Deutschland)

QVD-Oph (Abcam, UK)

α-Tocopherol (Vitamin E, Fluka, Deutschland)

N-Acetylcystein (NAC; Sigma-Aldrich, Deutschland)

Bisindolylmaleimid 1 (Bis 1; Cayman Chemical, USA)

Dimethylsulfoxid (DMSO; 67-68-5; Sigma-Aldrich, Deutschland)

Propidium Iodid (PI, 25535-16-4, Santa Cruz, USA)

Natriumcitrat (Sigma-Aldrich, Deutschland)

Triton X-100 (Serva, Deutschland)

Calcein AM (564061, Becton Dickinson, USA)

Tetramethylrhodamin Methylester-Perchlorate (T5425, Sigma-Aldrich, Deutschland)

WST-1 (11644807-001, Sigma-Aldrich, Deutschland)

Bicinchoninsäure (BCA) Protein Assay (23227, Thermo Fischer, USA)

2-, 7-Dichlorodihydrofluoresceindiacetat (H_2DCFDA; D-399, Life Technologies, USA)

NaCl (1.06404.1000, Merck, Deutschland)

Ethylendiamintetraessigsäure (E9884, Sigma-Aldrich, Deutschland)

NP-40 (85125, Thermo Fischer, USA)

Tris-(hydroxymethyl)-aminomethanhydrochlorid (1185-53-1, Carl Roth, Deutschland)

Pierce Protease and Phosphatase Inhibitor (A32959, Thermo Fischer, USA)

Tris-Base (T3253, Sigma-Aldrich, Deutschland)

37,2%-HCl (1.00317, Merck, Deutschland)

Natriumdodecylsulfat (SDS, L-4390, Sigma-Aldrich, Deutschland)

Glycerin (1.04093, Merck, Deutschland)

Bromphenolblau (1610404, Bio-Rad, USA)

β-Mercaptoethanol (M-7154, Sigma-Aldrich, Deutschland)

30% Acrylamid/Bis-acrylamid (1610154, Bio-Rad, USA)

Amonium Persulfat (APS, 1610700, Bio-Rad, USA)

TEMED (1610801, Bio-Rad, USA)

Tricin (5704-04-1, Carl Roth, Deutschland)

Nitrozellulose-Membran (Protran BA83 0,2 µm, Whatman, Deutschland)

10x Phosphate-buffered saline (PBS, 70011044, Fischer Scientific, USA)

Precision Plus Protein™ Dual Color Standards (Biorad, USA)

Tween20 (BP337-100, Fischer Bioreagents, USA)

Milchpulver (68514-61-4, Carl Roth, Deutschland)

Enhanced Chemi Luminescence ECL™ Westernblotting substrate (Thermo Fisher, USA)

Glycin (56-40-6, Carl Roth, Deutschland)

Primäre Antikörper:

- Kanninchen, Cell Signaling, USA:

    Caspase-3 (9662), gespaltene Caspase-3 (9664), Caspase-9 (9502), XIAP (2042), Mcl-1 (4572), Bcl-w (2724), Bcl-2 (2872)

- Maus, Cell Signaling, USA:

    Caspase-8 (9746)

- Maus, Santa Cruz Biotech, USA:

    c-FLIP (sc-5276), p21 (sc-6246), p53 (sc-126), p21(sc-6246), GAPDH (sc-32233), Bcl-x$_L$ (sc-8392), β-actin (sc-47778)

- Kaninchen polyklonal, Thermo Fisher, USA
    - PKCδ (PA587443)

Sekundärantikörper:

- Peroxidase-markierte Ziegen-Antikaninchen- und Ziegen-Anti-Maus-Antikörper (Dako, Deutschland)

2.2 Eingesetzte Zelllinien und ihre Kultivierungsbedingungen

Die Charakteristika der in dieser Arbeit verwendeten Zelllinien sind in Tabelle 1 aufgelistet. Alle Zelllinien wurden bei 37 °C, 5%igem CO_2-Gehalt und 95%-iger Luftfeuchtigkeit im Brutschrank mit RPMI 1640-Komplettmedium, welches aus 500 ml

RPMI 1640-Nährmedium, 10%-igem FBS, 1%-igem Penicillin/Streptomycin sowie 0,3%-igem L-Glutamin besteht, kultiviert.

Tabelle 1: Charakteristika der verwendeten Zelllinien (eigene Darstellung)

Zelllinie	Jahr Etablier ung	Demographie	Stadium/Gewe be-quelle	Immunophenotyp	Krankheits-erscheinung
MyLa (Kaltoft et al., 1992)	1990	82, kaukasischer Mann	IIA/Hautbiopsie	CD4$^+$ und CD8$^+$	Fortgeschrittene MF
HH (Starkebaum et al., 1991)	1986	61, kaukasischer Mann	IVB, Blut	CD2$^+$, CD3$^+$, CD4$^+$, CD5$^+$, CD30$^+$, CD8$^-$, CD25$^-$	Fortgeschrittene leukämische MF
HuT-78 (Gazdar et al., 1980)	1987	53, kaukasischer Mann	IVA, Blut	CD2$^+$, CD3$^+$, CD25$^+$, CD4$^+$, CD1$^-$, CD5$^-$, CD8$^-$, CD20$^-$	SS
SeAx (Kaltoft et al., 1987)	1987	66, kaukasische Frau	IVA, Blut	CD3$^+$, CD4$^+$, CD5$^+$	SS

Die Suspensionskulturen wurden alle 3-4 Tage passagiert, indem diese in ein 50 ml-Falcon Röhrchen überführt, zentrifugiert (1600 rpm/5 Min) und das Zellpellet in 10 ml frischem Medium resuspendiert und ausgesät wurden.

2.3 Konservierung und Auftauen der Zellen

Die Zellen wurden in 20% Zelldichte in Kryoröhrchen konserviert, zuerst auf -80 °C und anschließend auf -196 °C heruntergekühlt. Das Auftauen der Zellen erfolgte im 37 °C-Wasserbad. Die Zellsuspension wurde dann in 10 ml RPMI-Komplettmedium überführt, zentrifugiert (1600 rpm/5 Min), das Zellpellet in einem 10 ml RPMI-Komplettmedium resuspendiert und in Zelldichte von 10, 20 und 30% ausgesät.

2.4 Zellzahlbestimmung

Das Auszählen der Zellen erfolgte mittels Neubauer-Zählkammer. Die Zellzahl pro ml wurde aus dem Mittelwert der zwei in diagonal liegenden Quadranten und der Multiplikation mit 10^4 errechnet.

2.5 Verwendete Reagenzien

PEP005, S63845, ABT-263 und ABT-737, DKP-071 wurden für die Behandlung eingesetzt. Zur Hemmung der Caspaseaktivität erfolgte eine einstündige Vorinkubation der Zellen mit Pan-Caspase-Inhibitor QVD-Oph, zur Hemmung der PKC-Aktivität mit 1

µM Bis-1 für HH-Zellen und 0,25 µM für HuT-78-Zellen. Um ROS abzufangen erfolgte eine einstündige Vorbehandlung der Zellen mit 1 mM α-Tocopherol bzw. 1 mM NAC.

Für die Assays wurden 50000 Zellen pro Welle in 24-Well-Platten ausgesät. Die Kontrollzellen wurden mit 2%-igem DMSO in derselben Inkubationsbedingung behandelt.

2.6 Zellbiologische Methoden

2.6.1 Durchflusszytometrie

Zur Untersuchung von mehreren Zelleigenschaften auf Einzelzellebene mittels Durchflusszytometrie werden die einzelnen Fluoreszenz-markierten Zellen durch hydrodynamische Fokussierung an einem Laserstrahlbündel bestimmter Wellenlänge vorbeigeleitet. Die Elektronen des Fluoreszenzfarbstoffes werden durch monochromatischen Laserstrahl angeregt und auf ein höheres Energieniveau gebracht. Beim Rückfall auf das ursprüngliche Energieniveau werden Photonen emittiert und durch einen Detektor registriert. Die emittierte Photonenenergie steht im Verhältnis zu der Zellzahl proportional. Durch die Streu- und Beugungsintensität des Lichtes lassen sich ebenfalls Rückschlüsse auf die Größe und Granularität der Zellen ziehen. In dieser Arbeit erfolgte die Durchflusszytometrie mittels FACSCalibur Durchflusszytometer (BD Bioscience) und die Datenauswertung mittels CellQuest Software (BD Bioscience).

2.6.1.1 Nachweismethode – Sub-G1 Assay

Für den Nachweis der Apoptoseinduktion wurden die DNA der Zellen mit PI markiert. Der Farbstoff besitzt eine Anregung-/Emissionwellenlänge von 493/636 nm (Riccardi and Nicoletti, 2006). Die apoptotischen Zellen werden im Histogramm im Sub-G1-Peak dargestellt. Hierfür wurden die Zellen aus 24-Wellplatten geerntet, die Zellsuspension zentrifugiert (1600 rpm/5 Min), gewaschen (1600 rpm/5 Min) und in einer 200 µl, aus 40 µg/ml PI, 0,1%Natriumcitrat, 0,1%Triton X-100 zusammengesetzten PI-Lösung einstündig bei 4°C inkubiert. Die Detektion erfolgte mittels Fluoreszenzdetektors FL-3.

2.6.1.2 Nachweismethode – Zellviabilität

Die Zellviabilitätuntersuchung erfolgte mittels Calcein-Assay (Wang et al., 1993). Der Farbstoff Calcein AM wird in die Zellen durchdringen und durch die intrazellulären, aktiven Esterasen, welche ausschließlich in intakten Zellen verfügbar sind, in eine stark fluoreszierende Calcein hydrolysiert. Die Anregungs- und Emissionwellenlänge des Farbstoffs beträgt 496 und 520 nm. Die Zellen wurden aus 24-Wellplatten geerntet und

nach Zentrifugation (1600 rpm/5 Min) mit 1 ml PBS in 200 µl der frischen, aus der 5 mM Stammlösung 1:10000 mit DMSO verdünnten Arbeitslösung resuspendiert und bei 37 °C inkubiert. Danach wurden die Zellen mit 1 ml kaltem PBS verdünnt, zentrifugiert (1300 rpm/8 Min) und das Pellet in 200 µl kaltem PBS resuspendiert. Die Analyse erfolgte im Fluoreszenzdetektor FL-2.

2.6.1.3 Nachweismethode - mitochondriales Membranpotential (MMP)

Zur Untersuchung des MMPs wurde TMRM$^+$ mit einer Anregungs-/Emissionswellenlenge von 548/574 nm eingesetzt. Der Nachweis erfolgte durch die Anreicherung dieses kationischen Farbstoffes in den negativ-geladenen Mitochondrien. Die geernteten Zellen wurden zweimal mit eiskaltem PBS gewaschen (1600 rpm/5 Min), in 200 µl der 1 µM TMRM$^+$-Arbeitslösung resuspendiert und für 20 Min bei 37 °C inkubiert. Nach dem Waschen wurde die Zellsuspension in 200 µl PBS resuspendiert und umgehend im Fluoreszenzdetektors FL-2 gemessen.

2.6.1.4 Nachweismethode - reactive oxygen species (ROS)

Zum Nachweis der intrazellulären ROS wurde H$_2$DCFDA mit einer Anregungs-/Emissionswellenlänge von 484/535 nm verwendet. Hierbei wurden die Zellen mit 25 µl der 10 µM H$_2$DCFDA Arbeitslösung einstündig vor der Behandlung vorinkubiert. Als Positivkontrolle dienten 10 µl H$_2$O$_2$, die den Zellen einstündig vor dem Assaybeginn gegeben wurden. Die geernteten Zellen wurden anschließend zweimal mit PBS gewaschen (1600 rpm/5 Min), in 250 µl PBS resuspendiert und mittels Fluoreszenzdetektor FL-1 untersucht.

2.6.2 **Nachweismethode – Zellproliferation**

Die Quantifizierung der Zellproliferation basierte auf der Spaltung des wasserlöslichen Tetrazoliumsalzes WST-1 in einen Formazan-Farbstoff durch zelluläre mitochondriale Dehydrogenasen, welche ausschließlich in lebenden Zellen aktiv sind. Durch Erhöhung der Zellzahl wird die Aktivität der Enzyme und die Bildung von Formazan-Farbstoffes erhöht.

Für die Untersuchung wurden 10000 Zellen in einer 100 µl Zellsuspension in einer 96-Wellplatte kultiviert. Die behandelten Zellen wurden nach Zugabe von 5 µl WST-1 Reagenz im Dunklen einstündig bei Raumtemperatur inkubiert. Die Quantifizierung erfolgte in einem ELISA Reader bei 450 nm mit dem Programm Ahmed WST Assay.

2.7   SDS-PAGE und Westernblot

SDS Page und Westernblot diente der Untersuchung auf Proteinebene.

2.7.1.1 Probenvorbereitung

Zunächst wurden die Zellen zweimal mit eiskaltem PBS gewaschen (1600 rpm/5 Min) und anschließend einstündig bei 4 °C mit dem aus 150 mM NaCl, 1 mM EDTA, 1% NP-40, 50 mM Tris (pH 8,0) sowie Phosphatase- und Proteaseinhibitoren bestehenden Lysepuffer inkubiert, bei 4 °C zentrifugiert (1800 rpm/20 Min) und den Überstand auf Eis aufbewahrt.

Die Proteinkonzentration im Lysat wurde mittels BCA Protein Assay bestimmt. Das Verfahren beruht auf der Reduktion von Cu^{2+} zu Cu^+, welches sich anschließend mit BCA einen Farbkomplex ausbildet und mittels ELISA Reader bei 550 nm quantifizierbar ist. In 96-Wellplatte wurde insgesamt 20 µl Probenlösung aus einer Mischung von 19, 18 oder 17 µl PBS und entsprechend 1, 2 oder 3 µl Proteinextrakt gelegt. Für die Eichgerade wurde eine Eichlösung wie in Tabelle 2 zweifach vorbereitet. Anschließend wurden 200 µl Reaktionspuffer, welches frisch aus 4 µl Lösung A und 196 µl Lösung B zusammengesetzt wurden, in jede Welle gegeben, die Proben für 30 min bei 37 °C inkubiert und anschließend im ELISA Reader vermessen.

Für die weiteren Schritte wurden 20 µl Proteinproben mit 30 µg Proteingehalt vorbereitet. Das dafür notwendige Volumina (V1) der Proteinextrakte mit einer Konzentration von C1 wurde wie folgt berechnet: V1 = 30 µg/ml *0,02 ml / C1

Die Proteinproben setzten sich wie folgt zusammen:

V1 µl aus dem Proteinextrakt + 5 µl aus der 4x Laemmli Pufferlösung + (15-V1) µl PBS

Tabelle 2: Herstellung der Eichlösung für Eichgerade (eigene Darstellung)

2mg/ml BSA-Lösung (µl)	PBS (µl)
0	20
1	19
2	18
3	17

4	16
5	15
7,5	12,5
10	10

Die 4x Laemmli-Pufferlösung wurde wie folgt vorbereitet :

- 12,5 ml der 1 M Tris-HCl Pufferlösung pH 6,8 bestehend aus 24,23 g Tris-Base, 15,8 ml 37,2%-HCl und 184,2 ml Aqua bidest

- 4,6 g SDS

- 20 ml Glycerin

- Ein Tropfen von Bromphenolblau

- Aqua bidest add 45 ml

Die Pufferlösung wurden in 900 µl Aliquot bei -20°C gelagert und vor der Zugabe in die Proteinproben mit 100 µl β-Mercaptoethanol frisch versetzt. Durch SDS wurden die Proteine in ihre primäre Aminosäuresequenz denaturiert und gleichmäßig mit einer negativen Ladung versetzt. Das ß-Mercaptoethanol diente zusätzlich als Reduktionsmittel, welches die Schwefelbrücken der Proteine spalten. Die Inkubation erfolgte bei 95 °C für 10 Min.

2.7.1.2 SDS-PAGE (SDS-Polyacrylamidgelelektrophorese)

Mittels SDS-PAGE lassen sich die einzelnen Proteine durch ihre elektrophoretische Mobilität im elektrischen Feld voneinander auftrennen. Dafür wurden jeweils zwei Gelstücke, welche aus einem 6%-igen Sammelgel und einem 14%-igen Trenngel bestehen, in eine Elektrophoresekammer eingesetzt. Die innere Kammer wurde mit 1x konzentriertem kathodischem und die äußere Kammer mit 1x konzentriertem anodischem Laufpuffer gefüllt. Die einzelne Geltasche wurde mit 20 µl der Proteinproben beladen. Durch das Anlegen des elektronischen Feldes wanderten die negativ geladenen Proteine zur Anode und wurden nach Molekulargewicht aufgetrennt. Die Elektrophorese für das Sammelgel lief bei 80 V für 10 Min und für das Trenngel bei 120 V für 55 Min. Als Referenz für die Proteingröße wurde ein das Molekulargewichtstandard Precision Plus Protein™ Dual Color Standards verwendet.

Folgende Rezepte wurden verwendet:

- 6%-iges Sammelgel

Für zwei Gele: 3,1 ml Aqua bidest; 1,3 ml Polyacrylamid (30%); 1,25 ml Sammelgelpuffer pH 6,8; 0,05 ml SDS (10%); 100 µl APS (10%); 5 µl TEMED.

Für Sammelgelpuffer: 19,7 g Tris-Base; 1,0 g SDS; Aqua bidest add 500 ml, Einstellung auf pH 6,8 mit NaOH/HCl.

- 14%-iges Trenngel

    Für zwei Gele: 3,5 ml Aqua bidest, 5,3 ml Polyacrylamid (30%), 2,1 ml Trenngelpuffer pH 8,8; 0,106 ml SDS (10%); 200 µl APS (10%); 20 µl TEMED.

    Für Trenngelpuffer; 38,5 g Tris-Base; 9,3 g Tris-HCl; 1,0 g SDS; Aqua bidest add 500 ml, Einstellung auf pH 8,8 mit NaOH/HCl.

- Kathodischer Laufpuffer

    Für 10x konzentrierte Lösung: 120 g Tris Base; 180 g Tricin, 10 g SDS, Aqua bidest add 1 l, auf pH 8,45 mit NaOH/HCl einstellen.

- Anodischer Laufpuffer

    Für 10x konzentrierte Lösung: 240 g Glycin; Aqua bidest add 1 l, Einstellung auf pH 8,9 mit NaOH/HCl.

2.7.1.3 Westernblot

Wie die PAGE wurden beim Westernblot die negativ-geladenen Proteine durch einen elektrischen Strom von Anode zur Kathode und so auf die Membran im selben Muster wie im Gel transferiert.

Ein 9x6,5 cm großer Nitrozellulose-Membranstück, Filterpapieren und Schwämmen wurden im Transfer-Puffer getränkt. Das Blot-System wurde in folgender Reihenfolge luftblasenfrei aufgebaut: Schwamm, Filterpapiere, Gel, Nitrozellulose-Membran, 2 Filterpapiere, Schwamm. Danach wurde das System in Blotkammer, welcher den aus 6,04 g Tris Base, 28,8 g Glycin und 180 ml Aqua dest bestehenden Transferpuffer beinhaltet, so ausgerichtet, dass das Gel auf der anodischen und die Membran auf der kathodischen Seite lag. Das Bloten erfolgte einstündig bei 120 V auf Eis.

2.7.1.4 Membranblocking und Immunoblotting

Der Nachweis der Proteine erfolgte indirekt durch die spezifische Bindung von Antikörpern. Hierzu wurden die Blots dreimal für jeweils 5 Min mit 15 ml PBS-T, welches aus 100 ml 10xPBS, 900 ml Aqua dest und 1 ml Tween20 hergestellt wurde, gewaschen. Zur Absättigung der freien Bindungstellen wurde das Blot einstündig bei RT bei leichtem Schütteln mit 5%-igem, aus 5 g Milchpulver und 100 ml PBS-T bestehendem Milch-PBS-T inkubiert. Nach dreimaligem Waschen mit 15 ml PBS-T für jeweils 5 Min wurde das Blot

mit 2 ml primärem Antikörper über Nacht bei 4 °C bei leichtem Schütteln inkubiert. Das Blot wurde dreimal mit 15 ml PBS-T für jeweils 5 Min gewaschen und anschließend mit dem konjugierten Sekundär-Antikörper bei RT einstündig bei leichtem Schütteln inkubiert. Nach dreimaligem Waschvorgang war das Blot für die Detektion bereit. Die primären Antikörper von Cell Signaling wurden 1:1000, die primären Antikörper von Santa Cruz Biotech 1:500 und der Antikörper für PKCδ 1:1000 und die Sekundärantikörper 1:5000 vorverdünnt.

2.7.1.5 Immundetektion

Zur Detektion der membrangebundenen Proteine wurde ECL™ Westernblotting Substrate eingesetzt. Das Chemolumineszenz-Substrat ECL wurde durch im Sekundär-Antikörper gekoppelten Enzym Meerrettich Peroxidase (HRP) oxidiert und so auf ein erhöhtes instabiles Energieniveau gebracht. Beim Rückgang in die stabile Ausgangslage wird Energie als Licht freigesetzt, deren Intensität durch Phenol verstärkt wird. Zur Proteindetektion wurden die Blots mit 1 ml aus dem gleichen Anteil der beiden ECL-Lösungen bestehender ECL-Arbeitslösung überdeckt. Nach fünfminütiger Inkubation im Dunkeln bei RT wurde das Lichtsignal in der Maschine FUSION mit dem Programm FUSION detektiert.

2.7.1.6 Membranstripping

Zur Wiederverwendung des Blots wurden die Antikörper aus dem Blot entfernt, indem das Blot dreimal mit 10 ml Strippingpuffer pH 2,2, welches aus 1,5 g Glycin, 100 mg SDS, 1 ml Tween20 und Aqua dest add. 100 ml besteht, für 10 Min bei RT und leichtem Schütteln inkubiert und mit frischem Strippingpuffer für 10 Min geschwenkt wurde. Nach zweimaligem zehnminütigen Waschen mit 15 ml PBS-T und zweimaligem fünfminütigem Waschen war das Blot für ein erneutes Blocking (Abschnitt 2.6.3.4) bereit.

2.8 Statistische Analyse

Jedes Experiment wurde mindestens zweimal, jeweils mit Triplikaten, wiederholt. Der Mittelwert aus drei voneinander unabhängigen Experimenten wurde zur Auswertung der Experimente herangezogen. Die statistische Signifikanz wurde mit einem ungepaarten t-Test mit Excel berechnet. p-Werte unter 0,05 wurden als signifikant bewertet.

Für Westernblots wurden mindestens zwei Experimente mit unabhängigen Proteinextraktserien durchgeführt. Die Signale wurden mittels densitometrischer Analyse

und mit den jeweiligen β-Actin-Werten normalisiert. Für die Bcl-2 Proteine mit drei unabhängigen Experimenten wurden die statistische Signifikanz berechnet.

Die Identifizierung von synergistischen Effekten bei Kombinationsbehandlungen mit S63845 und ABT-263 wurde von Herrn Sinnberg mit dem Programm SyngeryFinder 3.0 durchgeführt. Die Bliss-Scoring-Methode wurde angewandt, und Delta-Scores (δ) ≥ 10 als synergistisch, während Werte zwischen -10 und 10 als additiv angesehen.

3 Ergebnisse

3.1 Unterteilung der CTCL-Zelllinien in empfindliche und resistente Gruppen gegenüber PEP005 und S63845

Um das Ausmaß der proapoptotischen Wirkung von PEP005 und S63845 in CTCL-Zellen zu untersuchen, wurden nach 24- bzw. 48-stündiger Behandlung die Apoptoserate sowie die Zellviabilität bestimmt.
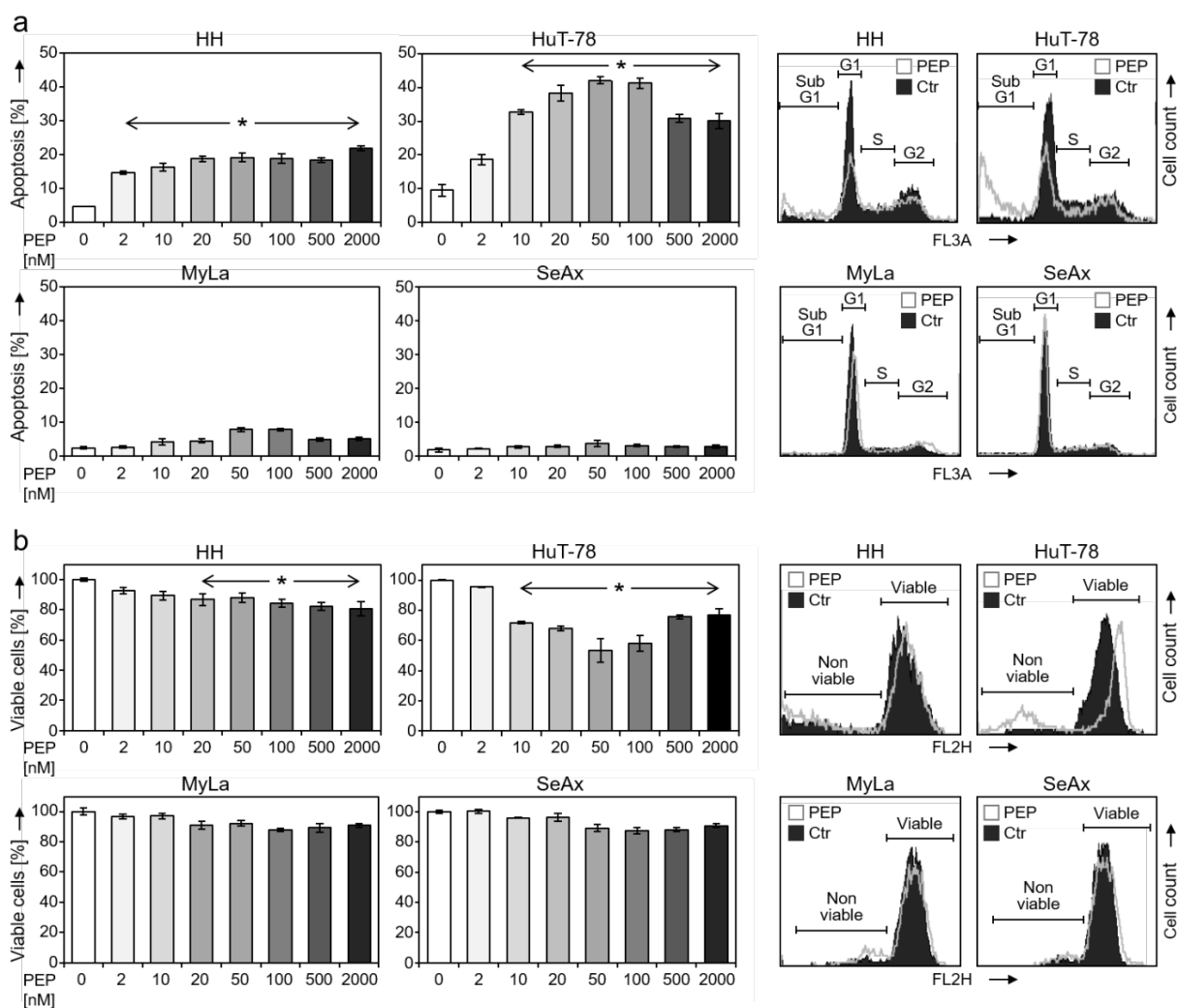

Abbildung 1. Konzentrationsabhängige Effekte von PEP005 auf CTCL-Zelllinien. Apoptoseinduktion (a) und Zellviabilität (b) wurden in HH, HuT-78, MyLa und SeAx nach 48h Inkubation mit 2, 10, 20, 50, 100, 500 und 2000 nM PEP005 bestimmt. Charakteristische Histogramme von mit 50 nM PEP005 behandelten Zellen (PEP) wurde in Überlagerungen mit den unbehandelten Zellen (Ctr) dargestellt. Zwei unabhängige Experimente ergaben ähnliche Daten. Die statistische Signifikanz zwischen behandelten und unbehandelten Zellen ist angegeben (*, p<0,05). (Aus Sumarni et al., 2021)
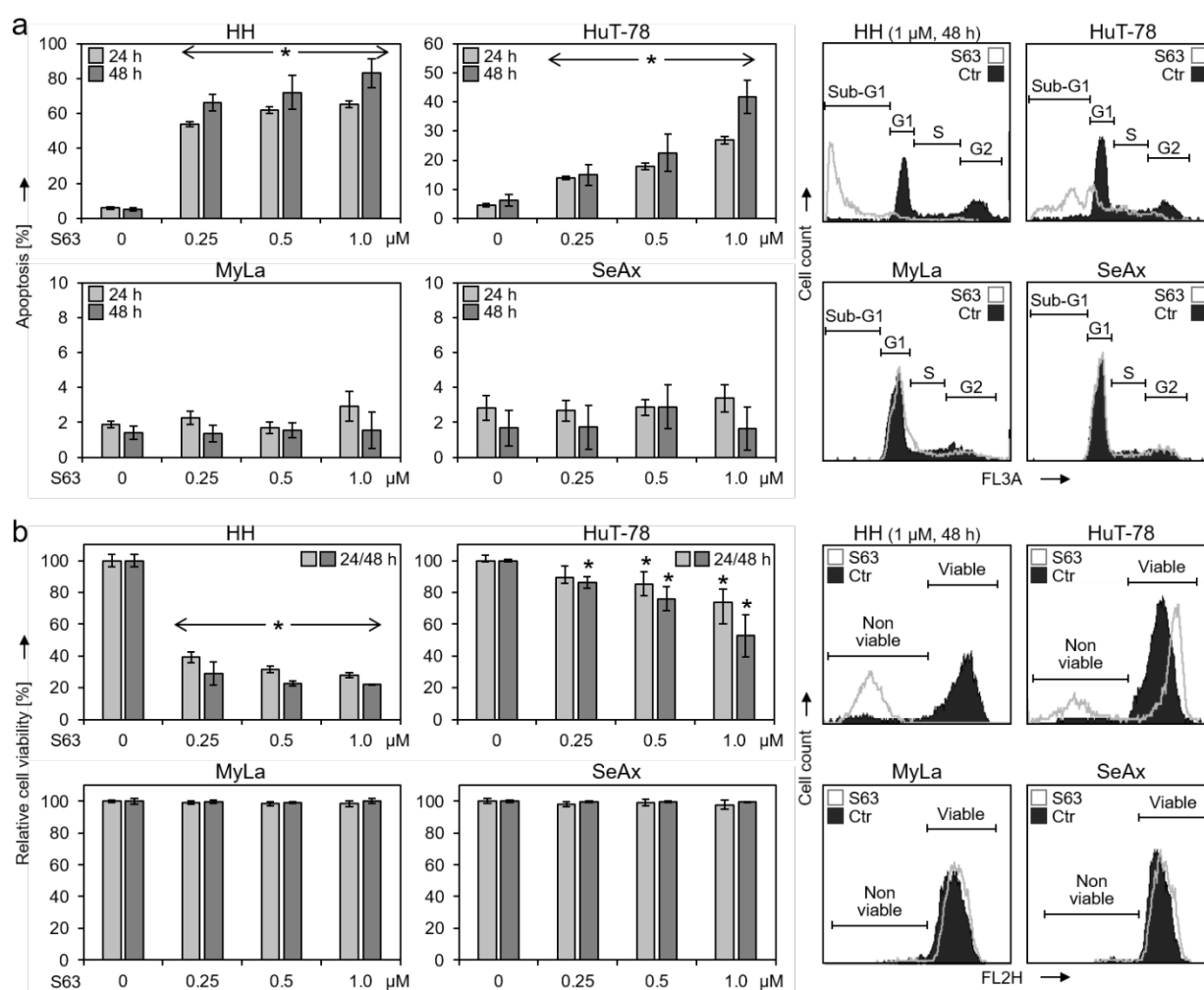
Abbildung 2. Konzentrations- und zeitabhängige Effekte von S63845 auf CTCL-Zelllinien. Apoptoseinduktion (a) und Zellviabilität (b) wurden in HH, HuT-78, MyLa und SeAx nach 24h bzw. 48h Inkubation mit 0,25, 0,5 und 1,0 µM S63845 bestimmt. Charakteristische Histogramme von mit 1 µM S63845 für 48h behandelten Zellen (S63), wurde in Überlagerungen mit den unbehandelten Zellen (Ctr) dargestellt. Drei unabhängige Experimente mit jeweils Dreifachwerten ergaben ähnliche Daten. Die statistische Signifikanz zwischen behandelten und unbehandelten Zellen ist angegeben (*, p<0,05). (Aus Sumarni et al., 2022)

PEP005 zeigte hohe proapoptotische Wirkung bei HH und HuT-78 (Abbildung 1). Die effektivste Konzentration war 50 mM, mit der die maximale Apoptoserate von 19% bei HH sowie 42% bei HuT-78 erreicht wurden. Die Zellviabilität bei HH und HuT-78 verringerte sich auf 88% bzw. 54% relativ zu Kontrolle. Bei MyLa und SeAx war der Effekt deutlich weniger ausgeprägt.

Zur Untersuchung der Zeitabhängigkeit wurden die Zellen für 24, 48 und 72 Stunden mit 50 nM PEP005 behandelt. Eine zeitabhängige Zunahme der Apoptoserate bis auf 39% in HH, 73% in HuT-78 sowie Zellviabilitätsverlust bis auf 52% bei HH bzw. 50% bei HuT-78 wurden beobachtet. Bei MyLa und SeAx lag die Apoptoserate bei höchstens 15% bzw. 13% und die Viabilität bei 75% bzw. 76% (Abbildung 3a und b).
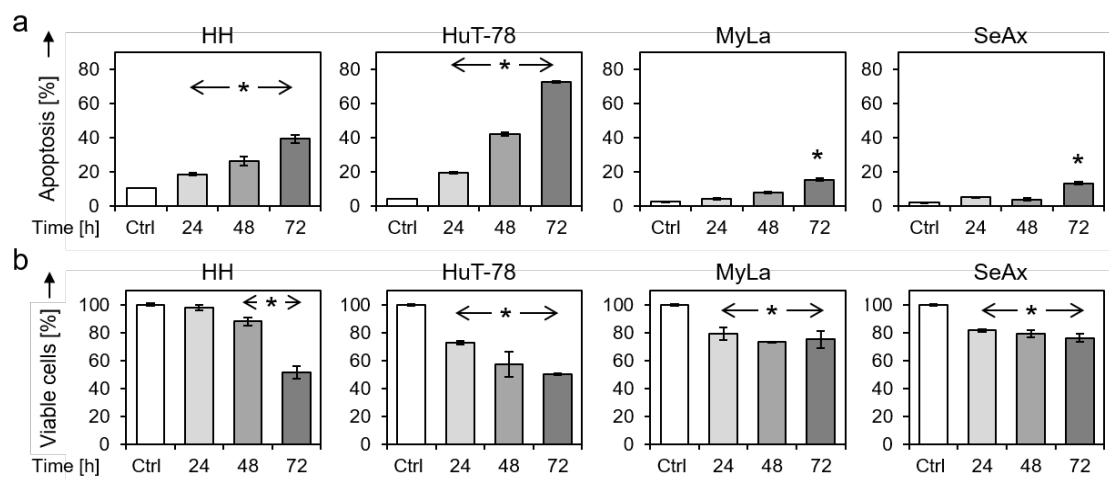
Abbildung 3. Zeitabhängige Effekte von PEP005 auf CTCL-Zelllinien. Apoptoseinduktion (a) und Zellviabilität (b) wurden in HH, HuT-78, MyLa und SeAx nach 24h 48h und 72hInkubation mit 50 nM PEP005 bestimmt. Zwei unabhängige Experimente mit jeweils Dreifachwerten ergaben ähnliche Daten. Die statistische Signifikanz zwischen behandelten und unbehandelten Zellen ist angegeben (*, p<0,05). (Aus Sumarni et al., 2021)

Bei S63845 ergab sich ein ähnliches Verteilungsmuster wie bei PEP005 (Abbildung 2). HH und HuT-78 waren sensitiv, während MyLa und SeAx resistent gegenüber S63845. Ein dosisabhängiger Anstieg der Apoptoserate nach 48-stündiger Behandlung auf bis zu 83% in HH sowie 42% in HuT-78 wurde beobachtet. Die Zellviabilität nahm dementsprechend auf 22% bei HH sowie auf 53% bei HuT-78 ab.

Zum Vergleich der S63845-Effekte in verschiedenen Zelllinien wurde der EC50 berechnet. Dies erfolgte basierend auf der Zellviabilität (Abbildung 4) und der Apoptoserate (Abbildung 5). Die Zellen wurden für 24 bzw. für 48 Stunden mit PEP005 in einer Konzentrationsreihe von 10 nM bis 2000 nM behandelt. Für HH ergab sich nach 48-stündiger Behandlung ein EC50 von 95 nM in Bezug auf der Apoptose bzw. 22 nM in Bezug auf der Zellviabilität, für HuT-78 1,4 µM und 110 nM. Bei den resistenten Zelllinien SeAx und MyLa wurde bei der höchsten Konzentration von 2 µM die EC50 noch nicht erreicht.
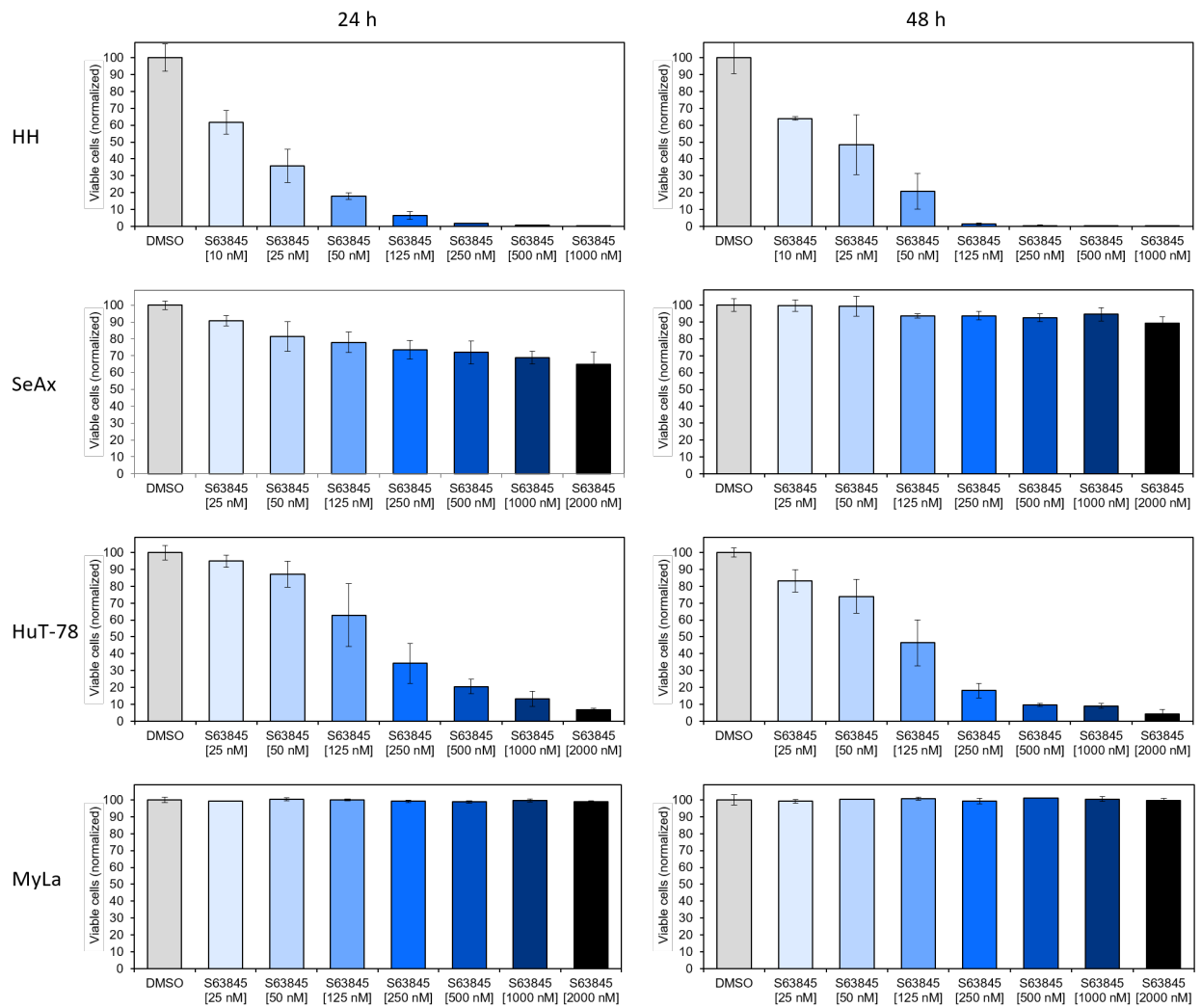
Abbildung 4. Konzentrations- und zeitabhängige Effekte von S63845 auf die Viabilität der CTCL-Zelllinien. Zwei unabhängige Experimente mit jeweils Dreifachwerten ergaben ähnliche Daten. (Aus Sumarni et al., 2022)
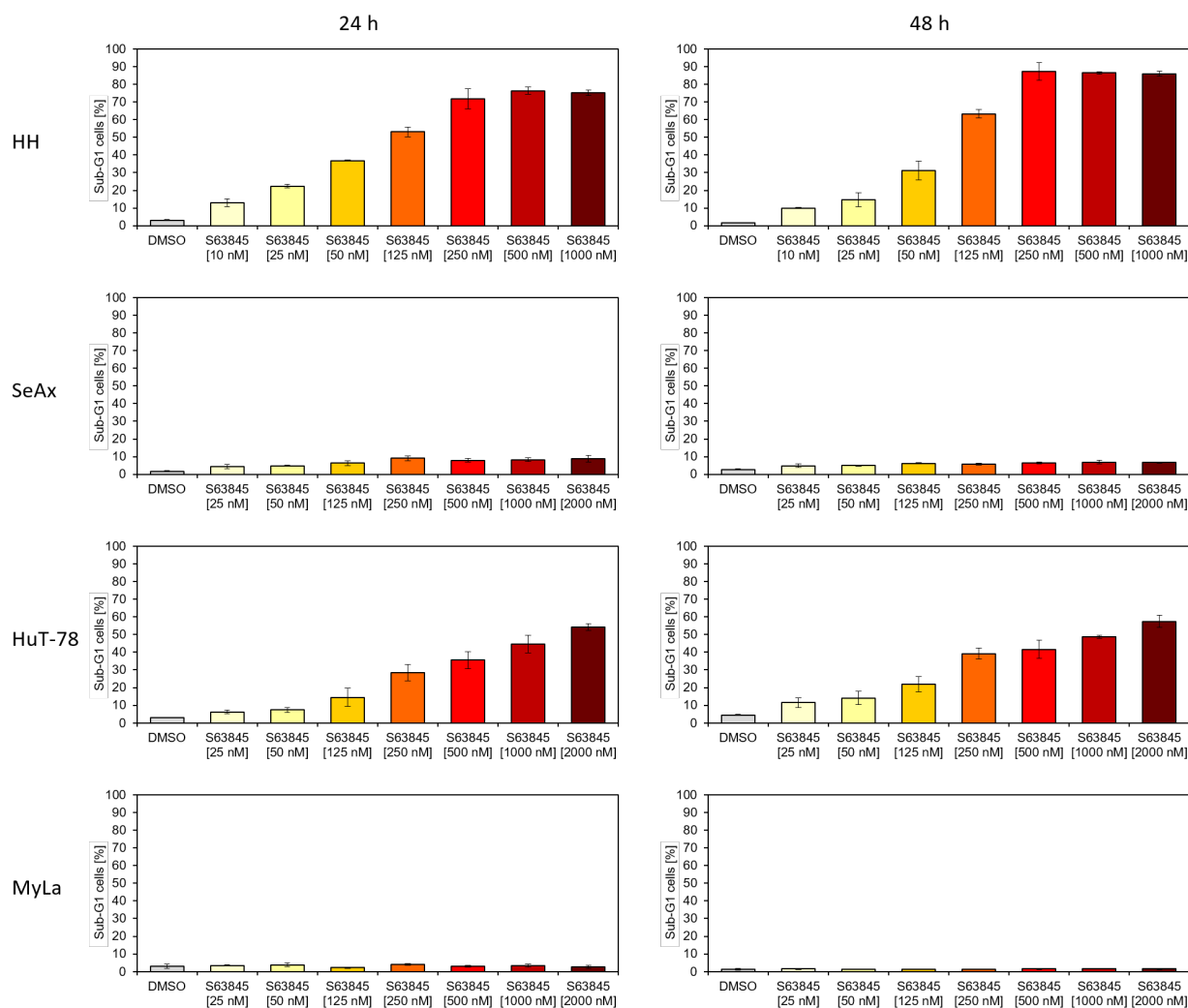
Abbildung 5. Konzentrations- und zeitabhängige Effekte von S63845 auf die Apoptoseinduktion der CTCL-Zelllinien. Zwei unabhängige Experimente mit jeweils Dreifachwerten ergaben ähnliche Daten. (Aus Sumarni et al., 2022)

DKP-071 zeigte eine proapoptotische Wirkung in allen drei verwendeten Zelllinien (Abbildung 6). Nach 48-stündiger Behandlung mit 10 µM DKP-071 wurde eine Apoptoserate von 17% in HH, 14% in HuT-78 sowie 13% in MyLa festgestellt. Die Viabilität verringerte sich dabei auf 23% bei MyLa, auf 1% bei HuT-78 bzw. auf 38% bei HH.
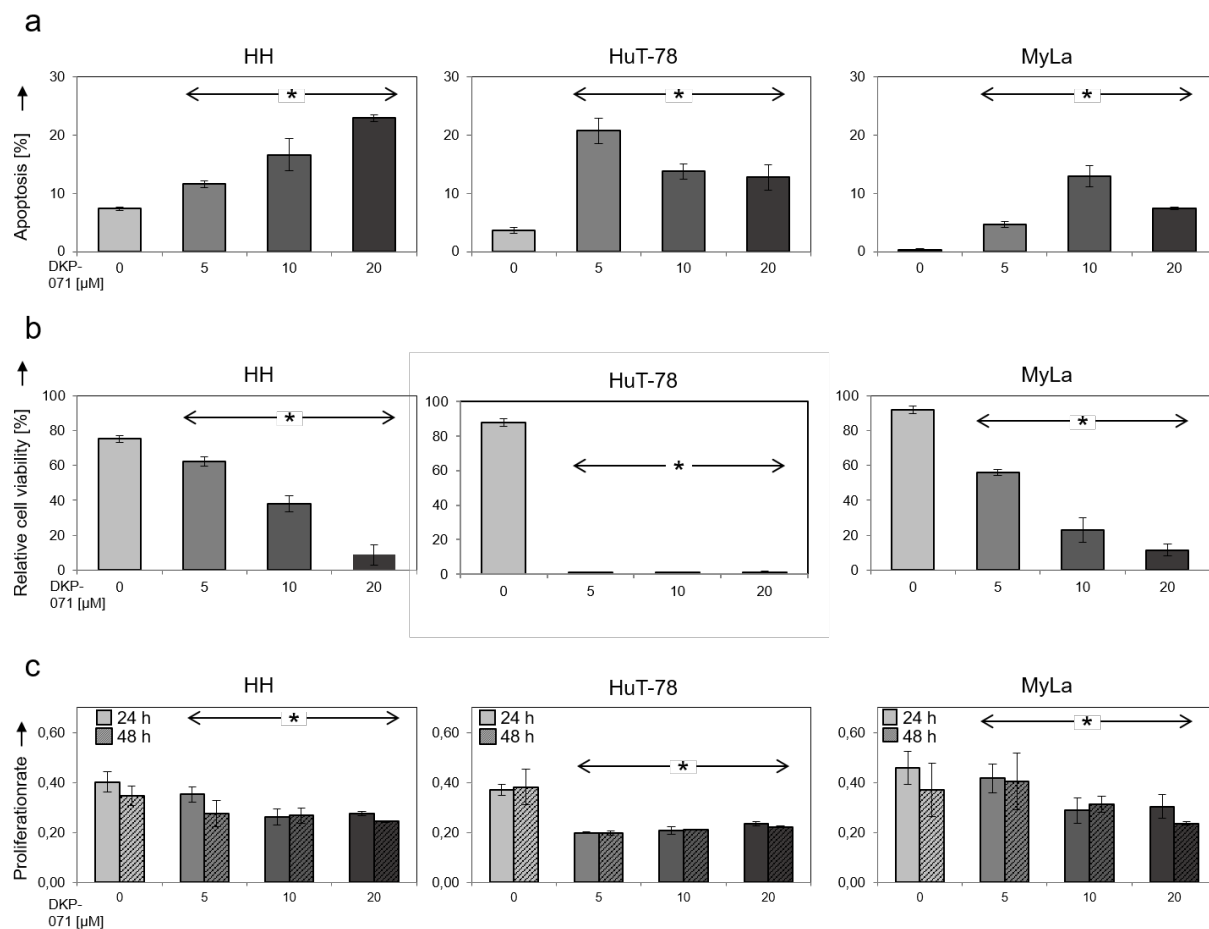
Abbildung 6. Effekt von DKP-071 auf die Apoptoseinduktion (a), Zellviabilität (b) und Proliferationsrate (c) der CTCL Zelllinien HH, HuT-78 und MyLa. Drei unabhängige Experimente mit jeweils Dreifachwerten ergaben ähnliche Daten. Die statistische Signifikanz zwischen behandelten und unbehandelten Zellen ist angegeben (, p<0,05). (Aus Soltan et al., 2019)*

3.2 Untersuchung des Einflusses von PEP005 und S63845 auf die Bildung von ROS und den Verlust an MMP

Der Effekt von PEP005 in den vier untersuchten CTCL-Zelllinien war unterschiedlich. So zeigte HuT-78 einen Verlust des MMPs von 36%, während bei HH, MyLa und SeAx der MMP-Verlust viel weniger ausgeprägt war. ROS dagegen nahm bei allen vier Zelllinien nach 24-stündiger Behandlung mit PEP005 zu (Abbildung 7).
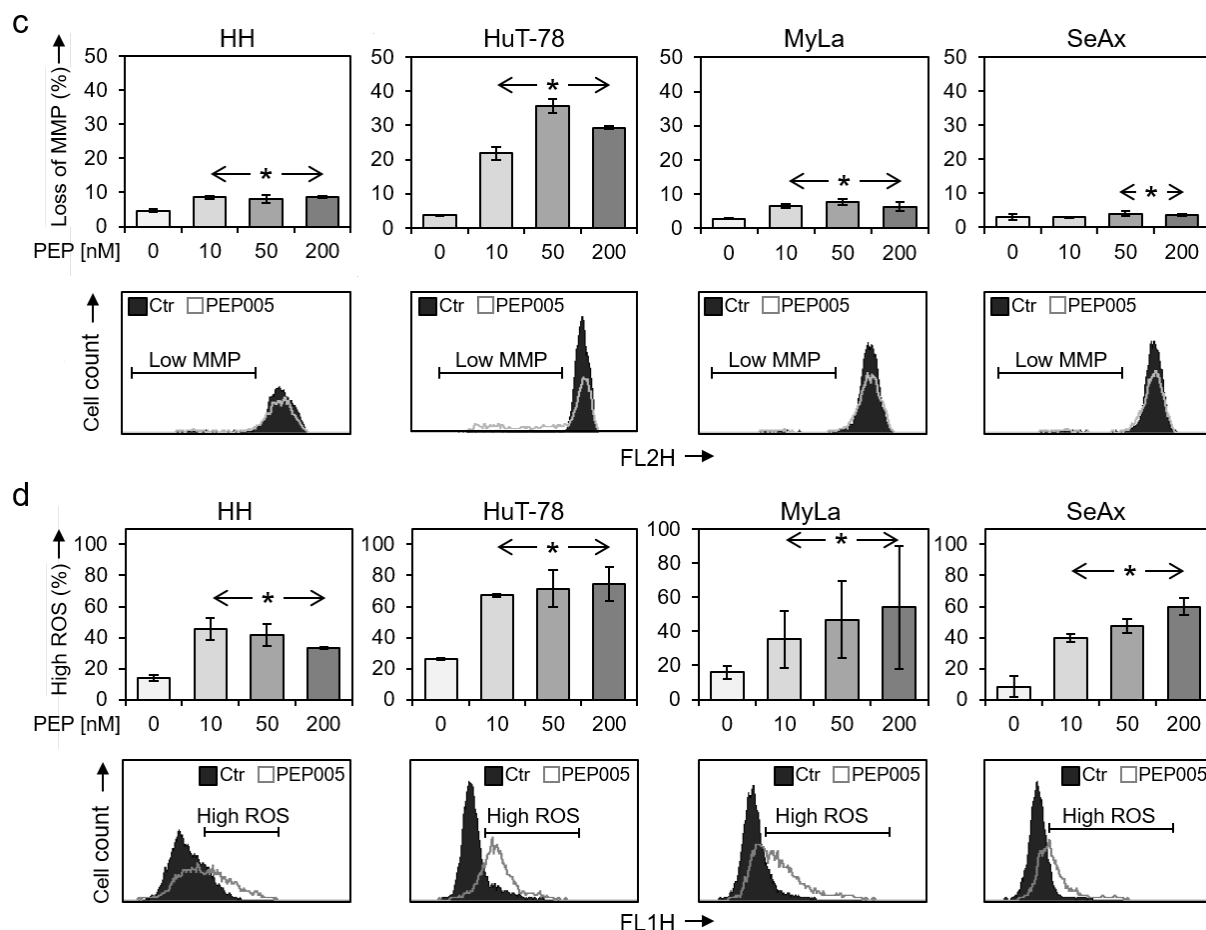
Abbildung 7. Konzentrationsabhängige Effekte von PEP005 auf MMP-Verlust (a) und ROS-Bildung (b) in CTCL-Zelllinien nach 24h Behandlung. Zwei unabhängige Experimente mit jeweils Dreifachwerten ergaben ähnliche Daten. Die statistische Signifikanz zwischen behandelten und unbehandelten Zellen ist angegeben (, p<0,05). Repräsentative Histogramme mit Überlappung von mit 50nM für 24h behandelten(PEP005) und unbehandelten(Ctr) Zellen sind in der folgenden Zeile dargestellt. (Aus Sumarni et al., 2021)*

Der Effekt von S63845 auf den MMP-Verlust wurde nach 4- und 24-stündiger Behandlung mit 0,25, 0,5 und 1,0 µM S63845 untersucht. Ein signifikanter, dosisabhängiger MMP-Verlust wurde nach 24 Stunden festgestellt (Abbildung 8). Bei HH betrug dieser 65%, 83%, 91%, bei HuT-78 21%, 25% und 35%. Bei MyLa und SeAx zeigte sich kein signifikanter MMP-Verlust. Desweiteren wurden bei HH und HuT-78 nach 24 Stunden eine Zunahme der ROS-Bildung bis auf 51% bzw. 26% beobachtet, während bei MyLa und SeAx die ROS-Bildung durch S63845 nicht signifikant erhöht war.
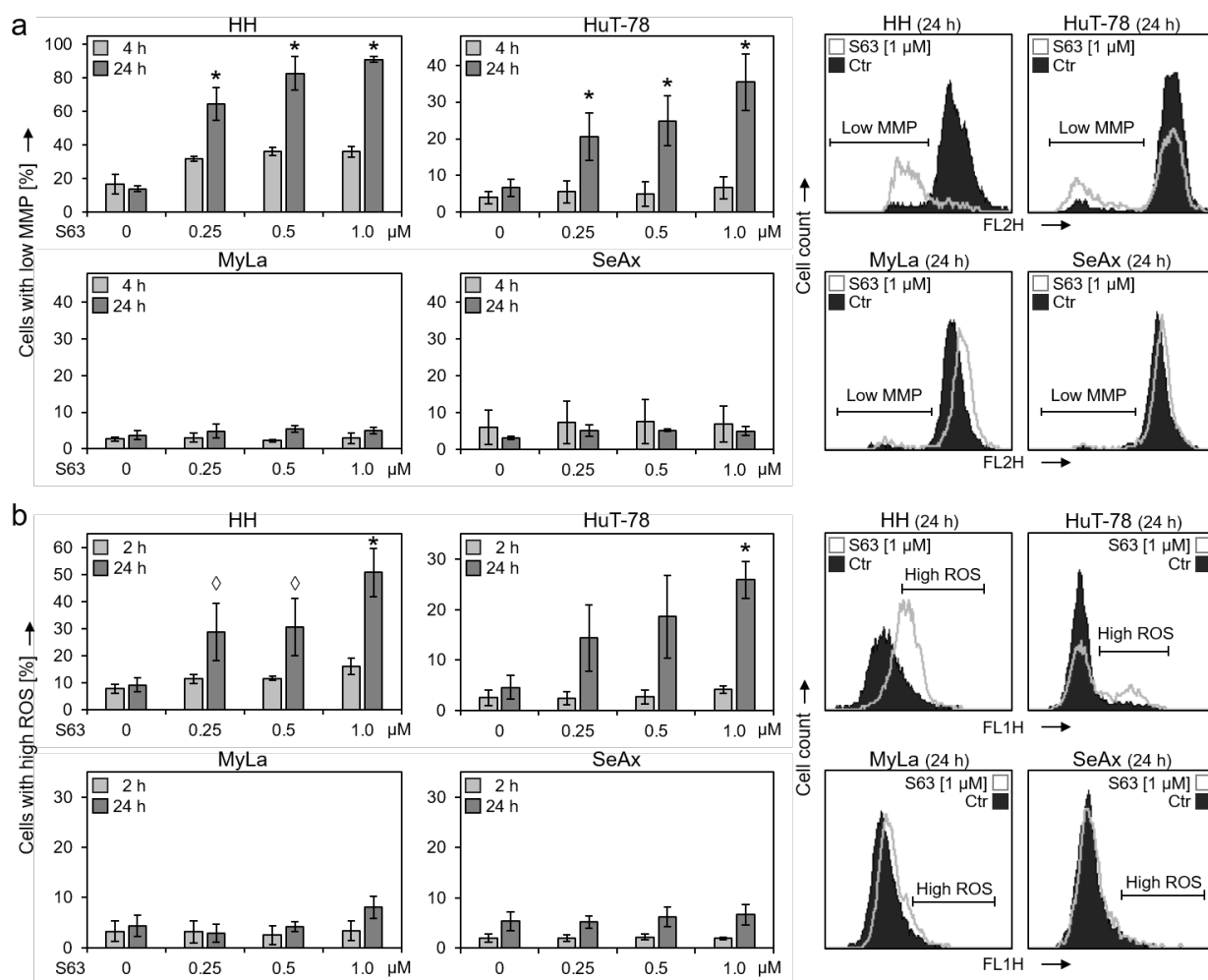
Abbildung 8. Konzentrations- und zeitabhängige Effekte von S63845 auf MMP-Verlust (a) und ROS-Bildung (b) in CTCL-Zelllinien. Repräsentative Histogramme mit Überlappung von mit 1 µM S63845 für 24h behandelten und unbehandelten(Ctr) Zellen sind rechts dargestellt. Mindestens zwei unabhängige Experimente mit jeweils Dreifachwerten ergaben ähnliche Daten. Die statistische Signifikanz (*, p<0,05) und der statistische Trend (◊, p<0,1) zwischen behandelten und unbehandelten Zellen ist angegeben. (Aus Sumarni et al., 2022)

3.3 Bedeutung der Caspasenaktivierung für die proapoptotische Wirkung von PEP005 und S63845

Die Prozessierung der Caspase-8 als Initiator-Caspase des extrinsischen und der Caspase-9 als Initiator-Caspase des intrinsischen Signalwegs dient als Hinweis auf die Initiierung proapoptotischer Caspase-Kaskaden. Interessanterweise wurde die stärkste Caspase-8 Prozessierung in den beiden PEP005-resistenten Zelllinien MyLa und SeAx beobachtet. Desweiteren konnte eine gewisse Caspase-9-Prozessierung in HuT-78, MyLa und SeAx (Abbildung 9a) festgestellt werden. Die 17 kDa aktive Caspase-3 sind demgegenüber nur in sensitiven Zellen detektierbar. Bei den resistenten Zellen MyLa und SeAx wurde die Caspase-3 bis zum nicht aktiven, 21 kDa langen Fragment prozessiert. Diese Ergebnisse deuteten darauf hin, dass die Apoptoseinduktion in den resistenten

Zellen erst nach der Aktivierung der Initiator Caspase-8 und der Prozessierung der Caspase-3 bis zum 21 kDa Zwischenprodukt blockiert wurde.

Bei den c-FLIP$_{L/S}$ sowie bei XIAP zeigten sich auffällige Unterschiede zwischen den sensitiven und resistenten zelllinien. In resistenten Zelllinien MyLa und SeAx wurden diese Proteine stark exprimiert, c-FLIP$_{L/S}$ wurden durch PEP005 sogar hochreguliert. Im Gegensatz dazu wurden c-FLIP$_{L/S}$ in HuT-78 schwach exprimiert; in HH wurden sie durch PEP005 herunterreguliert. Ebenfalls wurde XIAP in HH schwach exprimiert und durch PEP005 in HuT-78 herunterreguliert. Diese Ergebnisse zeigten die entscheidende, limitierende Rolle der Caspase-Antagonisten c-FLIP$_{L/S}$ und XIAP bei der Apoptoseinduktion durch PEP005. Die Expression des Tumorsuppressors und proapoptotischen Transkriptionsfaktors p53 hing mit der PEP005-Sensitivität negativ zusammen. In resistenten Zellen ist dieses Protein stark exprimiert, während es in HH und HuT-78 fehlte. Ähnliches zeigte sich beim Zellzyklus-Inhibitor p21. In MyLa und SeAx war die Expression des Proteins sehr stark ausgeprägt, während in HH fehlend. In HuT-78 folgte p21 der erwarteten Regulierung, d.h. dass p21 durch PEP005 hochreguliert wurde. Das Protein p21 könnte somit zur Hemmung der Zellproliferation in HuT-78 beitragen.
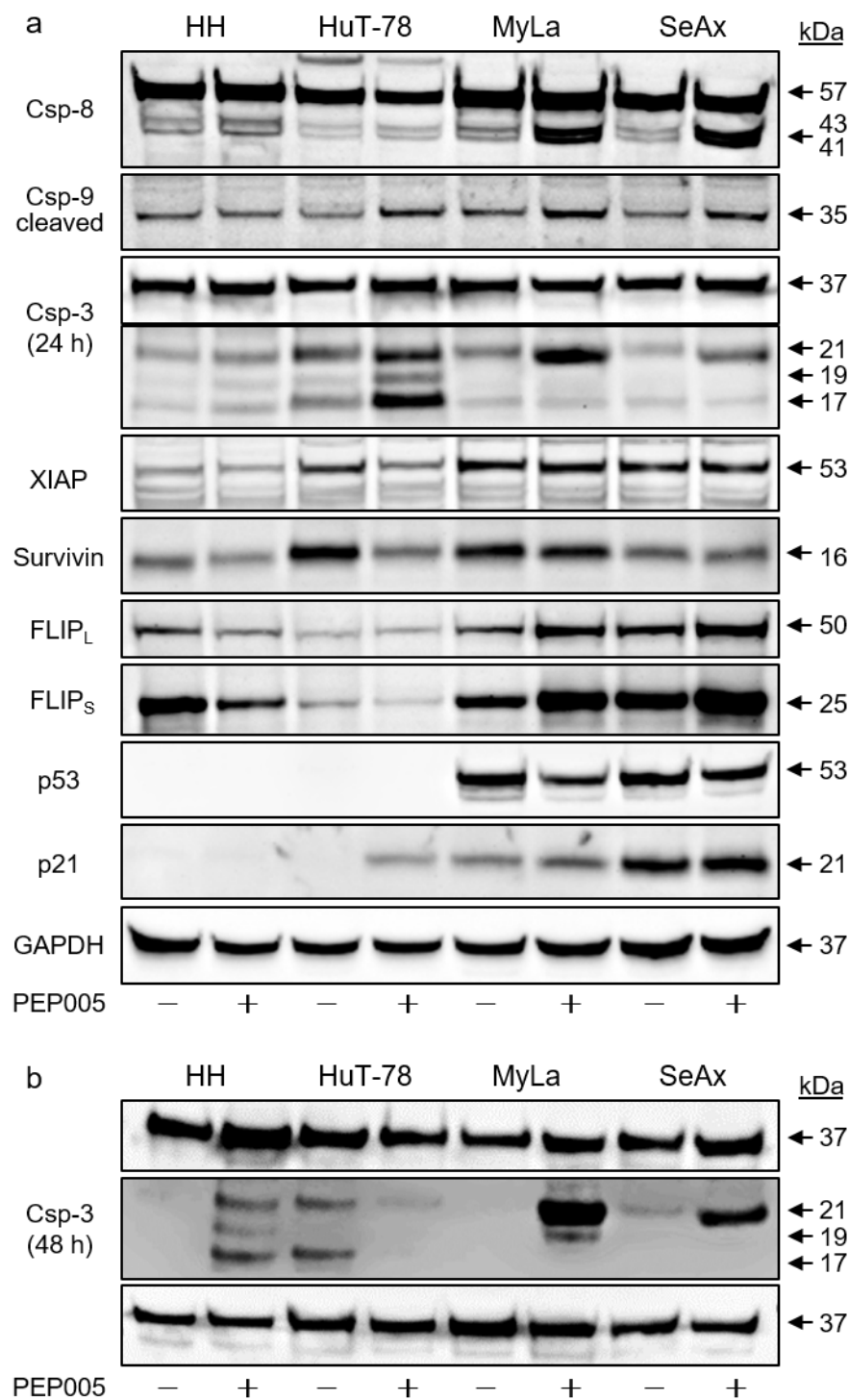
Abbildung 9. PEP005-Effekte auf Apoptose-regulierende Proteine in CTCL-Zellen. Die Zellen wurden mit 50 nM PEP005 für 24h inkubiert und die Proteinexpression mittels Westernblot Analyse untersucht. Für die Untersuchung der Caspase-3-Prozessierung wurde eine 48-stündige Behandlung untersucht (b). Eine gleichmäßige Proteinbeladung von 30 μg pro Geltasche wurde mit GAPDH (37kDa) überprüft. Zwei unabhängige Experimente zeigten vergleichbare Ergebnisse. (Aus Sumarni et al., 2021)

Desweiteren führte S63845 zur Zunahme der aktiven Caspase-3 (16 kDa-Bande) in den sensitiven Zelllinien HH und HuT-78 (Abbildung 10). Darüberhinaus waren in HH 44, 43 und 18 kDa großen Caspase-8 Spaltprodukte erkennbar, welches für eine Aktivierung der Caspase-8 durch S63845 sprach. In HuT-78 wurde stattdessen der Initiator der intrinsischen Apoptosewege Caspase-9, nachgewiesen durch die 36kDa Bande, aktiviert. Eine nicht näher zu erklärende Proteinbande von 35 kDa reagierte ebenfalls auf den Caspase-9-Antikörper. Da diese 35 kDa-Bande auch in unbehandelten Zellen zu sehen war, wurde sie nicht mit der Aktivierung von Caspase-9 in Verbindung gebracht.
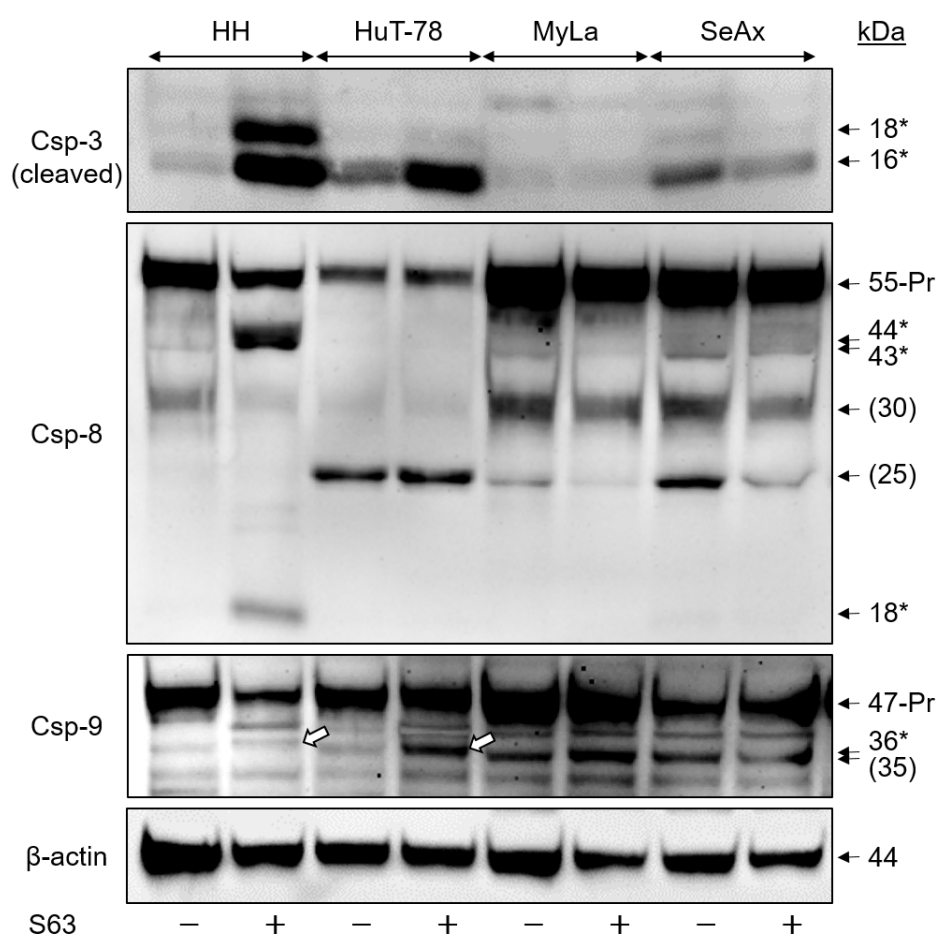
Abbildung 10. Überprüfung der Caspasenaktivierung durch S63845 auf Proteinebene der CTCL-Zellen mittels Westernblot. CTCL-Zellen wurden mit 1 µM S63845 für 48h behandelt. Die Blots zeigten die Caspase-3 (Spaltprodukte: 18, 16 kDa), Caspase-8 (Proform: 55 kDa; Spaltprodukte, 44, 43, 18 kDa) sowie Caspase-9 (Proform: 47 kDa; Spaltprodukt: 36 kDa). Spezifische Spaltprodukte sind durch (*) und die Spaltprodukte von Caspase-9 (36 kDa) sind durch weiße Pfeile gekennzeichnet.). Proteinbanden bei 30 und 25 kDa (Caspase-8) sowie 35 kDa (Caspase-9) sind keine spezifischen Banden. Das Housekeeping-Protein β-Actin (44 kDa) wurde als Ladekontrolle verwendet. Zwei unabhängige Serien von Proteinextrakten und Westernblot Analyse zeigten vergleichbare Ergebnisse. (Aus Sumarni et al., 2022)

3.4   Untersuchung der Rolle von PKCδ in der PEP005-induzierten Apoptose

Proapoptotische Aktivitäten wurden der aktiven PKCδ zugeschrieben. Das 78 kDa-Proform wird dabei zum 41 kDa größen, aktiven Endprodukt verarbeitet (Kato et al., 2009) (Zhao et al., 2012). In allen vier CTCL-Zelllinien führte PEP005 zur Aktivierung der PKCδ (Abbildung 12). Eine starke Reduzierung der 78 kDa-Proform, welche auf eine Weiterprozessierung dieser Proform hindeutet, war zu erkennen. Leider konnte dieses Endprodukt durch die in dieser Arbeit verwendeten Antikörper nicht detektiert werden. Desweiteren ließ sich die PKCδ-Prozessierung weder durch Pan-Caspase-Inhibitor QVD-Oph noch durch Antioxidant Vitamin E hemmen (Abbildung 11).
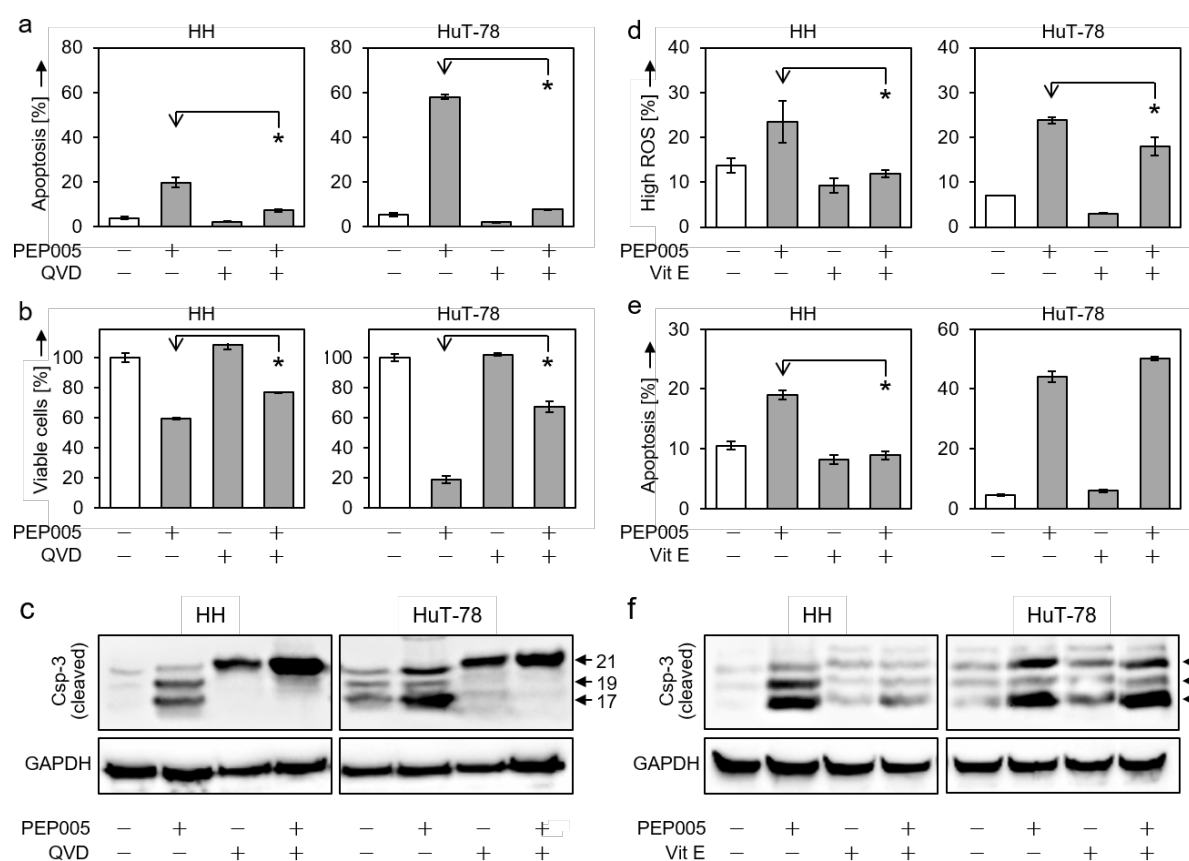
Abbildung 11. Hemmung des Effekts von PEP005 durch QVD-Oph und Vitamin E. Antagonistische Wirkung des 5 µM Pan-Caspase-Inhibitors QVD-Oph (QVD, a-c) und des 1 mM Antioxidants Vitamin E (Vit E, d-f) in HH- und HuT-78 bezüglich der Apoptoseinduktion (a,e, 48h), der Zellviabilität (b, 48h), der ROS-Bildung (d, 24h) und der Caspase-3-Prozessierung (c,f, 24h) wurde nachgewiesen. Mindestens zwei unabhängige Experimente zeigten vergleichbare Ergebnisse. Die statistische Signifikanz der Kombinationseffekte von PEP005 und QVD bzw. Vit E zu PEP005 allein wurde angegeben (*, p<0,05) (a,b,d,e). GAPDH (37 kDa) diente als Ladekontrolle. Zwei unabhängige Serien von Proteinextrakten und Westernblots ergaben vergleichbare Ergebnisse (c,f). (Aus Sumarni et al., 2021)

Die Rolle von PKCδ wurde mithilfe vom PKC-Inhibitor Bis-1 untersucht. Die entscheidende Rolle von PKCδ wurde dadurch hervorgehoben, dass die PEP005-induzierte Apoptose in HH und HuT-78 durch Bis-1 vollständig aufgehoben und die

Zellviabilität wiederhergestellt wurde (Abbildung 11). Während Bis-1 die PKCδ-Prozessierung selbst nicht beeinflusste, verhinderte es weitgehend die PEP005-vermittelte Prozessierung von Caspase-3, -8 und -9. Bis-1 inhibierte ebenfalls den PEP005-vermittelten Verlust von MMP (Abbildung 12g) und die ROS-Produktion (Abbildung 12h) in HuT-78.
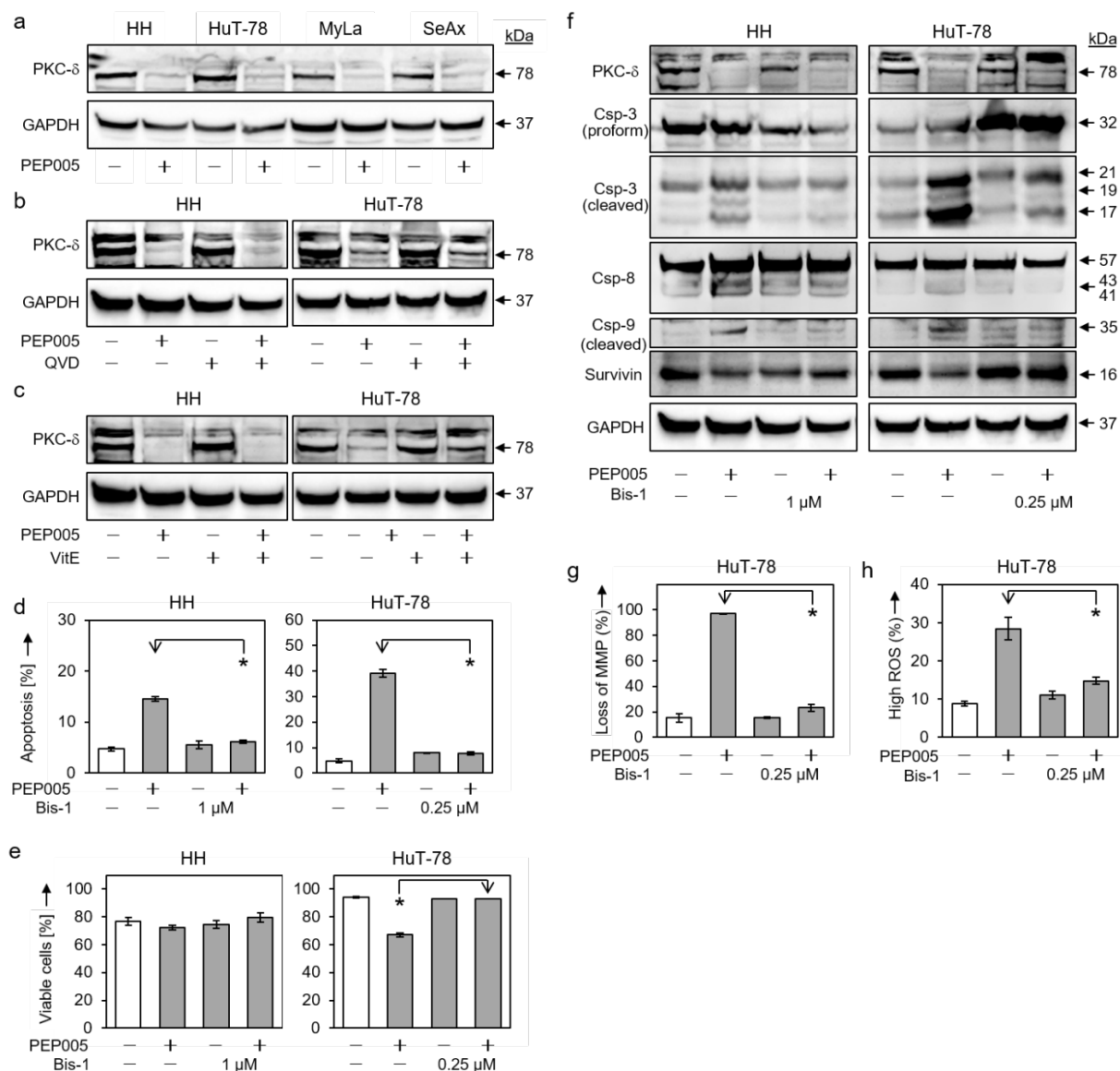

Abbildung 12. PEP005-Effekte auf PKCδ-Prozessierung in CTCL-Zellen. Die Blots zeigten den Effekt von 50 nM PEP005 (a) sowie in Kombination mit 5 µM QVD (b) oder mit 1 mM Vit E (c) auf die PKCδ-Expression in CTCL-Zellen. Das Housekeeping-Protein GAPDH (37 kDa) diente als Ladekontrolle. Zwei unabhängige Experimente zeigten vergleichbare Ergebnisse. Hemmung der Apoptose (d) und Wiederherstellung der Zellviabilität (e) in HH und HuT-78 durch 1h Vorbehandlung mit Bis-1 (HH: 1 µM, HuT-78: 0,25 µM) wurde nachgewiesen. Die Effekte von Bis-1 auf Apoptose-regulierende Proteine Caspase-3 (Proform, 32 kDa; Spaltprodukte, 21, 19, 17 kDa), Caspase-8 (Proform, 57 kDa, Spaltprodukte, 43/41 kDa) und Caspase-9 (Spaltprodukte, 35 kDa) wurden untersucht. Das Housekeeping-Protein GAPDH (37 kDa) diente als Ladekontrolle. Zwei unabhängige Experimente zeigten vergleichbare Ergebnisse. Der Effekt von Bis-1 auf den PEP005-induzierten MMP-Verlust (g) und ROS-Bildung (h) in HuT-78 wurde untersucht. Drei unabhängige Experimente zeigten vergleichbare Ergebnisse. Statistische Signifikanz zwischen PEP005 behandelten und PEP005 und Bis-1 behandelten Zellen ist angegeben (*, p<0,05). (Aus Sumarni et al., 2021)

3.5 Untersuchung der Effekte weiterer Inhibitoren von Bcl-Proteinen

Die Effekte von ABT-263 und ABT-737 zeigten ein anderes Muster. So ergab die 48-stündige Behandlung mit steigenden Konzentrationen von 0,01, 0,1 und 1 µM der beiden Substanzen eine hohe, dosisabhängige Sensitivität bei den S63845-resistenten Zelllinien MyLa und SeAx. Bei 1 µM ABT-263 lag die Apoptoserate bei MyLa und SeAx bei 73% bzw. 70%, während 43% und 35% Apoptose in HH und HuT-78 induziert wurde (Abbildung 14a). Bei MyLa und SeAx wurde die zur Kontrolle relative Zellviabilität durch auf 8% bzw. 7% gesenkt. Bei HH und HuT-78 betrug diese 60% bzw. 55% (Abbildung 14b). Der Unterschied zur Kontrolle war bei allen Zelllinien statistisch signifikant ($p < 0,05$).

Es zeigte sich weiterhin, dass die Bcl-2 Protein-Antagonisten sich gegenseitig in Kombinationen verstärkten. Bei allen Zelllinien wurden niedrigere Konzentrationen von ABTs (bis zu 0,1 µM) eingesetzt, bei HH 0,05 µM von S63845, um die gegenseitige Verstärkung besser zu erkennen. Gute Kombinationswirkungen wurden auf der Ebene der Zellviabilität erzielt. So wurden bei den sensitiven Zelllinien HH und HuT-78 die Wirkung von S63845 durch ABT-263 und ABT-737 weiter verstärkt. In HH sank die Zellviabilität weiter von 39% auf 20% bei Kombination von 0,05 µM S63845 mit 0,1 µM ABT-263 und auf 19% bei Kombination von 0,05 µM S63845 mit 0,1 µM ABT-737. Bei HuT-78 sank die Zellviabilität von 79% auf 24% bei Kombination von 1 µM S63845 mit 0,1 µM ABT-263 und auf 36% bei Kombination von 1 µM S63845 mit 0,1 µM ABT-73, wie auf der Abbildung 13 ersichtlich ist. Bei resistenten Zelllinien MyLa und SeAx hat die Kombination ebenfalls eine verstärkende Wirkung. So verringerte sich die Viabilität bei MyLa in Kombination von 1 µM S63845 mit 0,1 µM ABT-263 von 59% auf 21% und mit 0,1 µM ABT-737 von 87% auf 66%. Ähnlich zu MyLa wurde die Zellviabilität bei SeAx bei Kombination von 1 µM S63845 mit 0,1 µM ABT-263 von 19% auf 8% in Kombination mit 0,1 µM ABT-737 von 89% auf 39% reduziert. Auf der Ebene der Apoptoseinduktion waren die Wirkungen der Kombinationen im Vergleich zu den Einzelbehandlungen jedoch weniger ausgeprägt.

Um der Frage nachzugehen, ob diese Verstärkungen synergistisch waren, wurde eine Serie von Kombinationsexperimenten mit S63845 und ABT-263 durchgeführt. Mithilfe der Webanwendung SynergyFinder 3.0 von Ianevski et al (Manzano et al., 2018) wurde die Verstärkung der Effekte der Kombination auf die Verminderung der Zellviabilität sowie

die Apoptoseinduktion von Dr. Tobias Sinnberg berechnet. Bei HH und HuT-78 stellte sich die Kombination als weitgehend synergistisch (δ-Score > 10) fest (Abbildung 15). Bei MyLa und SeAx hingegen wurde bezüglich der Zellviabilität eine synergistische Beziehung mit δ > 10 für eine begrenzte Anzahl kombinierter Konzentrationen festgestellt. Auch für die Induktion der Apoptose lagen die δ-Werte bei diesen Zellen zwischen -10 und 10, was auf eine additive Wirkung hindeute.
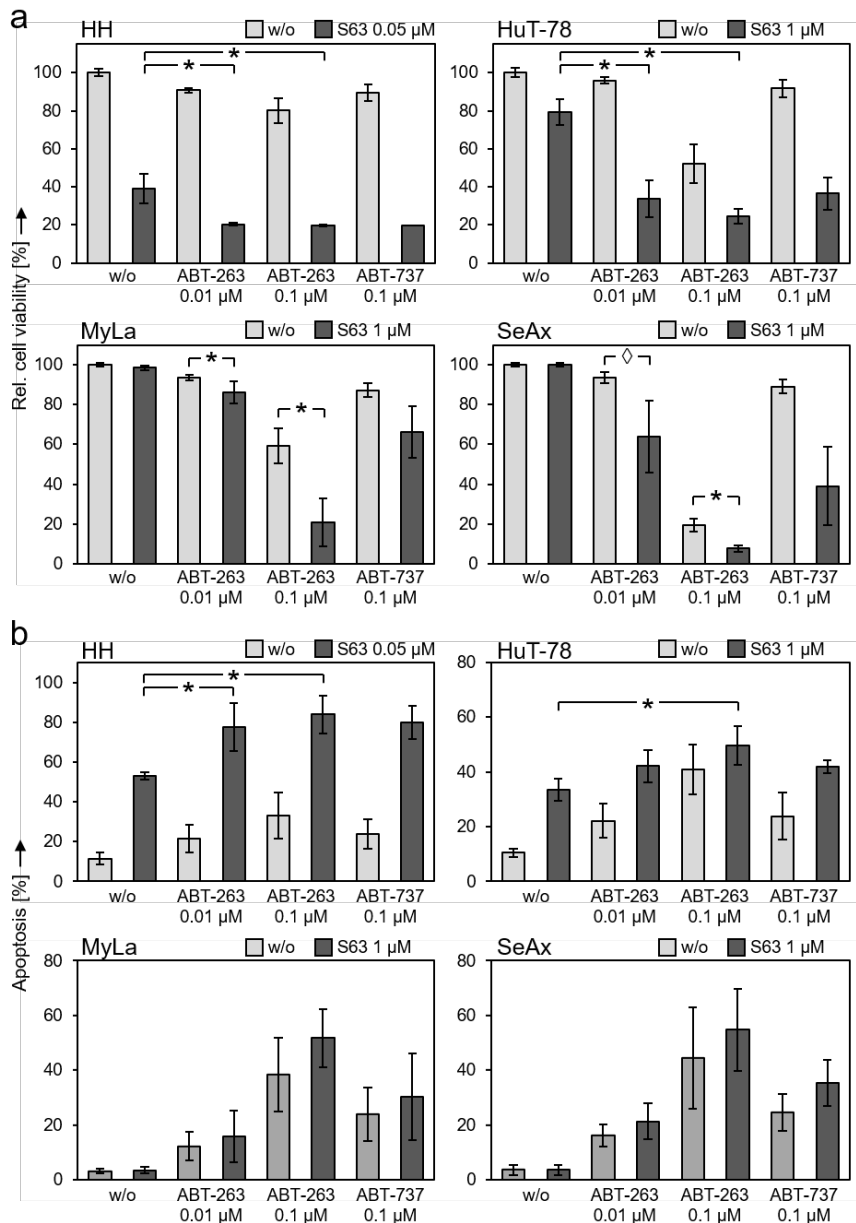
Abbildung 13. Effekte der Antagonisten-Kombinationen in CTCL-Zellen. Die Zellen wurden mit S63845 (HH: 0,05 μM; HuT-78, MyLa, SeAx: 1 μM, dunkle Balken), mit ABT-263 (0,01 und 0,1 μM), mit ABT-737 (0,1 μM) sowie mit Kombinationen behandelt. Zellviabilität (a) und Apoptoserate (b) wurden nach 48h bestimmt. Mindestens zwei unabhängige Experimente zeigten vergleichbare Ergebnisse. Statistische Signifikanz (*, p<0,05) oder statistische Trend (◊, p<0,1) sind angegeben. (Aus Sumarni et al., 2022)
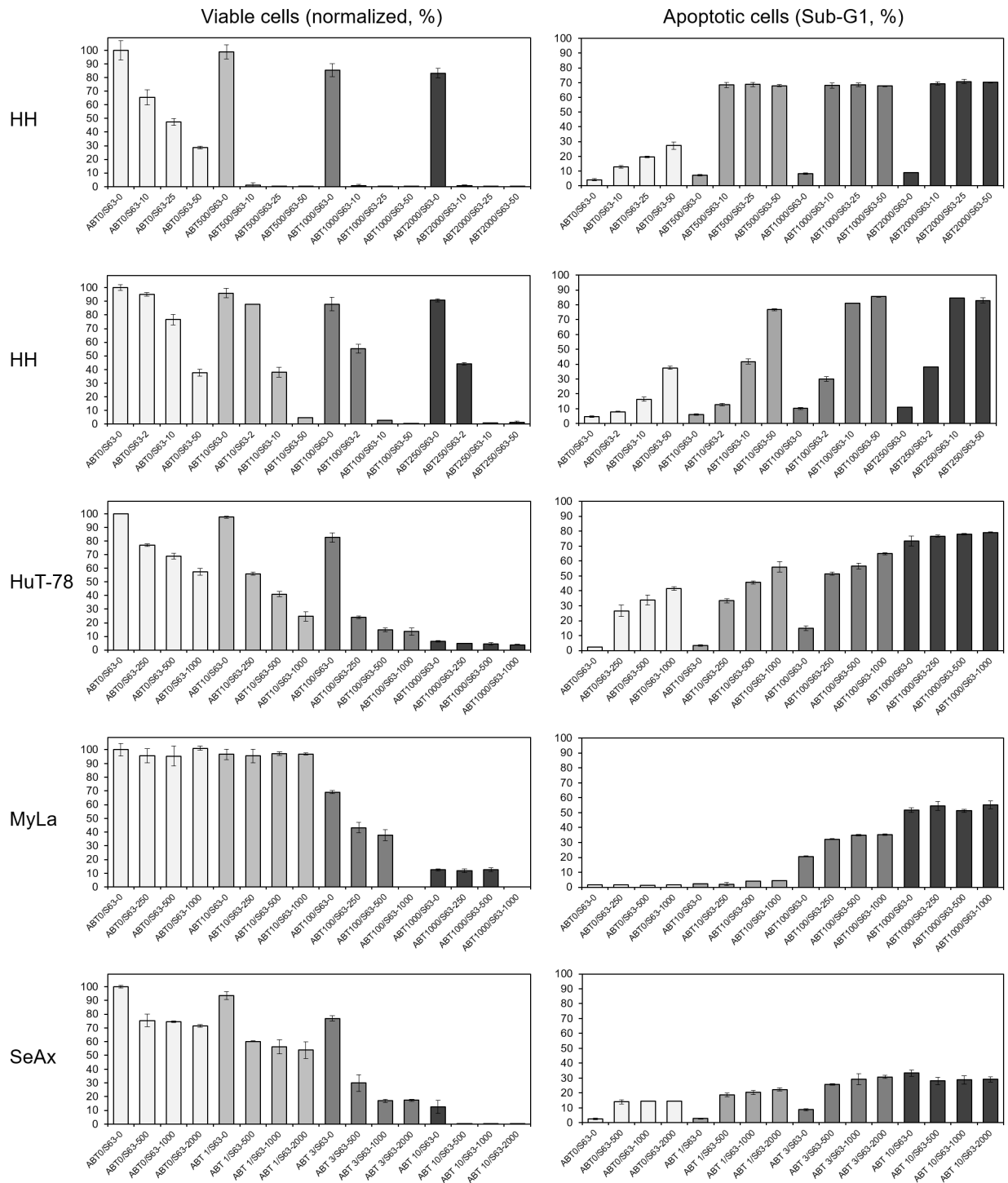
Abbildung 14. Effekte der Kombination von S63845 mit ABT-263 in CTCL-Zelllinien. Die Zellen wurden mit verschiedenen Konzentration der Inhibitoren (angegeben hinter den Namen der Inhibitoren in nM) für 24h inkubiert. Die Anzahl der viablen Zellen ist in Prozent relativ zu den unbehandelten Zellen und die Anzahl der apoptotischen Zellen in Prozent angegeben. (Aus Sumarni et al., 2022)

Die Auswirkung von S63845, ABT-263 und ABT-737 auf frisch isolierte PBMCs wurde ebenfalls untersucht. Die Proben stammten aus vier unabhängigen PBMC-Präparaten, die im gleichen Wachstumsmedium wie CTCL-Zellen kultiviert und 48 Stunden lang mit S63845 behandelt wurden. Es wurde eine vergleichbare proapotitische Wirkung

festgestellt. Die Zellviabilität lag nach 48-stündigen Behandlung mit 1 µM S63845 bei
31%, 17%, 6%, 4% und die Apoptoserate bei 54%, 49%, 43%, 41%. Ähnliche Effekte
wurden bei 1 µM ABT-263 und bei 1 µM ABT-737 beobachtet (Abbildung 16).

Abbildung 15. Berechnungen zum Synergismus der Antagonisten S63845 und ABT-263. Ausgehend von den Kombinationsexperimenten mit steigenden Konzentrationen für S63845 und ABT-263 wurde die Synergie in den vier CTCL-Zelllinien mithilfe des Programms SynergyFinder 3.0 berechnet. Delta-Scores >10 wiesen auf Synergismus hin, während Scores ≥-10 und ≤10 additive Effekte bedeuteten. (Aus Sumarni et al., 2022)
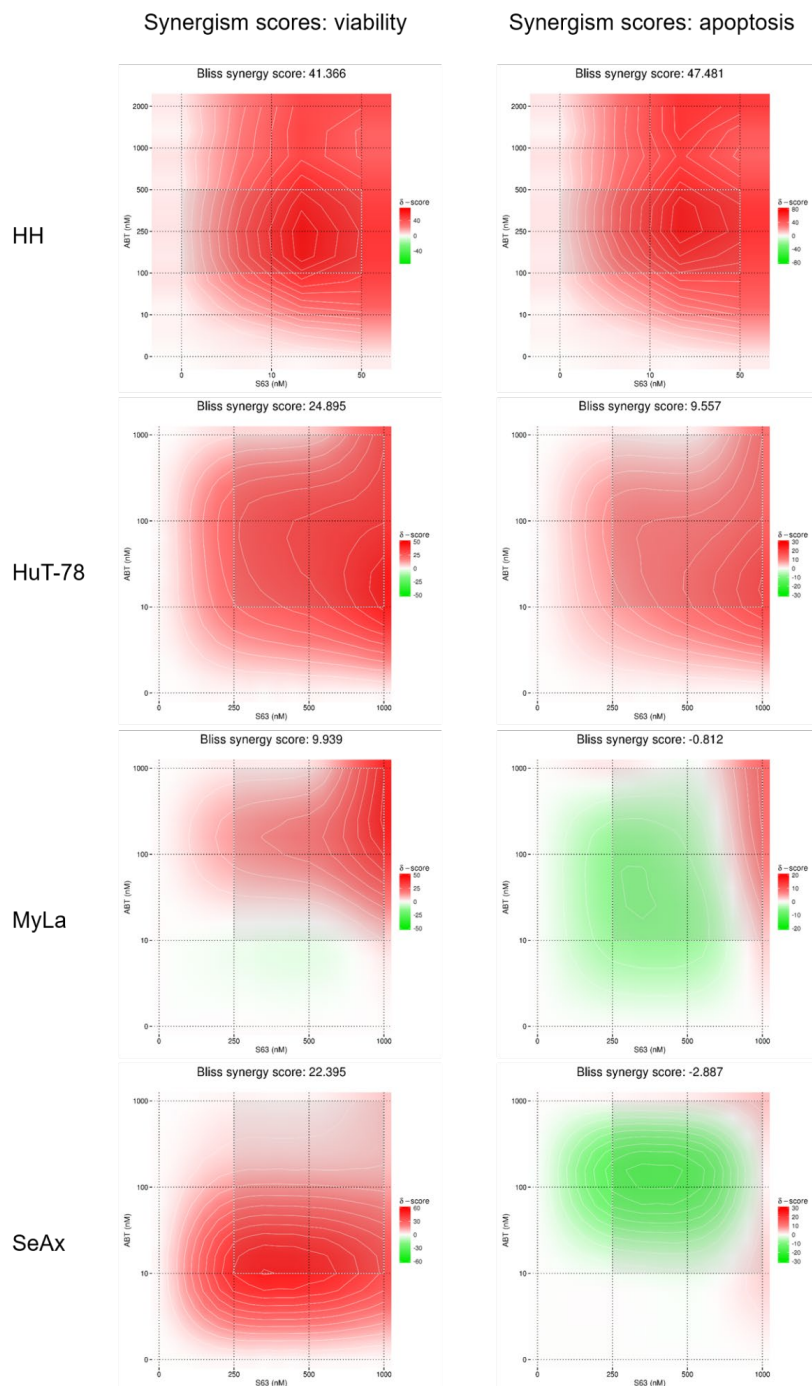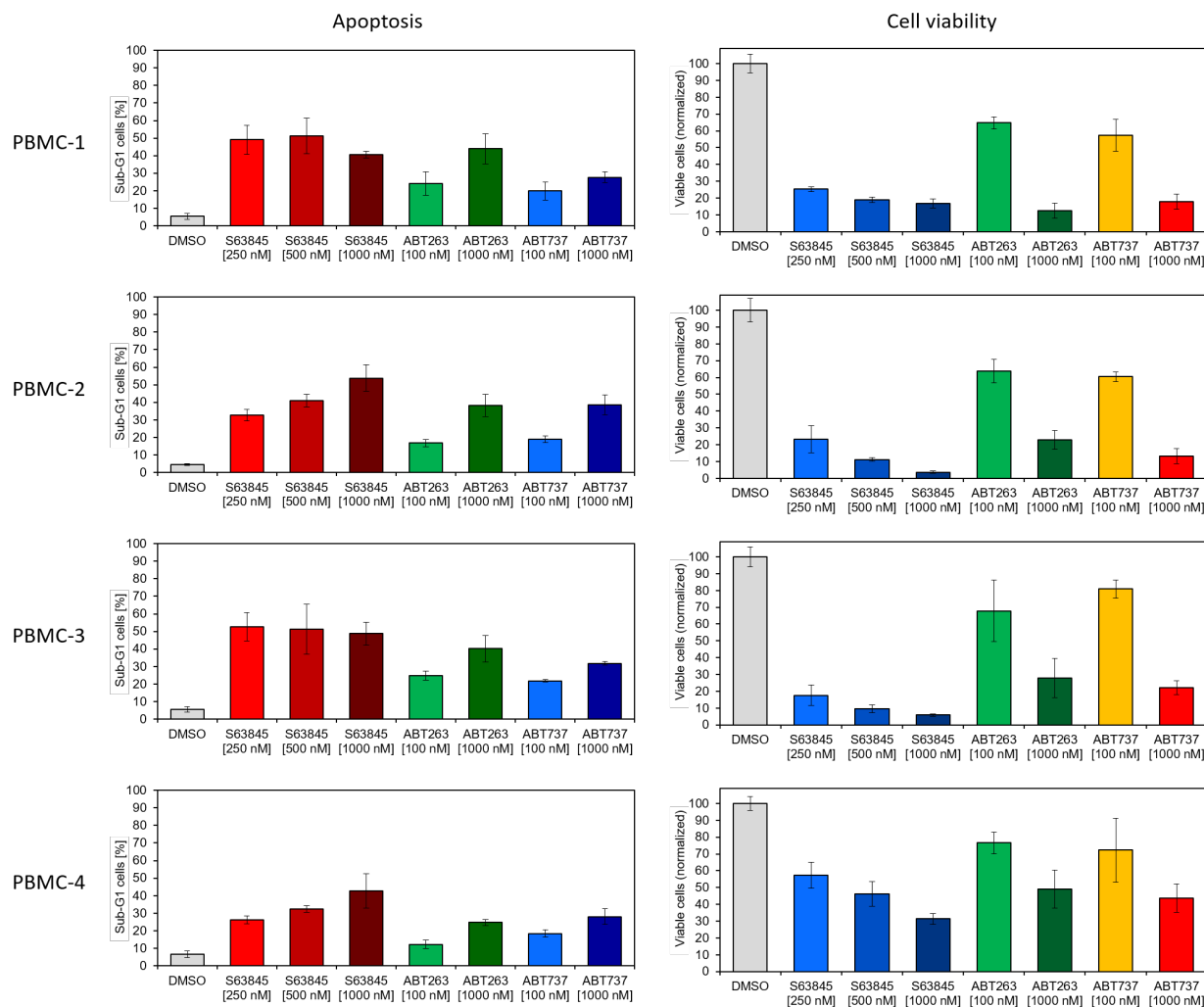
Abbildung 16. Effekte von S63845, ABT-263 und ABT-737 in PBMC. PBMC wurden aus dem Blut von vier gesunden Spendern isoliert, am selben Tag in 24-Wellenplatten ausgesät (100.000 Zellen pro Welle) und am nächsten Tag mit den Bcl-2 Protein-Antagonisten S63845, ABT-263 und ABT-737 in den angegebenen Konzentrationen behandelt. Die Kontrollzellen erhielten 2 µl DMSO. Nach 48h Inkubation wurde die Apoptoserate und die Zellviabilität bestimmt. (Aus Sumarni et al., 2022)

Um die unterschiedliche Sensitivität der CTCL-Zelllinien gegenüber den Bcl-2 Protein-Antagonisten besser zu verstehen, wurden vier antiapoptotischen Bcl-2 Proteine Mcl-1, Bcl-x$_L$, Bcl-2 und Bcl-w durch Westernblot untersucht (Abbildung 17). Dabei zeigte sich, dass Mcl-1 in den S63845-resistenten Zellen schwächer als in den sensitiven Zellen exprimiert wurden. Die Expression von Bcl-2 und Bcl-x$_L$ war in HH am schwächsten und in HuT-78 am stärksten. Der auffälligste Unterschied zwischen resistenten und sensitiven Zellen wurde bei Bcl-w festgestellt. Dieses Protein fehlte vollständig in HH und HuT-78, während es in MyLa und SeAx stark exprimiert wurde.

Abbildung 17. S63845-Effekt auf die Bcl-2 Proteine in CTCL-Zelllinien. Die Zellen wurden nach 48h Behandlung mit 1 µM S63845 (+) bzw. 1 µl DMSO (-) untersucht. Auf den Blots sind Mcl-1 (40 kDa), Bcl-x$_L$ (26 kDa), Bcl-2 (28 kDa) und Bcl-w (16 kDa) dargestellt. Das Housekeeping-Protein β-Actin (44 kDa) wurde als Ladekontrolle verwendet. Drei unabhängige Experimente zeigten vergleichbare Ergebnisse. (Aus Sumarni et al., 2022)

4 Diskussion

4.1 Interpretation der Ergebnisse und Einbettung der Ergebnisse in den bisherigen Forschungsstand
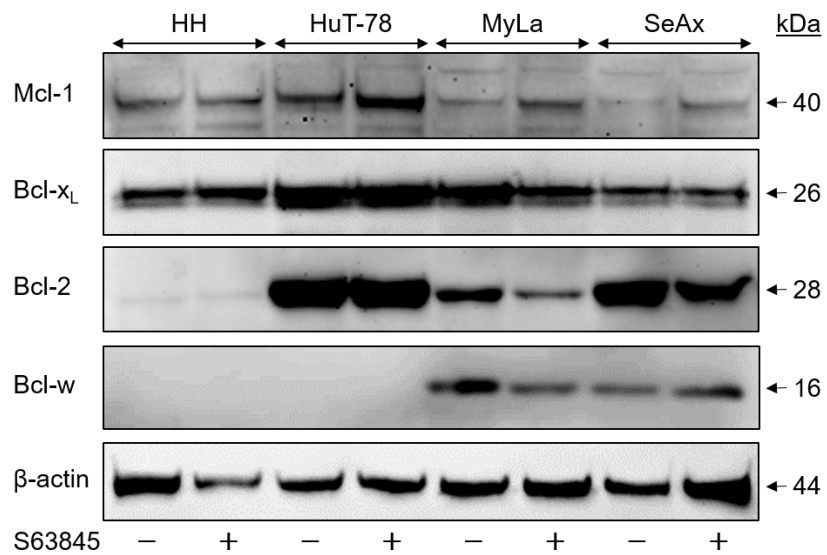
Im Rahmen dieser Arbeit wurden die Substanzen PEP005, S63845 und DKP-071 auf ihre proapoptotische Wirkung in CTCL-Zellen untersucht.

Gegenüber PEP005 zeigten sich bei zwei von vier Zelllinien, HH und HuT-78, eine signifikante Apoptoseinduktion sowie eine verringerte Zellviabilität und Zellproliferation. Die apoptotische Wirkung hing dabei nicht von der Herkunft der Zellen ab. So zeigte sich gegenüber PEP005 jeweils eine von den von MF- oder Sézary-Patienten stammenden Zelllinien entweder sensitiv (HH, HuT-78) oder resistent (MyLa, SeAx). Die Wirkkonzentration bei HH und HuT-78 lag im relativ moderaten Bereich von 50 nM. Dies wurde ebenfalls bei myeloischen Leukämiezellen, Melanomzellen sowie Darmkrebs-Zelllinien berichtet (Gillespie, et al. 2004) (Benhadji et al., 2008) (D. Wang & Liu, 2018) (Cozzi et al., 2006) (Hampson et al., 2005).

PEP005 führte zu einer vollständigen Prozessierung der Initiator Caspase-8 bei allen Zelllinien, während die vollständige Prozessierung der Caspase-3 bei sensitiven Zelllinien festgestellt wurde. Bei resistenten Zelllinien endete die Caspase-3-Prozessierung beim 21 kDa-Zwischenprodukt. In CTCL scheint Caspase-8 die Caspase-3-Aktivierung bis zum 21 kDa-Zwischenprodukt zu vermitteln, während die weitere Prozessierung der Caspase-3 bis zum aktiven Endprodukt einem Selbstprozessierungsmechanismus unterliegen soll. Diese Beobachtung wurde ebenfalls von Liu berichtet (Liu et al., 2005). Die Caspasen-Abhängigkeit der PEP005-vermittelten Apoptose wurde weiterhin mittels Pan-Caspase-Inhibitors (QVD-OPh) belegt, der die Apoptoserate stark reduzierte.

Zwischen PEP005-Sensitivität und der Expression und Regulation von c-FLIP und XIAP bestand ein signifikanter Zusammenhang. Die starke Expression von c-FLIP und XIAP in den resistenten Zelllinien, welche im Gegensatz zu den sensitiven Zelllinien nicht durch PEP005 zu unterdrucken war, deutete darauf hin, dass die konstitutiv hohe Expression von XIAP in resistenten Zellen die Aktivität und Aktivierung von Caspase-3 inhibierte. Diese entscheidende Rolle von Caspase-Antagonisten in CTCL-Zellen wurde in anderen Arbeiten beschrieben. So wurde c-FLIP durch SAHA und nichtsteroidales Antirheumatika

(NSAIDs), während XIAP durch SAHA und Pentoxifyllin herunterreguliert (Gahlot et al., 2010) (Al-Yacoub et al., 2012) (Braun et al., 2012).

Ein wesentlicher Schritt in den intrinsischen Apoptosewegen ist unter anderem der Verlust des MMPs (Tait & Green, 2010). In dieser Arbeit wurde ein signifikanter PEP005-vermittelter MMP-Verlust bei hoch sensitiven HuT-78 festgestellt. Bei PEP005-sensitiver HH war der MMP-Verlust nicht signifikant. Dass MMP-Verlust keinen Zusammenhang mit der PEP005-vermittelten Apoptose hat, wurde ebenfalls bei Melanomzellen beobachtet (Gillespie et al., 2004). PEP005 führte in CTCL zur erhöhten ROS-Produktion, allerdings sowohl in sensitiven als auch in resistenten CTCL-Zelllinien. Diese Ergebnisse wiesen darauf hin, dass ROS allein nicht ausreichend war, um Apoptose in resistenten Zellen zu induzieren und daher als zusätzlicher Promotor der PEP005-vermittelten Apoptose dienen sollte.

Die proapopotische Rolle von PKCδ bei PEP005-vermittelten Effekte wurde bisher in Leukämie-, Darmkrebs- und Melanomzellen nachgewiesen (Benhadji et al., 2008) (Cozzi et al., 2006). Die Aktivierung der PKCδ ließ sich durch die Prozessierung seiner 78 kDa-Proform in die aktive 41 kDa katalytische Domäne erkennen (Kato et al., 2009). In dieser Arbeit konnte ein PEP005-vermittelter Verlust der 78 kDa-Proform von PKCδ ebenfalls nachgewiesen werden, welcher auf die Aktivierung der PKCδ hindeutete. Anders als in glatten Muskelzellen, in denen Caspase-3 für die Aktivierung der PKCδ eine wichtige Rolle spielte (Kato et al., 2009), war die PEP005-vermittelte PKCδ-Aktivierung Caspase-unabhängig und fand sich sowohl in sensitiven als auch in resistenten CTCL-Zelllinien. Die PEP005-vermittelte PKCδ-Aktivierung in CTCL folgt somit einem anderen Mechanismus als dem in glatten Muskelzellen.

Die Befunde der vorliegenden Arbeit legen nahe, dass die PEP005-vermittelten Effekte eine vorgeschaltete PKCδ-Aktivierung bedürfen. Dies wurde durch Einsatz von Bis-1, einem Inhibitor der aktivierten PKC klar belegt. Die übergeordnete Rolle von PKCδ bei der PEP005-vermittelten Wirkung in CTCL-Zellen wurde dadurch deutlich, dass Bis-1 zwar nicht die Prozessierung von PKCδ selber aber alle nachgeschalteten Effekte wie Apoptoseinduktion, Caspase-3-Aktivierung, Induktion von ROS-Produktion, Verlust von MMP und Verlust der Zellviabilität inhibierte. Die aktive PKCδ scheint daher ein Hauptregulator bei der PEP005-vermittelten Apoptose in CTCL zu sein. Die Identifizierung von PKCδ als ein potenzielles therapeutisches Ziel beim CTCL ist einer der Hauptbefunde der vorliegenden Arbeit.

Die Substanz S63845 sowie andere BH3-Mimetika wurden entwickelt, um die Aktivität von proapoptotischen BH3-only-Proteinen nachzuahmen. Durch die Bindung an die antiapoptotischen Bcl-2 Proteine (Townsend et al., 2021) wird die Apoptoseresistenz überwunden. Während ABT-737 und ABT-263 die antiapoptotischen Proteine Bcl-2, Bcl-x_L und Bcl-w hemmt (Tse et al., 2008) (Oltersdorf et al., 2005), greift S63845 selektiv das antiapoptotische Protein Mcl-1 an (András Kotschy et al., 2016). Ähnlich wie bei PEP005 ergab sich bei S63845 eine klare Aufteilung in zwei vollständig resistente und zwei sensitive Zelllinien, die nicht mit der Herkunft der Zellen korrelierte. Im Gegensatz zu der unterschiedlichen Sensitivität der CTCL-Zelllinien hatten sich die Mehrzahl der Zelllinien von DLBCL, Burkitt-Lymphom oder primären Ergusslymphom als sensitiv gegenüber S63845 gezeigt (Klanova et al., 2022) (Manzano et al., 2018). Die meisten Zelllinien der akuten myeloischen Leukämie (AML) und des Multiplen Myeloms zeigten hohe Sensitivität hinsichtlich des Zellviabilitätsverlusts. Die Substanz S63845 vermittelte eine Caspase-3-Aktivierung in den sensitiven CTCL-Zelllinien. Desweiteren wurde in HH eine Caspase-8- und in HuT-78 eine Caspase-9-Prozessierung festgestellt. Dieses Ergebnis deutete darauf hin, dass S63845 in der Lage ist, sowohl extrinsische als auch intrinsische Apoptose-Signalwege zu aktivieren. Eine S63845-vermittelte Aktivierung von Caspase-3 wurde ebenfalls bei DLBCL- (Ewald et al., 2019), Burkitt-Lymphom- (Klanova et al., 2022) und AML- (Smith et al., 2020) Zellen berichtet. Neben Caspase-3-Aktivierung führte S63845 bei sensitiven Zelllinien zu einem signifikanten MMP-Verlust sowie zur erhöhten ROS-Produktion. Diese wurden ebenfalls bei DLBCL- (Ewald et al., 2019) und AML- (Smith et al., 2020) Zellen beobachtet .

Desweiteren hatten MyLa und SeAx, die gegenüber S63845 resistent waren, eine hohe Sensitivität, während HH und HuT-78, die gegenüber S63845 sensitiv waren, mäßige Sensitivität gegenüber ABT-263 und ABT-737. Es ließen sich somit in dieser Arbeit zwei CTCL-Zelllliniengruppen basierend auf deren Sensitivität auf die untersuchten BH-3 Mimetika unterscheiden: Zelllinien mit hoher Sensitivität gegenüber S63845 und mäßiger Sensitivität gegenüber ABTs oder Zelllinien mit niedriger Sensitivität gegenüber S63845 und hoher Sensitivität gegenüber ABTs.

In dieser Arbeit wurde gezeigt, dass Mcl-1 in den S63845-resistenten CTCL-Zelllinien schwächer exprimiert war, während die Expression von Bcl-2 und Bcl-x_L in der hochsensitiven HH am schwächsten war. Der auffälligste Unterschied wurde bei Bcl-w festgestellt, welches ausschließlich in CTCL-Zellen mit S63845-Resistenz und hoher Empfindlichkeit gegenüber ABT-263 und ABT-737 exprimiert wurde. Das

Zusammenspiel von verschiedenen antiapoptotischen Bcl-2 Proteinen scheint daher eine entscheidende Rolle bei der Sensitivität der CTCL gegenüber den verschiedenen BH3-Mimetika zu haben. So erwies sich die Expression von Bcl-w als stark genug, um die durch den Mcl-1-Inhibitor vermittelte Apoptoseinduktion zu hemmen, was wiederum mit einer erhöhten Sensitivität gegenüber ABT-263 und ABT-737 verbunden war. Umgekehrt dazu war das Überleben der CTCL-Zellen bei fehlender Bcl-w Expression besonders stark von Mcl-1 abhängig. Dies resultierte in einer hohen Sensitivität gegenüber S63845 sowie in der geringen Sensitivität gegenüber ABT-263 und ABT-737. Die Stärke der Expression von Bcl-2 und Bcl-x_L korrelierte sich in umgekehrter Weise mit der Sensitivität gegenüber der Mcl-1 Inhibition.

Die wichtige Rolle von Bcl-w bei der Tumorentstehung wurde ebenfalls bei B-Zell-Lymphomen, Burkitt-Lymphomen und DLBCL beschrieben (Adams et al., 2017). Die Herunterregulierung von Bcl-w in DLBCL-Zelllinien führte jedoch nicht zu einer Sensitivierung für S63845 (Diepstraten et al., 2020). Desweiteren hatten frühere Arbeiten einen Zusammenhang zwischen der S63845-Resistenz und der Bcl-x_L Expression gezeigt. So wurde eine hohe Bcl-x_L Expression bei S63845-sensitiven Lymphomzellen beobachtet. Dies deutete drauf hin, dass Bcl-x_L bei manchen Zelltypen die Hemmung von Mcl-1 funktionell kompensieren kann (A. Kotschy et al., 2016), vergleichbar wie es hier für Bcl-w beobachtet wurde.

BH3-Mimetika sind vielversprechende Kandidaten für den klinischen Einsatz bei Krebspatienten (Townsend et al., 2021). Aus diesem Grund wurde in dieser Arbeit die Sensitivität von PBMCs auf diese Substanzen untersucht. Entgegen der Erwartung wurde bei PBMC ebenfalls eine hohe Sensitivität gegenüber S63845, ABT-263 sowie ABT-737 bezüglich der Induktion von Apoptose und des Verlustes der Viabilität festgestellt. Aufgrund des begrenzten Umfangs dieser Untersuchungen wurde hier nicht näher darauf eingegangen, ob diese Effekte bei PBMCs *ex-vivo* ähnliche Effekte in der *in-vivo*-Umgebung widerspiegeln. So bleibt noch zu klären, ob die Überlebenssignale der im Wachstumsmedium kultivierten Zellen denen im Gewebe entsprechen. Diese Fragen könnten mit Tierversuchen und/oder in der klinischen Prüfung geklärt werden. Frühere Arbeiten bestätigten die gute Verträglichkeit von S63845 bei Mäusen (A. Kotschy et al., 2016)..

Bei dem Indirubin-Derivat DKP-071 zeigte sich eine generelle Sensitivität der CTCL-Zelllinien. Die Wirkmechanismen wurden von Dr. Marwan Soltan untersucht (Sumarni,U als Zweitautorin). Es stellte sich heraus, dass das Indirubin-Derivat die extrinsische

Apoptose-Kaskade über Caspase-8 und Caspase-3 durch Herunterregulierung der Caspase-antagonistischen Proteine c-FLIP und XIAP aktiviert. Desweiteren wurde ein starker ROS-Anstieg als frühe Reaktion auf die Behandlung mit DKP-071 beobachtet (Soltan et al., 2019). Die antioxidative Vorbehandlung bewies weiterhin die entscheidende Rolle von ROS, die allen anderen proapoptotischen Effekten vorangestellt war. ROS scheint als ein hochaktiver proapoptotischer Signalweg bei CTCL zu sein, welcher durch ein Indirubin-Derivat effizient aktiviert wurde (Soltan et al., 2019).

4.2 Klinische Wirksamkeit und zukünftige Forschung

PEP005 wurde als Hydrogel mit dem Handelsnamen Picato® zur topischen Behandlung von aktinischen Keratosen bei Erwachsenen von der Food and Drug Administration (FDA) und der Europäischen Arzneimittel-Agentur (EMA) in 2012 zugelassen. Aus der Auswertung von zwölf Studien zur Ermittlung vom Zusammenhang zwischen der Anwendung von Ingenolmebutat und Hautkrebs durch die Zulassungsbehörde Health Canada ergaben sich jedoch Hinweise auf neu induzierten Hautkrebs durch Ingenolmebutat. Ebenfalls hat die EMA diese Sicherheitsfrage geprüft und kam im April 2020 zu der Schlussfolgerung, dass Ingenolmebutat das Hautkrebsrisiko erhöhte und dass die Risiken den Nutzen überwogen. Am 11.02.2020 zog der Hersteller das Produkt freiwillig vom Markt der Europäischen Union zurück (Picato). Die gewonnenen Erkenntnisse aus dieser Arbeit tragen dazu bei, die Wirkung von PEP005 in Tumorzellen besser zu verstehen. PEP005 zeigte sich durch seine proapoptotische Wirkung als potentieller Kandidat für CTCL-Therapie.

Die Substanz ABT-263 zeigte in Kombination mit ABT-199 in einer Phase-I-Studie bei Patienten mit ALL oder lymphoblastischem Lymphom eine gute Wirksamkeit (Pullarkat et al., 2021). Weiterhin werden derzeit zwei Mcl-1-Inhibitoren, PRT1419 (Prelude, 2022) und S64315 (MIK665), in klinischen Studien Phase I/II für hämatologische Krebsarten untersucht. Der letztere ist mit S63845 chemisch verwandt und hat vergleichbare Aktivität (Szlávik et al., 2019). Derzeit befindet sich S64315 in einer klinischen Studie der Phase I für AML (H. Wang et al., 2021). Insgesamt deuteten unsere Ergebnisse auf ein vielversprechendes Ansprechen von CTCL-Zellen auf BH3-Mimetika hin. Die CTCL-Zelllinien waren hoch sensitiv entweder gegenüber dem Mcl-1-Inhibitor S63845 oder gegenüber den Bcl-2/Bcl-x$_L$/Bcl-w-Inhibitoren ABT-263 und ABT-737. Diese Ergebnisse werfen ein besseres Licht auf die besondere Rolle der antiapoptotischen Bcl-2 Proteine bei der Apoptoseregulierung in CTCL-Zellen. Darüberhinaus können therapeutische

Strategien in Betracht gezogen werden, die entweder auf Mcl-1-Inhibitoren oder auf ABT-263 oder einer Kombination aus beiden basieren. Die Bcl-w Expressionstärke könnte als möglicher Biomarker dienen, um die richtigen Patientengruppe zu erkennen.

Die ROS-Produktion wurde inzwischen als ein wichtiger zellulärer Schritt in der Apoptoseinduktion. Eine durch das Indirubin-Derivat DKP-071 ausgelöste Signalkaskade von ROS, Caspase-Antagonisten und der Aktivierung der extrinsischen Apoptosewege wurde bei CTCL nachgewiesen (Soltan et al., 2019).

Zusammenfassend lässt sich sagen, dass in dieser Arbeit die proapoptotische Wirkung des PKCδ Aktivators PEP005, des Mcl-1-Inhibitors S63845 sowie des Indirubin-Derivats DKP-071 in CTCL-Zelllinien nachgewiesen werden konnte. Um eine klinische Entwicklung weiter voranzutreiben, wären die Untersuchung von *ex-vivo*-Patientenproben und *in-vivo*-Tierversuche die nächsten Schritte. Wenn eine vergleichbare Effektivität in Patientenproben gegeben ist, wird die nächste große Herausforderung darin bestehen, Patienten zu identifizieren, die von diesen Strategien profitieren können.

5   Schlussfolgerungen

Zu den Hauptzielen der Krebstherapie gehören unter anderem die Eliminierung von Tumorzellen durch Apoptoseinduktion sowie die Überwindung der Apoptoseresistenz. Therapieansätze für CTCL-Patienten, die auf einer Apoptoseinduktion basieren, befinden sich bereits in der klinischen Anwendung. Jedoch sind die aktuell vefügbaren Therapien häufig unzureichend wirksam und die apoptotischen Signalwege in CTCL werden noch unzureichend verstanden.

In dieser Arbeit stellte der PKCδ Aktivator PEP005 als neuer potentieller Therapieansatz für CTCL dar. Die proapoptotische Wirkung von PEP005 wurde in zwei von vier CTCL-Zelllinien gezeigt, deren Mechanismus mit der Aktivierung der PKCδ und darauffolgenden Aktivierung von Caspase-3 verbunden war. Auf der Grundlage unserer *in-vitro*-Daten zeigte sich bei den resistenten Zelllinien neben der Expression von p53 und p21 ebenfalls eine verstärkte Expression von c-FLIP und XIAP. Diese molekularen Merkmale könnten möglicherweise als potenzielle Kandidaten für die Stratifizierung von Patienten dienen.

Bei der Untersuchung der Sensitivität der CTCL-Zellen auf BH-3 Mimetika zeigten zwei von vier CTCL-Zelllinien eine hohe Sensitivität gegenüber dem Mcl-1-Inhibitor S63845, während die zwei anderen Zelllinien mit geringer Sensitivität für S63845 eine hohe Sensitivität gegenüber den für Bcl-2, Bcl-w und Bcl- x_L spezifischen Inhibitoren ABT-263 und ABT-737 besaßen. Die S63845-resistenten Zelllinien zeigten eine schwächere Expression von Bcl-2 und Bcl-x_L sowie fehlende Bcl-w Expression. Die antiapoptotischen Bcl-2 Proteine scheinen bei der Apoptoseregulierung in CTCL eine besondere Rolle zu spielen. Dabei könnten sowohl der Mcl-1-Inhibitor S63845 als auch die Bcl-2/Bcl-x_L/Bcl-w-Inhibitoren ABT-263 und ABT-737 als potentielle Therapieansätze in Betracht gezogen werden. Die Bcl-w Expression könnte als Biomarker genutzt werden, um Patienten mit Therapieansprechen auf S63845 zu erkennen.

Die dritte untersuchte Substanz Indirubin-Derivat DKP-071 zeichnete sich in dieser Arbeit durch die effiziente Induktion der Apoptose bei den CTCL-Zellen und könnte daher als mögliche therapeutische Strategie für das CTCL angesehen werden.

Literaturverzeichnis

1.Adams CM, Kim AS, Mitra R, Choi JK, Gong JZ, Eischen CM. BCL-W has a fundamental role in B cell survival and lymphomagenesis. The Journal of Clinical Investigation. 2017;127(2):635-50.

2.Agar NS, Wedgeworth E, Crichton S, Mitchell TJ, Cox M, Ferreira S, Robson A, Calonje E, Stefanato CM, Wain EM, Wilkins B, Fields PA, Dean A, Webb K, Scarisbrick J, Morris S, Whittaker SJ. Survival outcomes and prognostic factors in mycosis fungoides/Sézary syndrome: validation of the revised International Society for Cutaneous Lymphomas/European Organisation for Research and Treatment of Cancer staging proposal. J Clin Oncol. 2010;28(31):4730-9.

3.Al-Yacoub N, Fecker LF, Möbs M, Plötz M, Braun FK, Sterry W, Eberle J. Apoptosis induction by SAHA in cutaneous T-cell lymphoma cells is related to downregulation of c-FLIP and enhanced TRAIL signaling. J Invest Dermatol. 2012;132(9):2263-74.

4.Bagherani N, Smoller BR. An overview of cutaneous T cell lymphomas. F1000Res. 2016;5.

5.Benhadji KA, Serova M, Ghoul A, Cvitkovic E, Le Tourneau C, Ogbourne SM, Lokiec F, Calvo F, Hammel P, Faivre S, Raymond E. Antiproliferative activity of PEP005, a novel ingenol angelate that modulates PKC functions, alone and in combination with cytotoxic agents in human colon cancer cells. British Journal of Cancer. 2008;99(11):1808-15.

6.Berger A, Quast SA, Plötz M, Hein M, Kunz M, Langer P, Eberle J. Sensitization of melanoma cells for death ligand-induced apoptosis by an indirubin derivative--Enhancement of both extrinsic and intrinsic apoptosis pathways. Biochem Pharmacol. 2011;81(1):71-81.

7.Blažević T, Heiss EH, Atanasov AG, Breuss JM, Dirsch VM, Uhrin P. Indirubin and Indirubin Derivatives for Counteracting Proliferative Diseases. Evid Based Complement Alternat Med. 2015;2015:654098.

8.Braun FK, Al-Yacoub N, Plötz M, Möbs M, Sterry W, Eberle J. Nonsteroidal anti-inflammatory drugs induce apoptosis in cutaneous T-cell lymphoma cells and enhance their sensitivity for TNF-related apoptosis-inducing ligand. J Invest Dermatol. 2012;132(2):429-39.

9.Cong H, Xu L, Wu Y, Qu Z, Bian T, Zhang W, Xing C, Zhuang C. Inhibitor of Apoptosis Protein (IAP) Antagonists in Anticancer Agent Discovery: Current Status and Perspectives. Journal of Medicinal Chemistry. 2019;62(12):5750-72.

10.Cozzi SJ, Parsons PG, Ogbourne SM, Pedley J, Boyle GM. Induction of senescence in diterpene ester-treated melanoma cells via protein kinase C-dependent hyperactivation of the mitogen-activated protein kinase pathway. Cancer Res. 2006;66(20):10083-91.

11.de Vos S, Leonard JP, Friedberg JW, Zain J, Dunleavy K, Humerickhouse R, Hayslip J, Pesko J, Wilson WH. Safety and efficacy of navitoclax, a BCL-2 and BCL-X(L) inhibitor, in patients with relapsed or refractory lymphoid malignancies: results from a phase 2a study. Leuk Lymphoma. 2021;62(4):810-8.

12.Diepstraten ST, Chang C, Tai L, Gong J-n, Lan P, Dowell AC, Taylor GS, Strasser A, Kelly GL. BCL-W is dispensable for the sustained survival of select Burkitt lymphoma and diffuse large B-cell lymphoma cell lines. Blood Advances. 2020;4(2):356-66.

13.Dobos G, Pohrt A, Ram-Wolff C, Lebbé C, Bouaziz JD, Battistella M, Bagot M, de Masson A. Epidemiology of Cutaneous T-Cell Lymphomas: A Systematic Review and Meta-Analysis of 16,953 Patients. Cancers (Basel). 2020;12(10).

14.Dummer R, Vermeer MH, Scarisbrick JJ, Kim YH, Stonesifer C, Tensen CP, Geskin LJ, Quaglino P, Ramelyte E. Cutaneous T cell lymphoma. Nat Rev Dis Primers. 2021;7(1):61.

15.Ewald L, Dittmann J, Vogler M, Fulda S. Side-by-side comparison of BH3-mimetics identifies MCL-1 as a key therapeutic target in AML. Cell Death & Disease. 2019;10(12):917.

16.Gahlot S, Khan MA, Rishi L, Majumdar S. Pentoxifylline augments TRAIL/Apo2L mediated apoptosis in cutaneous T cell lymphoma (HuT-78 and MyLa) by modulating the expression of antiapoptotic proteins and death receptors. Biochem Pharmacol. 2010;80(11):1650-61.

17.Gazdar AF, Carney DN, Bunn PA, Russell EK, Jaffe ES, Schechter GP, Guccion JG. Mitogen Requirements for the In Vitro Propagation of Cutaneous T-Cell Lymphomas. Blood. 1980;55(3):409-17.

18.Gillespie SK, Zhang XD, Hersey P. Ingenol 3-angelate induces dual modes of cell death and differentially regulates tumor necrosis factor-related apoptosis-inducing ligand-induced apoptosis in melanoma cells. Mol Cancer Ther. 2004;3(12):1651-8.

19.Gong JN, Khong T, Segal D, Yao Y, Riffkin CD, Garnier JM, Khaw SL, Lessene G, Spencer A, Herold MJ, Roberts AW, Huang DCS. Hierarchy for targeting prosurvival BCL2 family proteins in multiple myeloma: pivotal role of MCL1. Blood. 2016;128(14):1834-44.

20.Gootenberg JE, Ruscetti FW, Mier JW, Gazdar A, Gallo RC. Human cutaneous T cell lymphoma and leukemia cell lines produce and respond to T cell growth factor. J Exp Med. 1981;154(5):1403-18.

21.Hampson P, Chahal H, Khanim F, Hayden R, Mulder A, Assi LK, Bunce CM, Lord JM. PEP005, a selective small-molecule activator of protein kinase C, has potent antileukemic activity mediated via the delta isoform of PKC. Blood. 2005;106(4):1362-8.

22.Hossini AM, Eberle J. Apoptosis induction by Bcl-2 proteins independent of the BH3 domain. Biochem Pharmacol. 2008;76(11):1612-9.

23.Kaltoft K, Bisballe S, Dyrberg T, Boel E, Rasmussen PB, Thestrup-Pedersen K. Establishment of two continuous T-cell strains from a single plaque of a patient with mycosis fungoides. In Vitro Cell Dev Biol. 1992;28a(3 Pt 1):161-7.

24.Kaltoft K, Bisballe S, Rasmussen HF, Thestrup-Pedersen K, Thomsen K, Sterry W. A continuous T-cell line from a patient with Sézary syndrome. Arch Dermatol Res. 1987;279(5):293-8.

25.Kato K, Yamanouchi D, Esbona K, Kamiya K, Zhang F, Kent KC, Liu B. Caspase-mediated protein kinase C-delta cleavage is necessary for apoptosis of vascular smooth muscle cells. Am J Physiol Heart Circ Physiol. 2009;297(6):H2253-61.

26.Kaufmann SH, Karp JE, Svingen PA, Krajewski S, Burke PJ, Gore SD, Reed JC. Elevated Expression of the Apoptotic Regulator Mcl-1 at the Time of Leukemic Relapse. Blood. 1998;91(3):991-1000.

27.Kerr JF, Wyllie AH, Currie AR. Apoptosis: a basic biological phenomenon with wide-ranging implications in tissue kinetics. Br J Cancer. 1972;26(4):239-57.

28.Klanova M, Kazantsev D, Pokorna E, Zikmund T, Karolova J, Behounek M, Renesova N, Sovilj D, Kelemen CD, Helman K, Jaksa R, Havranek O, Andera L, Trneny M, Klener P. Anti-apoptotic MCL1 protein represents critical survival molecule for most Burkitt lymphomas and BCL2-negative diffuse large B-cell lymphomas. Molecular Cancer Therapeutics. 2022;21(1):89-99.

29.Klemke CD, Brenner D, Weiss EM, Schmidt M, Leverkus M, Gülow K, Krammer PH. Lack of T-cell receptor-induced signaling is crucial for CD95 ligand up-regulation and protects cutaneous T-cell lymphoma cells from activation-induced cell death. Cancer Res. 2009;69(10):4175-83.

30.Koch R, Christie AL, Crombie JL, Palmer AC, Plana D, Shigemori K, Morrow SN, Van Scoyk A, Wu W, Brem EA, Secrist JP, Drew L, Schuller AG, Cidado J, Letai A, Weinstock DM. Biomarker-driven strategy for MCL1 inhibition in T-cell lymphomas. Blood. 2019;133(6):566-75.

31.Kotschy A, Szlavik Z, Murray J, Davidson J, Maragno AL, Le Toumelin-Braizat G, Chanrion M, Kelly GL, Gong JN, Moujalled DM, Bruno A, Csekei M, Paczal A, Szabo ZB, Sipos S, Radics G, Proszenyak A, Balint B, Ondi L, Blasko G, Robertson A, Surgenor A, Dokurno P, Chen I, Matassova N, Smith J, Pedder C, Graham C, Studeny A, Lysiak-Auvity G, Girard AM, Gravé F, Segal D, Riffkin CD, Pomilio G, Galbraith LC, Aubrey BJ, Brennan MS, Herold MJ, Chang C, Guasconi G, Cauquil N, Melchiore F, Guigal-Stephan N, Lockhart B, Colland F, Hickman JA, Roberts AW, Huang DC, Wei AH, Strasser A, Lessene G, Geneste O. The MCL1 inhibitor S63845 is tolerable and effective in diverse cancer models. Nature. 2016;538(7626):477-82.

32.Kotschy A, Szlavik Z, Murray J, Davidson J, Maragno AL, Le Toumelin-Braizat G, Chanrion M, Kelly GL, Gong JN, Moujalled DM, Bruno A, Csekei M, Paczal A, Szabo ZB, Sipos S, Radics G, Proszenyak A, Balint B, Ondi L, Blasko G, Robertson A, Surgenor A, Dokurno P, Chen I, Matassova N, Smith J, Pedder C, Graham C, Studeny A, Lysiak-Auvity G, Girard AM, Gravé F, Segal D, Riffkin CD, Pomilio G, Galbraith LC, Aubrey BJ, Brennan MS, Herold MJ, Chang C, Guasconi G, Cauquil N, Melchiore F, Guigal-Stephan N, Lockhart B, Colland F, Hickman JA, Roberts AW, Huang DC, Wei AH, Strasser A, Lessene G, Geneste O. The MCL1 inhibitor S63845 is tolerable and effective in diverse cancer models. Nature. 2016;538(7626):477-82.

33.Liu H, Chang DW, Yang X. Interdimer processing and linearity of procaspase-3 activation. A unifying mechanism for the activation of initiator and effector caspases. J Biol Chem. 2005;280(12):11578-82.

34.Manzano M, Patil A, Waldrop A, Dave SS, Behdad A, Gottwein E. Gene essentiality landscape and druggable oncogenic dependencies in herpesviral primary effusion lymphoma. Nature Communications. 2018;9(1):3263.

35.Netchiporouk E, Gantchev J, Tsang M, Thibault P, Watters AK, Hughes JM, Ghazawi FM, Woetmann A, Ødum N, Sasseville D, Litvinov IV. Analysis of CTCL cell lines reveals important differences between mycosis fungoides/Sézary syndrome vs. HTLV-1(+) leukemic cell lines. Oncotarget. 2017;8(56):95981-98.

36.Oltersdorf T, Elmore SW, Shoemaker AR, Armstrong RC, Augeri DJ, Belli BA, Bruncko M, Deckwerth TL, Dinges J, Hajduk PJ, Joseph MK, Kitada S, Korsmeyer SJ, Kunzer AR, Letai A, Li C, Mitten MJ, Nettesheim DG, Ng S, Nimmer PM, O'Connor JM, Oleksijew A, Petros AM, Reed JC, Shen W, Tahir SK, Thompson CB, Tomaselli KJ, Wang B, Wendt MD, Zhang H, Fesik SW, Rosenberg SH. An inhibitor of Bcl-2 family proteins induces regression of solid tumours. Nature. 2005;435(7042):677-81.

37.Picato.

38.Prelude T. A Study of PRT1419 in Patients with Relapsed/Refractory Hematologic Malignancies. 2022.

39.Pullarkat VA, Lacayo NJ, Jabbour E, Rubnitz JE, Bajel A, Laetsch TW, Leonard J, Colace SI, Khaw SL, Fleming SA, Mattison RJ, Norris R, Opferman JT, Roberts KG, Zhao Y, Qu C, Badawi M, Schmidt M, Tong B, Pesko JC, Sun Y, Ross JA, Vishwamitra D, Rosenwinkel L, Kim SY, Jacobson A, Mullighan CG, Alexander TB, Stock W. Venetoclax and Navitoclax in Combination with Chemotherapy in Patients with Relapsed or Refractory Acute Lymphoblastic Leukemia and Lymphoblastic Lymphoma. Cancer Discov. 2021;11(6):1440-53.

40.Redza-Dutordoir M, Averill-Bates DA. Activation of apoptosis signalling pathways by reactive oxygen species. Biochimica et Biophysica Acta (BBA) - Molecular Cell Research. 2016;1863(12):2977-92.

41.Scarisbrick JJ, Quaglino P, Prince HM, Papadavid E, Hodak E, Bagot M, Servitje O, Berti E, Ortiz-Romero P, Stadler R, Patsatsi A, Knobler R, Guenova E, Child F, Whittaker S, Nikolaou V, Tomasini C, Amitay I, Prag Naveh H, Ram-Wolff C, Battistella M, Alberti-Violetti S, Stranzenbach R, Gargallo V, Muniesa C, Koletsa T, Jonak C, Porkert S, Mitteldorf C, Estrach T, Combalia A, Marschalko M, Csomor J, Szepesi A, Cozzio A, Dummer R, Pimpinelli N, Grandi V, Beylot-Barry M, Pham-Ledard A, Wobser M, Geissinger E, Wehkamp U, Weichenthal M, Cowan R, Parry E, Harris J, Wachsmuth R, Turner D, Bates A, Healy E, Trautinger F, Latzka J, Yoo J, Vydianath B, Amel-Kashipaz R, Marinos L, Oikonomidi A, Stratigos A, Vignon-Pennamen MD, Battistella M, Climent F, Gonzalez-Barca E, Georgiou E, Senetta R, Zinzani P, Vakeva L, Ranki A, Busschots AM, Hauben E, Bervoets A, Woei-A-Jin FJSH, Matin R, Collins G, Weatherhead S, Frew J, Bayne M, Dunnill G, McKay P, Arumainathan A, Azurdia R, Benstead K, Twigger R, Rieger K, Brown R, Sanches JA, Miyashiro D, Akilov O, McCann S, Sahi H, Damasco FM, Querfeld C, Folkes A, Bur C, Klemke CD, Enz P, Pujol R, Quint K, Geskin L, Hong E, Evison F, Vermeer M, Cerroni L, Kempf W, Kim Y, Willemze R. The PROCLIPI international registry of early-stage mycosis fungoides identifies substantial diagnostic delay in most patients. Br J Dermatol. 2019;181(2):350-7.

42.Smith VM, Dietz A, Henz K, Bruecher D, Jackson R, Kowald L, van Wijk SJL, Jayne S, Macip S, Fulda S, Dyer MJS, Vogler M. I. Specific interactions of BCL-2 family proteins mediate sensitivity to BH3-mimetics in diffuse large B-cell lymphoma. Haematologica. 2020;105(8):2150-63.

43.Soltan MY, Sumarni U, Assaf C, Langer P, Reidel U, Eberle J. Key Role of Reactive Oxygen Species (ROS) in Indirubin Derivative-Induced Cell Death in Cutaneous T-Cell Lymphoma Cells. Int J Mol Sci. 2019;20(5).

44.Spinner S, Crispatzu G, Yi JH, Munkhbaatar E, Mayer P, Höckendorf U, Müller N, Li Z, Schader T, Bendz H, Hartmann S, Yabal M, Pechloff K, Heikenwalder M, Kelly GL, Strasser A, Peschel C, Hansmann ML, Ruland J, Keller U, Newrzela S, Herling M, Jost PJ. Re-activation of mitochondrial apoptosis inhibits T-cell lymphoma survival and treatment resistance. Leukemia. 2016;30(7):1520-30.

45.Starkebaum G, Loughran TP, Jr., Waters CA, Ruscetti FW. Establishment of an IL-2 independent, human T-cell line possessing only the p70 IL-2 receptor. Int J Cancer. 1991;49(2):246-53.

46.Sumarni U, Reidel U, Eberle J. Targeting Cutaneous T-Cell Lymphoma Cells by Ingenol Mebutate (PEP005) Correlates with PKCδ Activation, ROS Induction as Well as Downregulation of XIAP and c-FLIP. Cells. 2021 Apr 23;10(5):987.

47.Sumarni U, Zhu J, Sinnberg T, Eberle J. Sensitivity of Cutaneous T-Cell Lymphoma Cells to the Mcl-1 Inhibitor S63845 Correlates with the Lack of Bcl-w Expression. Int J Mol Sci. 2022 Oct 18;23(20):12471.

48.Szlávik Z, Ondi L, Csékei M, Paczal A, Szabó ZB, Radics G, Murray J, Davidson J, Chen I, Davis B, Hubbard RE, Pedder C, Dokurno P, Surgenor A, Smith J, Robertson A, LeToumelin-Braizat G, Cauquil N, Zarka M, Demarles D, Perron-Sierra F, Claperon A, Colland F, Geneste O, Kotschy A. Structure-Guided Discovery of a Selective Mcl-1 Inhibitor with Cellular Activity. J Med Chem. 2019;62(15):6913-24.

49.Tait SWG, Green DR. Mitochondria and cell death: outer membrane permeabilization and beyond. Nature Reviews Molecular Cell Biology. 2010;11(9):621-32.

50.Townsend PA, Kozhevnikova MV, Cexus ONF, Zamyatnin AA, Soond SM. BH3-mimetics: recent developments in cancer therapy. Journal of Experimental & Clinical Cancer Research. 2021;40(1):355.

51.Tse C, Shoemaker AR, Adickes J, Anderson MG, Chen J, Jin S, Johnson EF, Marsh KC, Mitten MJ, Nimmer P, Roberts L, Tahir SK, Xiao Y, Yang X, Zhang H, Fesik S, Rosenberg SH, Elmore SW. ABT-263: a potent and orally bioavailable Bcl-2 family inhibitor. Cancer Res. 2008;68(9):3421-8.

52.Valiulienė G, Vitkevičienė A, Skliutė G, Borutinskaitė V, Navakauskienė R. Pharmaceutical Drug Metformin and MCL1 Inhibitor S63845 Exhibit Anticancer Activity in Myeloid Leukemia Cells via Redox Remodeling. Molecules (Basel, Switzerland). 2021;26(8):2303.

53.Wang D, Liu P. Ingenol-3-Angelate Suppresses Growth of Melanoma Cells and Skin Tumor Development by Downregulation of NF-κB-Cox2 Signaling. Med Sci Monit. 2018;24:486-502.

54.Wang H, Guo M, Wei H, Chen Y. Targeting MCL-1 in cancer: current status and perspectives. J Hematol Oncol. 2021;14(1):67.

55.Wenzel S, Grau M, Mavis C, Hailfinger S, Wolf A, Madle H, Deeb G, Dörken B, Thome M, Lenz P, Dirnhofer S, Hernandez-Ilizaliturri F J, Tzankov A, Lenz G. MCL1 is deregulated in subgroups of diffuse large B-cell lymphoma. Leukemia. 2013;27(6):1381-90.

56.Willemze R, Cerroni L, Kempf W, Berti E, Facchetti F, Swerdlow SH, Jaffe ES. The 2018 update of the WHO-EORTC classification for primary cutaneous lymphomas. Blood. 2019;133(16):1703-14.

57.Willemze R, Jaffe ES, Burg Gn, Cerroni L, Berti E, Swerdlow SH, Ralfkiaer E, Chimenti S, Diaz-Perez JL, Duncan LM, Grange F, Harris NL, Kempf W, Kerl H, Kurrer M, Knobler R, Pimpinelli N, Sander C, Santucci M, Sterry W, Vermeer MH, Wechsler J, Whittaker S, Meijer CJLM. WHO-EORTC classification for cutaneous lymphomas. Blood. 2005;105(10):3768-85.

58.Xiao Z, Hao Y, Liu B, Qian L. Indirubin and meisoindigo in the treatment of chronic myelogenous leukemia in China. Leuk Lymphoma. 2002;43(9):1763-8.

59.Zhang J, Anastasiadis PZ, Liu Y, Thompson EA, Fields AP. Protein Kinase C (PKC) βII Induces Cell Invasion through a Ras/Mek-, PKCι/Rac 1-dependent Signaling Pathway*. Journal of Biological Chemistry. 2004;279(21):22118-23.

60.Zhao M, Xia L, Chen GQ. Protein kinase cδ in apoptosis: a brief overview. Arch Immunol Ther Exp (Warsz). 2012;60(5):361-72.

61.Zhivkova V, Kiecker F, Langer P, Eberle J. Crucial role of reactive oxygen species (ROS) for the proapoptotic effects of indirubin derivative DKP-073 in melanoma cells. Mol Carcinog. 2019;58(2):258-69.

Eidesstattliche Versicherung

„Ich, Uly Sumarni, versichere an Eides statt durch meine eigenhändige Unterschrift, dass ich die vorgelegte Dissertation mit dem Thema Überprüfung neuer therapeutische Strategien in Zellen des kutanen T-Zell-Lymphoms und deren Wirkung auf die Apoptoseregulation (Novel Therapeutic Strategies for Cutaneous T-Cell-Lymphoma and Its Effect on Apoptosis Regulation) selbstständig und ohne nicht offengelegte Hilfe Dritter verfasst und keine anderen als die angegebenen Quellen und Hilfsmittel genutzt habe.
Alle Stellen, die wörtlich oder dem Sinne nach auf Publikationen oder Vorträgen anderer Autoren/innen beruhen, sind als solche in korrekter Zitierung kenntlich gemacht. Die Abschnitte zu Methodik (insbesondere praktische Arbeiten, Laborbestimmungen, statistische Aufarbeitung) und Resultaten (insbesondere Abbildungen, Graphiken und Tabellen) werden von mir verantwortet.

Ich versichere ferner, dass ich die in Zusammenarbeit mit anderen Personen generierten Daten, Datenauswertungen und Schlussfolgerungen korrekt gekennzeichnet und meinen eigenen Beitrag sowie die Beiträge anderer Personen korrekt kenntlich gemacht habe (siehe Anteilserklärung). Texte oder Textteile, die gemeinsam mit anderen erstellt oder verwendet wurden, habe ich korrekt kenntlich gemacht.

Meine Anteile an etwaigen Publikationen zu dieser Dissertation entsprechen denen, die in der untenstehenden gemeinsamen Erklärung mit dem Erstbetreuer, angegeben sind. Für sämtliche im Rahmen der Dissertation entstandenen Publikationen wurden die Richtlinien des ICMJE (International Committee of Medical Journal Editors; www.icmje.og) zur Autorenschaft eingehalten. Ich erkläre ferner, dass ich mich zur Einhaltung der Satzung der Charité – Universitätsmedizin Berlin zur Sicherung Guter Wissenschaftlicher Praxis verpflichte.

Weiterhin versichere ich, dass ich diese Dissertation weder in gleicher noch in ähnlicher Form bereits an einer anderen Fakultät eingereicht habe.

Die Bedeutung dieser eidesstattlichen Versicherung und die strafrechtlichen Folgen einer unwahren eidesstattlichen Versicherung (§§156, 161 des Strafgesetzbuches) sind mir bekannt und bewusst."

Datum/Unterschrift

Anteilserklärung an den erfolgten Publikationen

Uly Sumarni hatte folgenden Anteil an den folgenden Publikationen:

Publikation 1: Sumarni U, Zhu J, Sinnberg T, Eberle J. Sensitivity of Cutaneous T-Cell Lymphoma Cells to the Mcl-1 Inhibitor S63845 Correlates with the Lack of Bcl-w Expression. International Journal of Molecular Sciences. 2022.

Beitrag im Einzelnen: Aus meiner experimentellen Arbeit und statistischen Auswertung sind die Abbildung 1 bis Abbildung 5 entstanden. Ebenfalls war ich bei den Experimenten für die Figure S1, S2 sowie S3 beteiligt. Neben der Konzeptualisierung, formalen Analyse, Untersuchung und Methodologie war ich bei der Erstellung vom ursprünglichen Entwurf sowie beim Korrekturlesen beteiligt.

Publikation 2: Sumarni U, Reidel U, Eberle J. Targeting Cutaneous T-Cell Lymphoma Cells by Ingenol Mebutate (PEP005) Correlates with PKCδ Activation, ROS Induction as Well as Downregulation of XIAP and c-FLIP. Cells. 2021

Beitrag im Einzelnen: Aus meiner experimentellen Arbeit und statistischen Auswertung sind die Abbildung 1 bis Abbildung 5 entstanden. Neben Methodik, Validierung, formale Analyse, Untersuchung und Datenkuratierung war ich bei der Erstellung des ursprünglichen Entwurfs sowie bei der Überprüfung und Bearbeitung des Schreibens beteiligt.

Publikation 3: Soltan MY, Sumarni U, Assaf C, Langer P, Reidel U, Eberle J. Key Role of Reactive Oxygen Species (ROS) in Indirubin Derivative-Induced Cell Death in Cutaneous T-Cell Lymphoma Cells. International Journal of Molecular Sciences. 2019.

Beitrag im Einzelnen: Aus meiner experimentellen Arbeit ist ein Teil von Abbildung 7 der Publikation entstanden. Dabei wurden zweifache Versuche für die Untersuchung des dosisabhängigen Effekts von DKP-071 auf die Apoptoseinduktion und Zellviabilität nach 48-stündiger Behandlung, sowie Proliferationsrate nach 24- und 48-stündiger Behandlung bei drei CTCL-Zelllinien (HH, HuT78, MyLa) durchgeführt. Diese wurden vom Reviewer des Journals angefordert.

_____

Unterschrift, Datum und Stempel des/der erstbetreuenden Hochschullehrers/in

_____

Unterschrift des Doktoranden/der Doktorandin

Auszug aus der Journal Summary List

- Sumarni U, Zhu J, Sinnberg T, Eberle J. Sensitivity of Cutaneous T-Cell Lymphoma Cells to the Mcl-1 Inhibitor S63845 Correlates with the Lack of Bcl-w Expression. International Journal of Molecular Sciences. 2022 Oct 18;23(20):12471. doi: 10.3390/ijms232012471. PMID: 36293331; PMCID: PMC9604298.

Journal Data Filtered By: **Selected JCR Year: 2021** Selected Editions: SCIE,SSCI
Selected Categories: **"BIOCHEMISTRY and MOLECULAR BIOLOGY"** Selected
Category Scheme: WoS
Gesamtanzahl: 296 Journale

Rank	Full Journal Title	Total Cites	Journal Impact Factor	Eigenfaktor
1	NATURE MEDICINE	141,857	87.241	0.23255
2	CELL	362,236	66.850	0.53397
3	Molecular Cancer	32,250	41.444	0.03386
4	Signal Transduction and Targeted Therapy	11,026	38.104	0.01781
5	Annual Review of Biochemistry	25,139	27.258	0.01962
6	Molecular Plant	20,242	21.949	0.02339
7	MOLECULAR CELL	94,258	19.328	0.13937
8	NUCLEIC ACIDS RESEARCH	284,490	19.160	0.33755
9	NATURE STRUCTURAL & MOLECULAR BIOLOGY	33,999	18.361	0.04689
10	TRENDS IN MICROBIOLOGY	19,957	18.230	0.02015
11	CYTOKINE & GROWTH FACTOR REVIEWS	9,002	17.660	0.00625
12	MOLECULAR ASPECTS OF MEDICINE	8,986	16.337	0.00615
13	Nature Chemical Biology	31,125	16.174	0.04456
14	TRENDS IN MOLECULAR MEDICINE	14,585	15.272	0.01381
15	NATURAL PRODUCT REPORTS	14,564	15.111	0.01079
16	PROGRESS IN LIPID RESEARCH	7,982	14.673	0.00444
17	TRENDS IN BIOCHEMICAL SCIENCES	22,957	14.264	0.02170
18	EMBO JOURNAL	80,536	14.012	0.05438
19	MOLECULAR PSYCHIATRY	33,324	13.437	0.04914
20	Molecular Systems Biology	11,036	13.068	0.01483
21	EXPERIMENTAL AND MOLECULAR MEDICINE	12,199	12.153	0.01698

Selected JCR Year: 2021; Selected Categories: "BIOCHEMISTRY and MOLECULAR BIOLOGY"

Rank	Full Journal Title	Total Cites	Journal Impact Factor	Eigenfaktor
64	BIOFACTORS	5,614	6.438	0.00307
65	International Review of Cell and Molecular Biology	3,388	6.420	0.00314
66	MOLECULAR MEDICINE	7,039	6.376	0.00402
67	Food & Function	27,282	6.317	0.02290
68	Biochimica et Biophysica Acta-Gene Regulatory Mechanisms	8,926	6.304	0.00707
69	INTERNATIONAL JOURNAL OF MOLECULAR SCIENCES	211,517	6.208	0.24907
70	Computational and Structural Biotechnology Journal	6,436	6.155	0.00945
71	JOURNAL OF MOLECULAR BIOLOGY	66,672	6.151	0.03581
72	JOURNAL OF NUTRITIONAL BIOCHEMISTRY	15,277	6.117	0.00837
73	Frontiers in Molecular Biosciences	6,864	6.113	0.01068
74	BIOCONJUGATE CHEMISTRY	19,624	6.069	0.01508
75	Biomolecules	21,742	6.064	0.02602
76	GLYCOBIOLOGY	10,212	5.954	0.00650
77	STRUCTURE	17,734	5.871	0.01779
78	MACROMOLECULAR BIOSCIENCE	9,240	5.859	0.00565
79	FASEB JOURNAL	59,831	5.834	0.04452
80	ACS Chemical Neuroscience	12,168	5.780	0.01655
81	BIOELECTROCHEMISTRY	7,093	5.760	0.00463
82	JOURNAL OF ENZYME INHIBITION AND MEDICINAL CHEMISTRY	8,156	5.756	0.00580
83	Journal of Genetics and Genomics	3,129	5.723	0.00327
84	Acta Crystallographica Section D-Structural Biology	23,006	5.699	0.02041
85	REDOX REPORT	2,247	5.696	0.00082

Selected JCR Year: 2021; Selected Categories: "BIOCHEMISTRY and MOLECULAR BIOLOGY"

4

- Sumarni, U.; Reidel, U.; Eberle, J. Targeting Cutaneous T-Cell Lymphoma Cells by Ingenol Mebutate (PEP005) Correlates with PKCδ Activation, ROS Induction as Well as Downregulation of XIAP and c-FLIP. *Cells* **2021**, *10*, 987. https://doi.org/10.3390/cells10050987

Journal Data Filtered By: **Selected JCR Year: 2021** Selected Editions: SCIE,SSCI
Selected Categories: **"CELL BIOLOGY"** Selected Category Scheme: WoS
Gesamtanzahl: 194 Journale

Rank	Full Journal Title	Total Cites	Journal Impact Factor	Eigenfaktor
1	NATURE REVIEWS MOLECULAR CELL BIOLOGY	66,072	113.915	0.07790
2	NATURE MEDICINE	141,857	87.241	0.23255
3	CELL	362,236	66.850	0.53397
4	CELL RESEARCH	29,215	46.297	0.04003
5	CANCER CELL	57,294	38.585	0.07359
6	Signal Transduction and Targeted Therapy	11,026	38.104	0.01781
7	Cell Discovery	5,318	38.079	0.01319
8	Cell Metabolism	61,067	31.373	0.08630
9	NATURE CELL BIOLOGY	55,078	28.213	0.06043
10	Cell Stem Cell	35,867	25.269	0.05806
11	TRENDS IN CELL BIOLOGY	20,498	21.167	0.02577
12	MOLECULAR CELL	94,258	19.328	0.13937
13	Science Translational Medicine	52,639	19.319	0.09144
14	NATURE STRUCTURAL & MOLECULAR BIOLOGY	33,999	18.361	0.04689
15	CYTOKINE & GROWTH FACTOR REVIEWS	9,002	17.660	0.00625
16	Journal of Extracellular Vesicles	11,679	17.337	0.01126
17	Cell Reports Medicine	2,183	16.988	0.00524
18	Protein & Cell	6,830	15.328	0.00937
19	TRENDS IN MOLECULAR MEDICINE	14,585	15.272	0.01381
20	EMBO JOURNAL	80,536	14.012	0.05438

1

Selected JCR Year: 2021; Selected Categories: "CELL BIOLOGY"

Rank	Full Journal Title	Total Cites	Journal Impact Factor	Eigenfaktor
43	CELLULAR & MOLECULAR BIOLOGY LETTERS	2,684	8.702	0.00250
44	CURRENT OPINION IN CELL BIOLOGY	16,077	8.386	0.01479
45	Journal of Molecular Cell Biology	3,664	8.185	0.00506
46	Stem Cell Research & Therapy	19,072	8.079	0.01980
47	JOURNAL OF CELL BIOLOGY	76,617	8.077	0.04412
48	CURRENT OPINION IN STRUCTURAL BIOLOGY	13,407	7.786	0.01689
49	HISTOPATHOLOGY	14,098	7.778	0.01493
50	AMERICAN JOURNAL OF RESPIRATORY CELL AND MOLECULAR BIOLOGY	16,259	7.748	0.01386
51	Cells	40,461	7.666	0.06054
52	Cell Communication and Signaling	6,412	7.525	0.00736
53	SEMINARS IN CELL & DEVELOPMENTAL BIOLOGY	15,850	7.499	0.01742
54	Tissue Engineering Part B-Reviews	5,132	7.376	0.00285
55	Oxidative Medicine and Cellular Longevity	37,850	7.310	0.03931
56	Stem Cell Reports	12,127	7.294	0.02370
57	Cell Death Discovery	3,965	7.109	0.00619
58	CELLULAR ONCOLOGY	3,031	7.051	0.00296
59	INFLAMMATION RESEARCH	6,771	6.986	0.00491
60	CELL BIOLOGY AND TOXICOLOGY	2,678	6.819	0.00176
61	Stem Cell Reviews and Reports	4,340	6.692	0.00391
62	JOURNAL OF CELLULAR PHYSIOLOGY	45,492	6.513	0.04482
63	International Review of Cell and Molecular Biology	3,388	6.420	0.00314

- Soltan MY, Sumarni U, Assaf C, Langer P, Reidel U, Eberle J. Key Role of Reactive Oxygen Species (ROS) in Indirubin Derivative-Induced Cell Death in Cutaneous T-Cell Lymphoma Cells. International Journal of Molecular Sciences. 2019.

Journal Data Filtered By: **Selected JCR Year: 2021** Selected Editions: SCIE,SSCI
Selected Categories: **"BIOCHEMISTRY and MOLECULAR BIOLOGY"** Selected
Category Scheme: WoS
Gesamtanzahl: 296 Journale

Rank	Full Journal Title	Total Cites	Journal Impact Factor	Eigenfaktor
1	NATURE MEDICINE	141,857	87.241	0.23255
2	CELL	362,236	66.850	0.53397
3	Molecular Cancer	32,250	41.444	0.03386
4	Signal Transduction and Targeted Therapy	11,026	38.104	0.01781
5	Annual Review of Biochemistry	25,139	27.258	0.01962
6	Molecular Plant	20,242	21.949	0.02339
7	MOLECULAR CELL	94,258	19.328	0.13937
8	NUCLEIC ACIDS RESEARCH	284,490	19.160	0.33755
9	NATURE STRUCTURAL & MOLECULAR BIOLOGY	33,999	18.361	0.04689
10	TRENDS IN MICROBIOLOGY	19,957	18.230	0.02015
11	CYTOKINE & GROWTH FACTOR REVIEWS	9,002	17.660	0.00625
12	MOLECULAR ASPECTS OF MEDICINE	8,986	16.337	0.00615
13	Nature Chemical Biology	31,125	16.174	0.04456
14	TRENDS IN MOLECULAR MEDICINE	14,585	15.272	0.01381
15	NATURAL PRODUCT REPORTS	14,564	15.111	0.01079
16	PROGRESS IN LIPID RESEARCH	7,982	14.673	0.00444
17	TRENDS IN BIOCHEMICAL SCIENCES	22,957	14.264	0.02170
18	EMBO JOURNAL	80,536	14.012	0.05438
19	MOLECULAR PSYCHIATRY	33,324	13.437	0.04914
20	Molecular Systems Biology	11,036	13.068	0.01483
21	EXPERIMENTAL AND MOLECULAR MEDICINE	12,199	12.153	0.01698

Selected JCR Year: 2021; Selected Categories: "BIOCHEMISTRY and MOLECULAR BIOLOGY"

Rank	Full Journal Title	Total Cites	Journal Impact Factor	Eigenfaktor
64	BIOFACTORS	5,614	6.438	0.00307
65	International Review of Cell and Molecular Biology	3,388	6.420	0.00314
66	MOLECULAR MEDICINE	7,039	6.376	0.00402
67	Food & Function	27,282	6.317	0.02290
68	Biochimica et Biophysica Acta-Gene Regulatory Mechanisms	8,926	6.304	0.00707
69	INTERNATIONAL JOURNAL OF MOLECULAR SCIENCES	211,517	6.208	0.24907
70	Computational and Structural Biotechnology Journal	6,436	6.155	0.00945
71	JOURNAL OF MOLECULAR BIOLOGY	66,672	6.151	0.03581
72	JOURNAL OF NUTRITIONAL BIOCHEMISTRY	15,277	6.117	0.00837
73	Frontiers in Molecular Biosciences	6,864	6.113	0.01068
74	BIOCONJUGATE CHEMISTRY	19,624	6.069	0.01508
75	Biomolecules	21,742	6.064	0.02602
76	GLYCOBIOLOGY	10,212	5.954	0.00650
77	STRUCTURE	17,734	5.871	0.01779
78	MACROMOLECULAR BIOSCIENCE	9,240	5.859	0.00565
79	FASEB JOURNAL	59,831	5.834	0.04452
80	ACS Chemical Neuroscience	12,168	5.780	0.01655
81	BIOELECTROCHEMISTRY	7,093	5.760	0.00463
82	JOURNAL OF ENZYME INHIBITION AND MEDICINAL CHEMISTRY	8,156	5.756	0.00580
83	Journal of Genetics and Genomics	3,129	5.723	0.00327
84	Acta Crystallographica Section D-Structural Biology	23,006	5.699	0.02041
85	REDOX REPORT	2,247	5.696	0.00082

Selected JCR Year: 2021; Selected Categories: "BIOCHEMISTRY and MOLECULAR BIOLOGY"

Druckexemplar(e) der Publikation(en)

Article

Sensitivity of Cutaneous T-Cell Lymphoma Cells to the Mcl-1 Inhibitor S63845 Correlates with the Lack of Bcl-w Expression

Uly Sumarni, Jiaqi Zhu, Tobias Sinnberg [ID] and Jürgen Eberle *[ID]

Department of Dermatology, Venerology und Allergology, Skin Cancer Center, Charité—Universitätsmedizin Berlin, 10117 Berlin, Germany
* Correspondence: juergen.eberle@charite.de; Tel.: +49-30-450-518-383

Abstract: Long-term, curative treatment of cutaneous T-cell lymphomas (CTCL) remains a major challenge. Therapy resistance is often based on apoptosis deficiency, and may depend on antiapoptotic Bcl-2 proteins, such as Bcl-2, Bcl-x_L, Bcl-w and Mcl-1. For their targeting, several antagonists have been generated, which mimic the Bcl-2 homology domain 3 (BH3 mimetics). As dysregulation and overexpression of Mcl-1 has been reported in CTCL, the use of Mcl-1 inhibitors appears as an attractive strategy. Here, we investigated the effects of the selective Mcl-1 inhibitor S63845 in a series of four CTCL cell lines, in comparison to ABT-263 and ABT-737 (inhibitors of Bcl-2, Bcl-x_L and Bcl-w). In two cell lines (HH, HuT-78), S63845 resulted in significant apoptosis induction, decrease in cell viability, loss of mitochondrial membrane potential and caspase activation, while two other cell lines (MyLa, SeAx) remained completely resistant. An inverse correlation was found, as S63845-resistant cells were highly sensitive to ABT-263/-737, and S63845-sensitive cells showed only moderate sensitivity to ABTs. Combinations of S63845 and ABT-263 partially yielded synergistic effects. As concerning Bcl-2 protein expression, weaker Mcl-1 expression was found in S63845-resistant MyLa and SeAx, while for Bcl-2 and Bcl-x_L, the lowest expression was found in the highly sensitive cell line HH. The most striking difference between S63845-resistant and -sensitive cells was identified for Bcl-w, which was exclusively expressed in S63845-resistant cells. Thus, CTCL may be efficiently targeted by BH3 mimetics, providing the right target is preselected, and Bcl-w expression may serve as a suitable marker.

Keywords: non-Hodgkin lymphoma; Bcl-2 proteins; BH3 mimetics

1. Introduction

Approximately 5% of non-Hodgkin lymphomas are characterized by primary cutaneous manifestation and clonal proliferation of skin-homing memory T cells, thus forming a distinct group of cutaneous T-cell lymphomas (CTCL). The group encloses mycosis fungoides, Sézary syndrome and CD30^{+} lymphoproliferative disorders [1,2]. In addition to severe effects on patient's quality of life, about 30% of early-stage CTCL patients undergo disease progression within 10 years by developing tumors as well as by dissemination to lymph nodes, blood and internal organs. Tumor progression is accompanied by reduced 5-year survival rates of only 18% [3]. According to detailed insights into CTCL pathogenesis, several therapeutic strategies have been identified, including TLR7/8 agonist, talimogene laherparepvec, histone deacetylase inhibitors, PI3K inhibitors as well as immune-stimulating antibodies [4]. Nevertheless, long-term, curative treatment remains a major challenge, and the search for new therapeutic approaches continues.

The elimination of tumor cells by apoptosis induction represents a principle goal in cancer therapy; thus, therapy resistance may be frequently explained by apoptosis deficiency [5,6]. As for CTCL, several therapeutic approaches have been related to apoptosis induction, as phototherapy, photopheresis, the retinoid bexarotene and the histone deacetylase inhibitor vorinostat [7–10].

Apoptosis can be induced through extrinsic and intrinsic pathways. Extrinsic proapoptotic pathways are initiated by death ligand binding to appropriate death receptors and the formation of death-receptor-bound signaling complexes [11]. On the other hand, intrinsic apoptosis pathways can be activated by different types of cellular damage as well as by dysregulation, such as oncogene activation, resulting in loss of mitochondrial membrane potential, mitochondrial permeabilization and release of proapoptotic mitochondrial proteins into the cytoplasm [12,13]. This may be further associated with ROS production [14].

A characteristic hallmark in apoptosis pathways is represented by caspase activation. Thus, death receptor ligation results in initiator caspase-8 activation [11], and mitochondria-released cytochrome c results in the formation of the apoptosome complex and initiator caspase-9 activation [13]. Initiator caspases can activate the major effector caspase-3 in signaling cascades through protease cleavage, which then can cleave a large number of death substrates, with the final result of DNA fragmentation and apoptosis induction [15].

Intrinsic proapoptotic pathways are critically controlled by the family of Bcl-2 proteins, which includes antiapoptotic (e.g., Bcl-2, Mcl-1, Bcl-x_L and Bcl-w), proapoptotic BH3-only (e.g., Bid, Bad, Noxa, Puma and Bim) as well as multidomain proapoptotic proteins, such as Bax and Bak. While Bax and Bak are supposed to mediate mitochondrial pores to release proapoptotic factors, they are bound and inhibited by antiapoptotic Bcl-2 proteins, which themselves can be inhibited by the group of BH3-only proteins [16].

As for Mcl-1, accumulating evidence has indicated its critical pro-survival roles in different cell types under physiological as well as malignant conditions. While its expression is tightly regulated at the levels of transcription and protein stability in normal cells, it may be deregulated in tumors [17,18]. Thus, chromosomal amplification, increased mRNA and protein expression were correlated to disease progression and chemotherapy resistance in hematopoietic cancer cells [19,20].

Targeting of antiapoptotic Bcl-2 proteins can be achieved by BH3 mimetics, small molecule inhibitors with structural homology to the Bcl homology domain 3 (BH3). Their binding to the hydrophobic groove of antiapoptotic Bcl-2 proteins prevents their ability to bind other proapoptotic family members [21]. BH3 mimetics with specificity for Bcl-2, Bcl-x_L and Bcl-w as ABT-263/navitoclax and ABT-737, as well as mimetics with specificity for Mcl-1 as S63845, have been developed [22–24]. ABT-263 represents an orally available analog of ABT-737, which aims to overcome the limited solubility of ABT-737 [22]; ABT-263 has already been tested in clinical trials for patients with hematological malignancies [25].

Dysregulation and overexpression of Mcl-1 was reported in non-Hodgkin and T-cell lymphomas. Mcl-1 expression was also seen in CTCL cell lines as well as in skin lesions from CTCL patients. In biopsies of patients from different CTCL stages, a trend towards increased Mcl-1 expression was found along with an increase in tumor stage [26–28]. Thus, the use of selective Mcl-1 inhibitors appears as an attractive therapeutic strategy. In this study, we investigated the effects of S63845 in comparison to ABT-263 and ABT-737 in a series of four CTCL cell lines. The data revealed a subdivision of CTCL cells into two groups with regard to their sensitivity profiles. Mechanisms and causes of resistance were further investigated, resulting in the identification of the selective expression of Bcl-w in S63845-resistant cells.

2. Results

2.1. CTCL Cell Lines Are Classified as Either Sensitive or Resistant to Mcl-1 Inhibition

For evaluation of the possible therapeutic potential of selective Mcl-1 inhibitors in CTCL, four representative cell lines (HH, HuT-78, MyLa and SeAx) were treated with increasing concentrations of S63845 (0.25, 0.5, 1.0 μM). Apoptotic rates were determined by sub-G1 assay, and cell viability was determined by calcein staining at 24 h and 48 h. While two cell lines (HH and HuT-78) showed strong response to S63845, cell lines MyLa and SeAx were completely resistant. A dose-dependent increase in apoptotic rates was found in sensitive cells: 66%/72%/83% (in HH) and 15%/23%/42% (HuT-78) for 0.25/0.5/1.0 μM

S63845 at 48 h, respectively (Figure 1a). In parallel, cell viability was strongly decreased to 22% (HH) and to 53% (HuT-78; 1 μM, 48 h; Figure 1b).
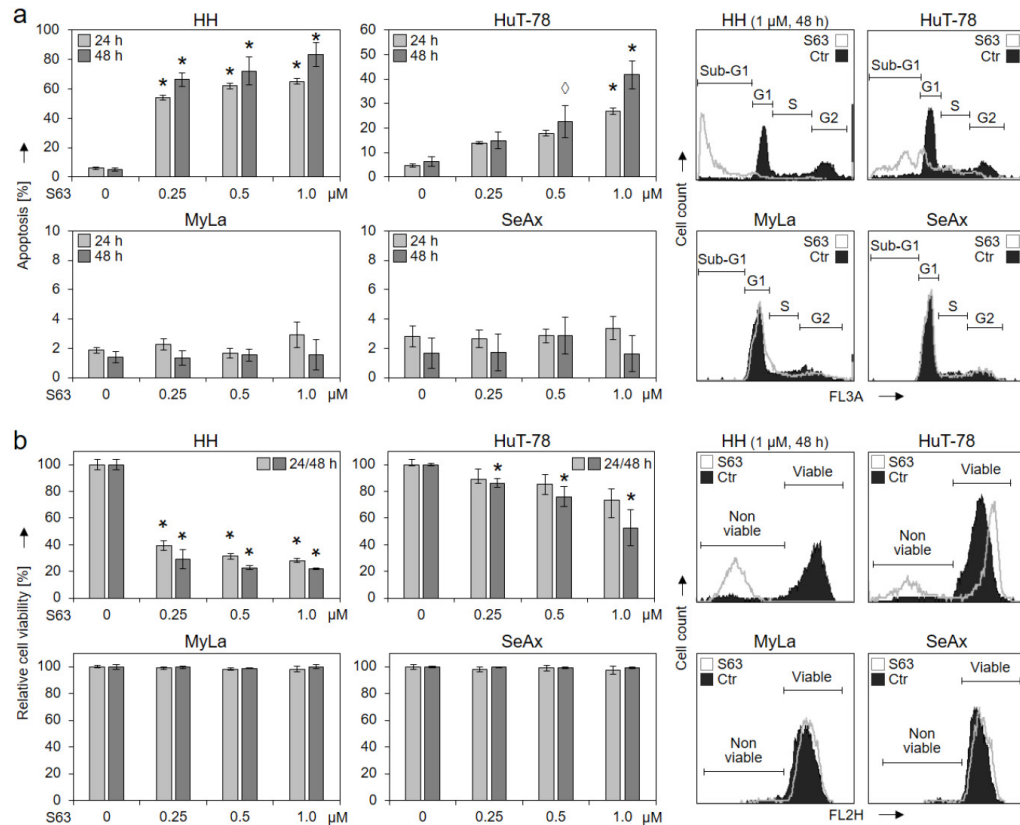

Figure 1. Induced apoptosis and decreased cell viability by S63845 in 2/4 CTCL cell lines. Cell lines HH, HuT-78, MyLa and SeAx were treated with increasing concentrations of S63845 (0.25, 0.5, 1.0 μM). After 24 and 48 h, apoptotic rates were determined by sub-G1 assay (**a**), and rates of cell viability were determined by calcein staining (**b**). Apoptotic rates correspond to percentages of sub-G1 cells (cells with fragmented DNA). Cell viability values were calculated in relation to non-treated controls (0), which were set to 100%. Characteristic histograms of controls (Ctr) and of cells treated for 48 h with S63845 (1 μM) are shown on the right side in overlays. Cell populations in cell cycle phases G1, S, G2 and sub-G1 (**a**) as well as non-viable and viable cells (**b**) are indicated. Mean values of triplicates ± SD of representative experiments are shown. At least three independent experiments were performed, which showed highly comparable results. Statistical significance was calculated from the mean values of independent experiments and is shown for treated cells vs. controls (*, $p < 0.05$). For some values, a statistical trend is also indicated (◊, $p < 0.1$).

To determine EC50 values for S63845, additional experiments were performed for the four cell lines, including concentrations between 10 nM and 2 μM of S63845. Cell viability (Supplementary Figure S1) and apoptosis (Figure S2) were determined after 24 h and 48 h. As for HH at 48 h, 22 nM was determined for 50% loss of cell viability and 95 nM for 50% induced apoptosis. As for HuT-78 at 48 h, 110 nM was determined for 50% loss of cell viability and at 1.4 μM for 50% induced apoptosis. As for the resistant cell lines SeAx and

MyLa, even the highest concentration (2 μM) was not sufficient; thus EC50 was >2 μM (Figures S1 and S2).

2.2. Activation of Apoptosis-Related Pathways by S63845

Loss of mitochondrial membrane potential (MMP), which represents a key trigger of intrinsic mitochondrial apoptosis pathways, was monitored at 4 h and at 24 h of treatment. Significant and dose-dependent loss of MMP was found at 24 h in response to treatments with 0.25, 0.5 and 1.0 μM of S63845 in HH (65%, 83% and 91%) as well as in HuT-78 (21%, 25% and 35%), while MyLa and SeAx showed no response (Figure 2a).
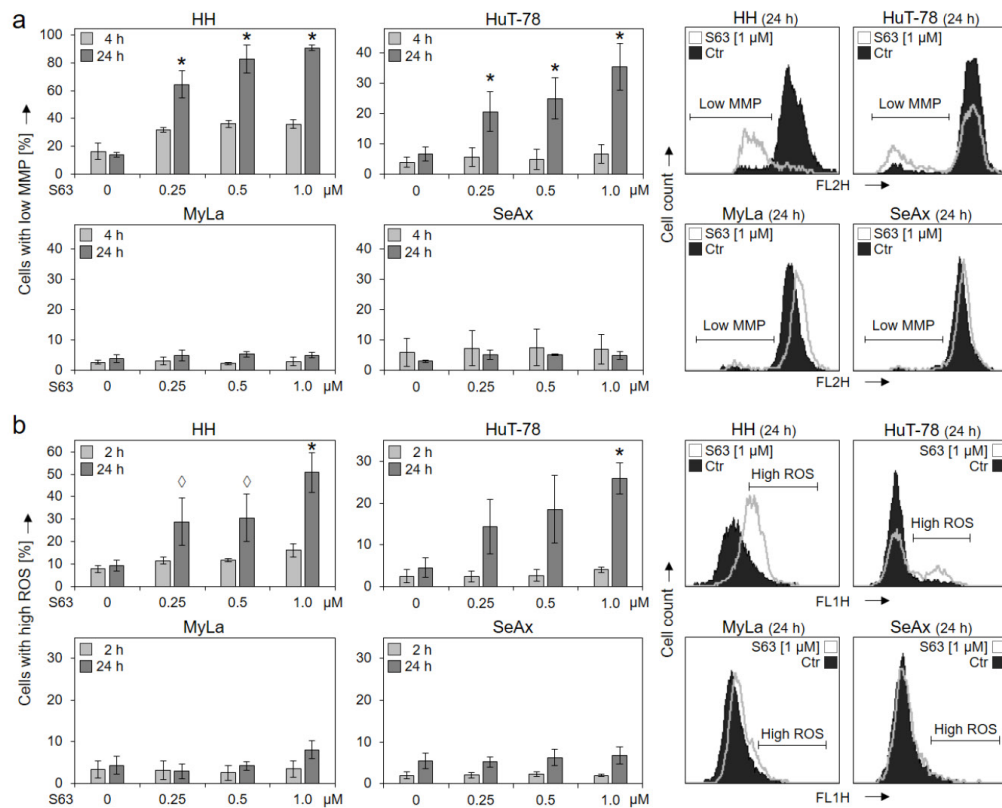
Figure 2. Loss of MMP and enhanced ROS levels in sensitive cells. Cell lines HH, HuT-78, MyLa and SeAx were treated with increasing concentrations of S63845 (0.25, 0.5, 1.0 μM). Changes of mitochondrial membrane potential (MMP, TMRM$^+$ staining) were determined at 4 h and at 24 h of treatment (**a**); levels of reactive oxygen species (ROS, H$_2$DCF-DA staining) were determined at 2 h and at 24 h of treatment (**b**). Representative histograms (overlays of cells treated for 24 h with 1 μM S63845 vs. controls, Ctr) are given on the right side. Mean values of triplicates ± SD of representative experiments are shown here; three independent experiments were performed for 24 h, which had highly comparable results; two experiments were performed for 2 h/4 h (each one with triplicates). Statistical significance (24 h) was calculated from the mean values of independent experiments and is shown for treated cells vs. controls (*, $p < 0.05$). For some values, a statistical trend is also indicated (◊, $p < 0.1$).

Increased levels of reactive oxygen species (ROS) may result from mitochondrial activation and mitochondrial leakage and may activate further cell death pathways in cancer cells [29]. Again, HH and HuT-78 showed increased ROS after 24 h in 51% and 26% of cells (c = 1 µM), respectively, while no clear response was seen in MyLa and SeAx (max. 8% ± 2%; Figure 2b).

Activation of caspase cascades via caspase-8 to caspase-3 or via caspase-9 to caspase-3 are central in apoptosis regulation. Indicating the contribution of caspases, we found strong activation of effector caspase-3 in the two sensitive cell lines, seen in Western blots by the major activated cleavage product of 16 kDa. In contrast, no induction of the 16 kDa form was seen by S63845 treatment in MyLa and SeAx, although weakly expressed in non-treated SeAx cells (Figure 3).
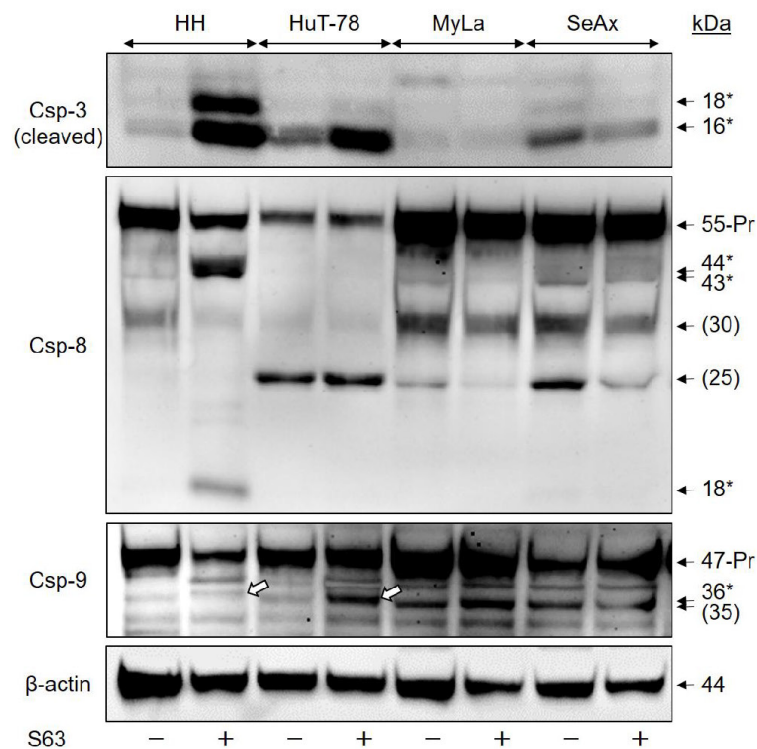
Figure 3. Caspase activation by S63845. CTCL cell lines were treated with 1 µM S63845, and activation of caspase cascade was determined at 48 h in Western blotting by analysis of the induced, specific cleavage products, as compared to DMSO-treated controls. Each 30 µg of proteins were loaded per lane. Blots were probed with antibodies for the cleaved forms of the major proapoptotic effector caspase-3 (cleavage products: 18, 16 kDa), for caspase-8, the initiator caspase of extrinsic pathways (proform: 55 kDa; cleavage products, 44, 43, 18 kDa) as well as for caspase-9, the initiator caspase of intrinsic pathways (proform, 47 kDa; cleavage product: 36 kDa). Specific cleavage products are indicated by (*), the cleavage products of caspase-9 (36 kDa) are further indicated by white arrows in the figure). Protein bands at 30 and 25 kDa (caspase 8) as well as 35 kDa (caspase-9) were not specified and do not reflect caspase activation (put in brackets). The housekeeping protein β-actin (44 kDa) was used as loading control. Two independent series of protein extracts and Western blotting experiments revealed highly comparable results.

In HH, caspase-3 activation correlated with activation of caspase-8, the initiator caspase of extrinsic apoptosis pathways, seen by the cleavage products of 44, 43 and 18 kDa. Furthermore, caspase-9, the initiator caspase of the intrinsic apoptosis pathway, was activated in HuT-78, as seen by a cleavage product of 36 kDa. A non-specified, close protein band of 35 kDa was responsive to caspase-9 antibody. As this 35 kDa band was also seen in non-treated cells, it may thus not be related with caspase-9 activation (Figure 3). Thus, S63845 treatment was able to trigger both extrinsic and intrinsic caspase cascades in different sensitive cell lines, which was excluded in resistant cells.

Caspase activation was quantified by densitometric analysis of the activated processing products of 16 kDa for caspase-3, 18 kDa for caspase-8 as well as 36 kDa for caspase-9. After normalization by the respective β-actin values, induction factors were calculated from two independent experiments, and median values were formed, resulting in median induction factors. Thus, the median induction factors for caspase-3 were 16 (HH) and 4 (HuT-78), while the factors were 1.2 and 0.9 for MyLa and SeAx, respectively. The median induction factors for caspase-8 were 28 (HH), whereas there was no significant caspase-8 activation in HuT-78, MyLa and SeAx. The caspase-9 median induction factor for HuT-78 was determined as 2.6, whereas it was 1.9 (HH), 1.2 (MyLa) and 0.9 (SeAx).

2.3. High Sensitivity of MyLa and SeAx to ABT-263 and ABT-737

The comparison with ABT-263 and ABT-737, which target the antiapoptotic Bcl-2 proteins Bcl-2, Bcl-x_L and Bcl-w, revealed an inverse correlation. Thus, treatment with increasing concentrations (0.01, 0.1 and 1 μM) for 48 h showed particularly high and dose-dependent sensitivity of the S63845-resistant cell lines MyLa and SeAx. For 1 μM ABT-263, apoptosis induction in MyLa and SeAx was at 73% and 70%, respectively, while only 43% and 35% apoptosis was induced in HH and HuT-78 (Figure 4a).

Largely comparable, cell viability was strongly decreased in MyLa and SeAx by 1 μM ABT-263 to 8% and 7% of controls, while the effect was only 60% and 55% in HH and HuT-78, respectively (Figure 1b). It may thus be concluded that the survival of HH and HuT-78 was particularly dependent on Mcl-1, while the survival of MyLa and SeAx was based on the other Bcl-2 proteins. As determined from at least three independent experiments, the response of MyLa and SeAx to ABT-263 (0.1 and 1 μM) in terms of apoptosis induction and loss of cell viability was significantly higher than in HH and HuT-78 ($p < 0.01$).

2.4. Effects of Bcl-2 Protein Antagonists Are Mutually Enhanced in Combinations

We investigated whether CTCL cells may be even better targeted by the combination of different BH3 mimetics. Lower concentrations of ABTs (down to 0.1 μM) were applied in all cell lines, and only 0.05 μM of S63845 was applied in HH, to better recognize any mutual enhancement. Good combination effects were obtained at the level of cell viability. Thus, in S63845-sensitive HH and HuT-78, effects of S63845 were further enhanced by ABT-263 and ABT-737. In HH, cell viability further decreased from 39% (0.05 μM S63845) to 20% (combination with 0.1 μM ABT-263) and to 19% (combination with 0.1 μM ABT-737). In HuT-78, cell viability decreased from 79% (1 μM S63845) to 24% (combination with 0.1 μM ABT-263) and to 36% (0.1 μM ABT-737) (Figure 5a).

Although MyLa and SeAx were not responsive to S63845 alone, the cell viability already decreased in response to ABT-263 and ABT-737 was further reduced in combinations with S63845. Thus, cell viability in MyLa was reduced from 59% (0.1 μM ABT-263) to 21% in combination with 1 μM S63845, and it was reduced from 87% (0.1 μM ABT-737) to 66% in combination. Similarly in SeAx, cell viability was reduced from 19% (0.1 μM ABT-263) to 8% in combination with 1 μM S63845, and it was reduced from 89% (0.1 μM ABT-737) to 39% in combination (Figure 5a). At the level of apoptosis induction, however, the effects of combinations were less pronounced, as compared to single treatments (Figure 5b).
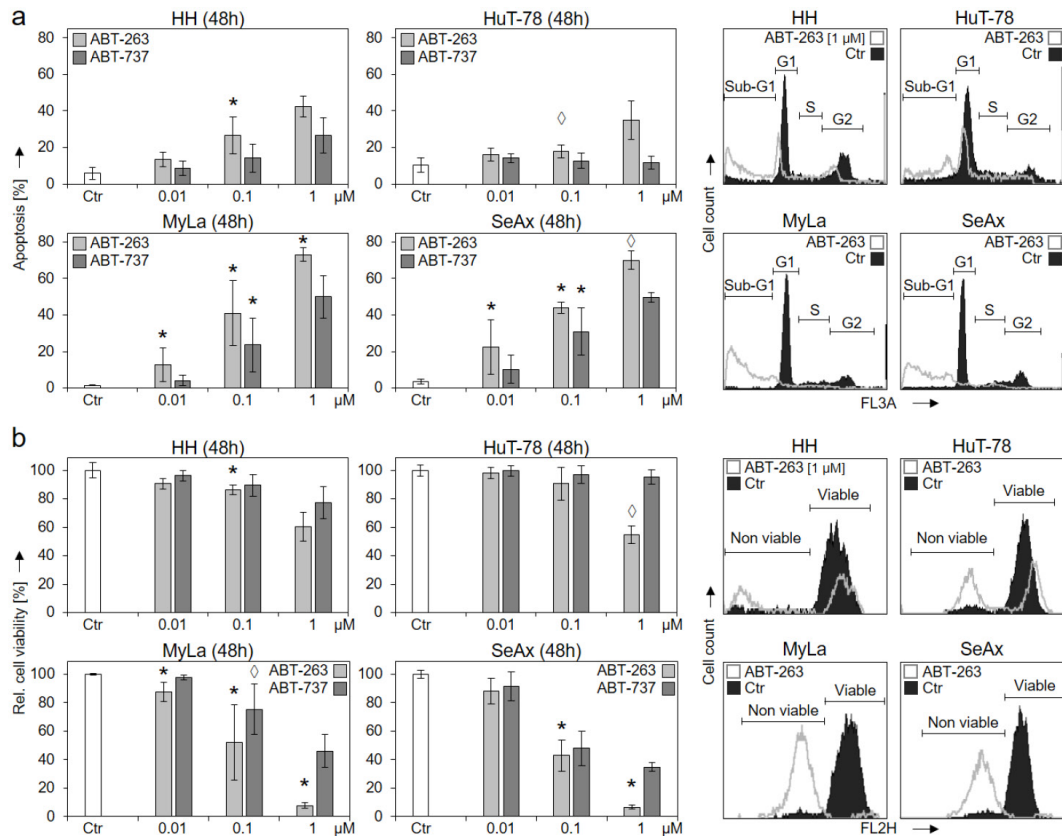
Figure 4. Strong response of S63845-resistant cells to ABT-263 and ABT-737. CTCL cell lines were treated with increasing concentrations (0.01, 0.1, 1 μM) of ABT-263 (light grey) and ABT-737 (dark grey). Apoptotic rates (**a**) were determined by sub-G1 assay, and cell viability rates (**b**) were determined by calcein staining at 48 h. Apoptotic rates correspond to percentages of sub-G1 cells (cells with fragmented DNA). Cell viability values were calculated in relation to non-treated controls (Ctr), which were set to 100%. Example histograms of controls and of cells treated with 1 μM ABT-263 are shown on the right side in overlays. Cell populations in cell cycle phases G1, S, G2 and sub-G1 (**a**) as well as non-viable and viable cells (**b**) are indicated. Mean values of triplicates ± SD of representative experiments are shown. At least three independent experiments (each one with triplicates) were performed for ABT-263 (0.01, 0.1 and 1 μM) as well as for ABT-737 (0.1 μM), which showed highly comparable results. Statistical significance was calculated from the mean values of independent experiments, and is shown for treated cells vs. controls (*, $p < 0.05$). For some values, a statistical trend was also indicated (◊, $p < 0.1$). For ABT-737 (0.01 and 1 μM) only two independent experiments (each one with triplicates) were performed. Thus, here, median values are given, and no statistical significance is indicated.
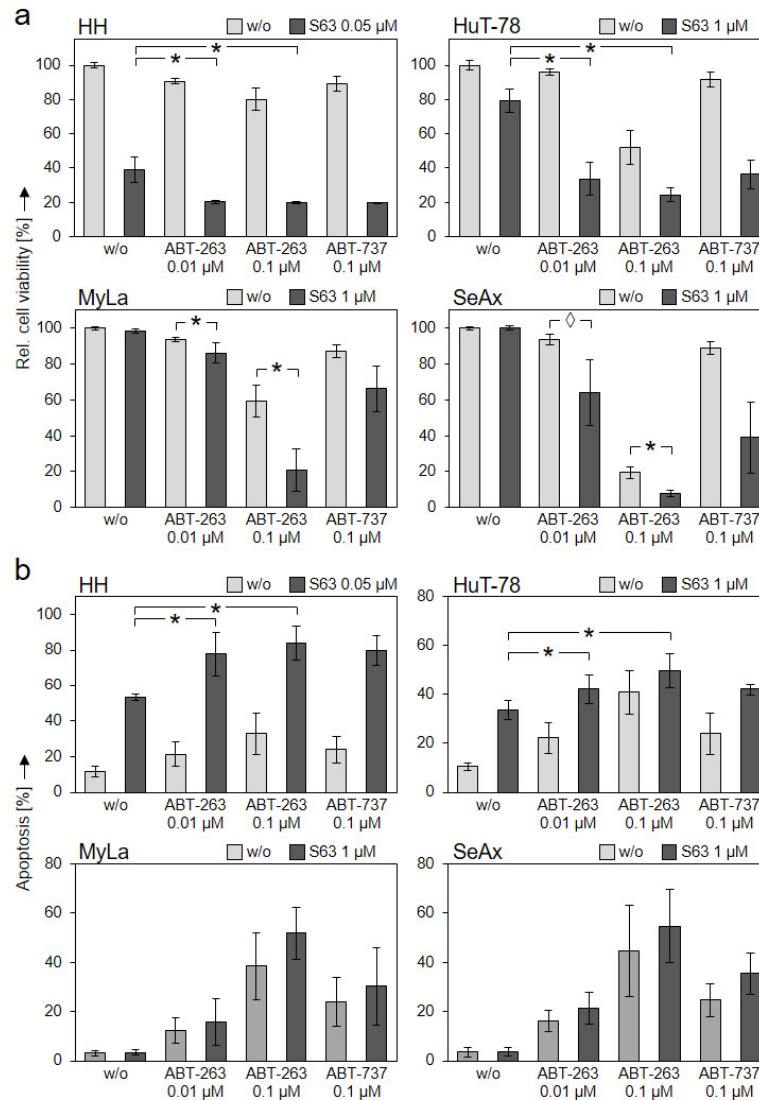
Figure 5. Further enhanced effects by antagonist combinations. CTCL cell lines were treated with S63845 (HH: 0.05 μM; HuT-78, MyLa, SeAx: 1 μM, dark bars), with ABT-263 (0.01 and 0.1 μM), with ABT-737 (0.1 μM) as well as with respective combinations. Cell viability (calcein staining, (**a**)) and apoptotic rates (sub-G1 assay, (**b**)) were determined after 48 h. Cell viability values were calculated in relation to non-treated controls, which were set to 100%; apoptotic rates correspond to percentages of sub-G1 cells (cells with fragmented DNA). Mean values of triplicates $\pm$ SD of representative experiments are shown. At least three independent experiments (each one with triplicate values) were performed for ABT-263 combinations, which showed highly comparable results. For ABT-737 combinations, two independent experiments (each one with triplicate values) revealed comparable results. Statistical significance (ABT-263) was calculated from the mean values of independent experiments, and is shown for cells treated with combinations vs. single treatments (*, $p < 0.05$). For some values, a statistical trend is also indicated ($\Diamond$, $p < 0.1$).

For addressing the question of whether these enhancements were synergistic, a large series of combination experiments with increasing concentrations of the antagonists S63845 and ABT-263 were performed (Supplementary Figure S3). Using the web application SyngeryFinder 3.0 created by Ianevski et al. [30], the enhancement of viability reduction and apoptosis induction in HH and HuT-78 cells was calculated as largely synergistic (δ score > 10). Over larger concentration ranges, the δ score was >40 in HH, and 10–40 in HuT-78, respectively. On the other hand, for cell viability in MyLa and SeAx, a synergistic relationship with δ > 10 was seen only for a limited number of combined concentrations. Additionally, for the induction of apoptosis, the δ scores were between -10 and 10 in these cells, suggesting an additive effect (Supplementary Figure S4).

The effects of Bcl-2 protein antagonists were, however, not restricted to CTCL cells, as shown in experiments with freshly isolated PBMCs. Thus, four independent PBMC preparations cultured in the same growth medium as CTCL cells and treated for 48 h with S63845 showed comparably reduced cell viability and induced apoptosis as sensitive CTCL cells. Thus, cell viability was reduced at 48 h to 31%, 17%, 6% and 4%, and apoptosis was induced to 54%, 49%, 43% and 41% (S63845, 1 μM). Similar effects were seen for ABT-263 (1 μM) and for ABT-737 (1 μM) (Supplementary Figure S5).

2.5. Expression of Bcl-w Correlates with Variant Sensitivities

To obtain a better understanding of the possible causes of variation in the sensitivity of CTCL cell lines to the different Bcl-2 protein antagonists, expression levels of four major antiapoptotic Bcl-2 proteins (Mcl-1, Bcl-x_L, Bcl-2 and Bcl-w) were investigated by Western blotting. As suppression of Mcl-1 activity might affect the protein levels, we included CTCL samples before and after S63845 treatment (48 h, 1 μM).

Mcl-1 protein was generally expressed in all four CTCL cell lines (Figure 6). However, its expression was weaker in S63845-resistant CTCL cell lines than in sensitive cells, as calculated after densitometric quantification and normalization by β-actin from three independent WB experiments ($p < 0.05$). When the mean expression in HH was set to 100% ($\pm 34\%$), it was 102% $\pm$ 57% in HuT-78, but only 61 $\pm$ 43% and 58 $\pm$ 34% in MyLa and SeAx, respectively. In contrast, both Bcl-2 and Bcl-x_L were most weakly expressed in HH (Figure 6). As for Bcl-x_L, quantitative analysis of three independent experiments revealed a relative expression in HH of 27% $\pm$ 9%, as compared to HuT-78 (100% $\pm$ 34%), MyLa (75% $\pm$ 24%) and SeAx (71% $\pm$ 57%; $p < 0.01$). The expression of Bcl-2 was quantified from two independent experiments, but as there was no difference between ($-$S63845) and ($+$S63845) samples; all four values were used for analysis. Thus, expression of Bcl-2 was 6% $\pm$ 5% in HH, as compared to HuT-78 (100% $\pm$ 7%), MyLa (27% $\pm$ 8%) and SeAx (74% $\pm$ 20%). The most striking difference between S63845-resistant and -sensitive cells was identified at the level of Bcl-w expression. This protein was completely lacking in HH and HuT-78 (<1%), while it was significantly expressed in MyLa (100% $\pm$ 20%) and SeAx (97% $\pm$ 26%), as determined from three independent experiments (Figure 6).

These data support a hypothesis according to which apoptosis resistance in MyLa and SeAx is particularly based on Bcl-w, while Mcl-1 is important for HH and HuT-78. Whereas in HuT-78, MyLa and SeAx, the antiapoptotic potential of Bcl-x_L and Bcl-2 can diminish the effects of the Mcl-1 inhibitor S63845, the cell line HH was particularly dependent on Mcl-1, and thus, S63845 showed the strongest effects.
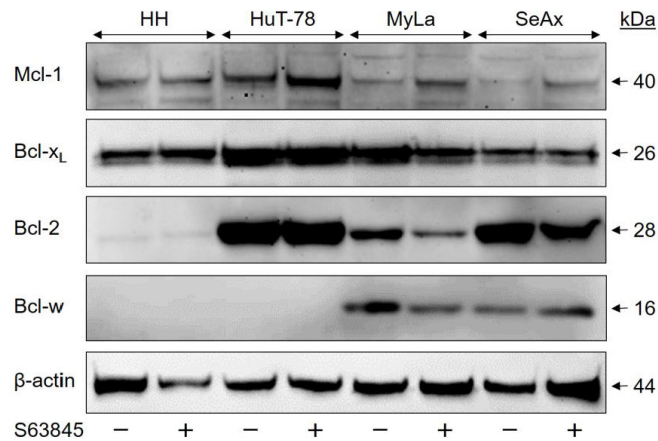
Figure 6. Variant expression of the Bcl-2 family proteins in CTCL cells. CTCL cell lines treated for 48 h with S63845 (1 μM, +) were compared to control cells (DMSO, −). In each lane, 30 μg of proteins were loaded. Blots were probed with antibodies for Mcl-1 (40 kDa), Bcl-x_L (26 kDa), Bcl-2 (28 kDa) and Bcl-w (16 kDa). The housekeeping protein β-actin (44 kDa) was used as a loading control. Three independent series of protein extracts and Western blotting experiments revealed highly comparable results.

3. Discussion

Activation of proapoptotic signaling pathways is an important goal in cancer therapy, which is often blocked by antiapoptotic Bcl-2 proteins. The targeting of Bcl-2 proteins thus appears as a promising strategy. A number of BH3 mimetics have been developed, which mimic the activity of proapoptotic BH3-only proteins and bind to the antiapoptotic Bcl-2 counterparts [21]. In this way, the blockage of apoptosis may be overcome, leading to either direct apoptosis induction or increased therapy sensitivity. Among the first BH3 mimetics, ABT-737 and ABT-263 were shown to inhibit Bcl-2, Bcl-x_L and Bcl-w [22,23].

As for Mcl-1, its important roles have been reported in hematopoietic cancer cells of different types, such as multiple myeloma (MM) [31], diffuse large B-cell lymphoma (DLBCL) [19], mantle cell lymphoma (MCL) [32] as well as in non-Hodgkin and T-cell lymphomas [26,27]. The development of BH3 mimetics with specificity for Mcl-1, e.g., S63845, enabled selective Mcl-1 targeting, which may also be used in therapeutic approaches [24]. When applying S63845 in four CTCL cell lines, we observed a clear division between two completely resistant cell lines and two sensitive cell lines, the latter characterized by induced apoptosis and decreased cell viability. The response was not correlated to the cells' origin, being derived either from MF or Sézary patients.

In contrast to the here-reported two, out of four, resistant CTCL cell lines, the vast majority of other lymphoma cell lines have previously been reported as sensitive. For example, apoptosis induction by S63845 was seen in 13 cell lines of DLBCL, in four out of five cell lines of Burkitt lymphoma (BL) and in 11 cell lines of primary effusion lymphoma [33,34]. As concerning cell viability, all investigated cell lines of AML and 23/25 cell lines of multiple myeloma showed IC50 values of <1 μM. For chronic myeloid leukemia (CML), all of the five investigated cell lines were reported as resistant to S63845 [24,35]. Thus, the question was addressed, which factors decide the variation in the sensitivity of CTCL cells.

Apoptosis can be mediated through extrinsic and intrinsic caspase cascades via caspase-8 and caspase-9, respectively, which finally results in the activation of the major effector caspase-3 [15]. Caspase activation appears to be of particular importance for apoptosis induction in CTCL cells, as seen in response to different treatments, e.g., histone

deacetylase inhibitors, non-steroidal anti-inflammatory drugs or inhibitors for protein kinase C delta [9,36,37]. Additionally, in response to S63845, significant caspase-3 activation was evident in sensitive CTCL cells, caspase-8 processing was seen in HH, and caspase-9 processing was seen in HuT-78, suggesting that both extrinsic and intrinsic caspase pathways may be activated by S63845. Caspase-3 activation in response to S63845 was also reported in DLBCL, Burkitt lymphoma and AML cells [33,35,38].

Loss of mitochondrial membrane potential represents an essential step in intrinsic apoptosis pathways [13], which may be further associated with ROS production [14]. In response to S63845, significant loss of MMP and ROS production was observed at 24 h in sensitive CTCL cell lines, suggesting the contribution of these pathways. Loss of MMP in response to S63845 was also reported in DLBCL and AML cells [35,38]. To date, ROS have not been investigated in most lymphoma studies, but their induction was also found in two AML cell lines at 24 h in response to S63845 [39]. Thus, as resistant CTCL cell lines were completely lacking caspase activation as well as loss of MMP and ROS production in response to S63845, the causes of their resistance had to be sought more above in the pathway.

Our comparison with two alternative BH3 mimetics (ABT-263 and ABT-737), which target Bcl-2, Bcl-x_L and Bcl-w, revealed a particular inverse correlation. Namely, high sensitivity to these ABTs was found in S63845-resistant MyLa and SeAx cells, while S63845-sensitive HH and HuT-78 showed only moderate sensitivity to ABTs. It appears that CTCL cells can be targeted, in principle, by BH3 mimetics, providing the right ones are chosen. Efficacy of ABT-737 was also reported in several other lymphoid cancer cells [40], while resistance was also reported in cell lines of, for example, CLL, ALL [41], MCL [42] and multiple myeloma [43]. As for ABT-263, both sensitive and resistant cell lines of different hematological tumors have been reported [22,23].

Thus, CTCL cell lines differentiated in two groups characterized either by high sensitivity to S63845 and only moderate sensitivity to ABTs, or by S63845 resistance and high sensitivity to ABTs. We aimed to explain these varying responses by differences in the expression of antiapoptotic Bcl-2 proteins. Via Western blot analysis, we showed that Mcl-1 protein was more weakly expressed in S63845-resistant CTCL cell lines, whereas Bcl-2 and Bcl-x_L expression was weakest in the highly sensitive cell line HH. The most striking difference was identified for Bcl-w, which was exclusively expressed in CTCL cells with S63845 resistance and high sensitivity to ABT-263 and -737. These findings suggest that survival of CTCL cells may be critically controlled by the different antiapoptotic Bcl-2 proteins. Once Bcl-w is expressed, it is strong enough to prevent apoptosis induction through Mcl-1 inhibition, but exhibits high sensitivity to ABT-263 and -737. Vice versa, when Bcl-w is lacking, CTCL survival particularly depends on Mcl-1, resulting in a high S63845 sensitivity and reduced sensitivity to ABT-263 and -737. In this setting, Bcl-2 and Bcl-x_L may have contributory roles. When they are weakly expressed, the sensitivity to Mcl-1 inhibition further increases.

Important roles of Bcl-w have also been described in B-cell lymphoma, Burkitt lymphoma and DLBCL [44]. However, the downregulation of Bcl-w in DLBCL cell lines did not sensitize them to S63845 [45]. Another inverse correlation was reported for Bcl-x_L in AML, CML and DLBCL cells, where S63845 resistance correlated with high Bcl-x_L expression, suggesting that in these cells, Bcl-x_L may functionally compensate for the inhibition of Mcl-1 [24,38].

BH3 mimetics represent promising candidates for clinical application in cancer patients [21]. In this study, we also found high sensitivity of isolated PBMCs to S63845 as well as to ABT-263 and ABT-737, in terms of apoptosis induction and loss of cell viability. However, it remains to be clarified, whether the response of cultured PBMCs ex vivo may reflect a similar response in the in vivo situation. Cultured normal cells in growth medium may lack essential survival signals that may be provided in the tissue. Finally, animal experiments and the clinical testing may answer this question. So far, S63845 has been described as well tolerated by mice, with no significant weight loss observed [24], and it

is currently in a phase I clinical trial [46]. Also, suitable safety profiles were reported for ABT-263 in phase I/II clinical trials for hematological malignancies [47].

In terms of clinical efficacy, ABT-263 has reportedly shown efficacy in combination with another BH3 mimetic (ABT-199) in a phase I trial with patients with ALL or lymphoblastic lymphoma [48]. For targeting Mcl-1, two Mcl-1 inhibitors are currently being evaluated in ongoing phase I/II clinical trials for different hematological cancers, namely PRT1419 [49] and S64315 (MIK665). The latter is chemically related to S63845, and shows comparable activity [50]. Open questions of dosing and the safety profile resulted in the termination of some previous studies. Currently, S64315 is in a phase I clinical trial to evaluate the maximal tolerated dose and the recommended dose for expansion. Further studies are planned to evaluate the tolerability, safety and antitumor activity of S64315 in different lymphoid tumors [46]. As Mcl-1 is a promising target in cancer treatment, there is much hope that Mcl-1-based strategies may also be well tolerated.

Taken together, our findings indicate promising responses of CTCL cells to BH3 mimetics. CTCL cell lines were either highly sensitive to the inhibition of Mcl-1 (S63845) or to the inhibition of Bcl-2/Bcl-x_L/Bcl-w (ABT-263, ABT-737). Sensitivity to S63845 was correlated with diminished expression of Bcl-2 and Bcl-x_L and in particular with a complete lack of Bcl-w expression. These findings shed more light on the particular roles of antiapoptotic Bcl-2 proteins in apoptosis control in CTCL cells. Furthermore, therapeutic strategies may be considered that are either based on Mcl-1 inhibitors or on ABT-263, or a combination of both. Expression levels of Bcl-w in tumor T cells may be used as a biomarker to identify the right targets.

4. Materials and Methods

4.1. Cell Culture and Treatment

Four representative CTCL cell lines were used in this study: MyLa derived from a plaque biopsy of a patient with MF [51]; SeAx [52] and HuT-78 [53] derived from peripheral blood mononuclear cells of patients with Sézary syndrome; and HH (ATCC, Manassas, VA, USA; CRL2105) derived from peripheral blood of a patient with aggressive CTCL [54]. Cells were maintained at 37 °C and 5% CO_2 in RPMI 1640 growth medium (Life Technologies, Darmstadt, Germany) supplemented with fetal calf serum (FCS, 10%), L-glutamine (600 μM) and antibiotics. Cells were generally passaged twice a week.

For the different assays, 5×10^4 cells were seeded per well in 24-well plates. Cells were treated with 0.01–2 μM S63845 (CAS# 1799633-27-4, Hölzel Diagnostika, Cologne, Germany), 0.01–1 μM ABT-263 (CAS# 923564-51-6, Biozol, Eching, Germany) and 0.01–1 μM ABT-737 (CAS# 852808-04-9, Biozol). Control cells received the solvent DMSO in the same concentration as used for treatment (max. 0.4%).

For control, human peripheral blood mononuclear cells (PBMCs) were isolated from full blood of healthy, voluntary donors (20 mL). All donors were informed about the use of their material. For reasons of data protection, samples were anonymized and randomized. PBMCs were isolated by a Ficoll 400 density gradient (Biocoll, Bio&SELL, Feucht/Nürnberg, Germany). Cells were washed in cold PBS, and healthy cells were counted after trypan blue staining. For assays, PBMCs were seeded the same day in 24-well plates (100,000 cells/well). Treatment with Bcl-2 protein agonists started after 24 h, and assays were performed after 48 h of treatment.

4.2. Determination of Apoptosis, Cytotoxicity, Cell Viability and Cell Proliferation

Quantification of apoptosis was performed by cell cycle analysis and sub-G1 assay. Harvested cells were lysed in hypotonic buffer containing sodium citrate (0.1%), Triton-X 100 (0.1%) and propidium iodide (PI, Sigma-Aldrich, St. Louis, MO, USA, 40 μg/mL). Thus, cells were lysed, and isolated cell nuclei were stained for at least 1 h with propidium iodide at 4 °C. Cells in G1, G2 and S phases as well as sub-G1 cells were quantified by flow cytometry at FL3A with a FACSCalibur (BD Bioscience, Bedford, MA, USA). Due to the

washing out of small DNA fragments, nuclei with less DNA than G1 (sub-G1) correspond to apoptotic cells.

Cell viability was determined by staining cells with calcein-AM (PromoCell, Heidelberg, Germany), which is converted through intracellular esterase activity in viable cells to the green fluorescent calcein. Cells, grown and treated in 24-well plates, were harvested and stained for 1 h with 0.5 μM calcein-AM at 37 °C. After labeling, cells were washed with PBS and measured by flow cytometry (FL2H).

4.3. Determination of Mitochondrial Membrane Potential and Reactive Oxygen Species (ROS)

The potential across the mitochondrial membrane was quantified by staining cells with the fluorescent dye $TMRM^+$ (tetramethylrhodamine methyl ester, Sigma-Aldrich). Cells, grown and treated in 24-well plates, were harvested and stained for 20 min at 37 °C in 1 μM $TMRM^+$. After washing twice with PBS, cell staining was quantified by flow cytometry (FL2H).

For the determination of intracellular ROS levels, cells grown in 24-well plates were preincubated for 1 h with the fluorescent dye H_2DCFDA (2′,7′-dichlorofluorescin diacetate, D-399, Thermo Fisher Scientific, Hennigsdorf, Germany, 10 μM), before starting treatment with effectors. After 2–24 h of treatment, cells were harvested, washed two times with PBS and analyzed by flow cytometry (FL1H). As positive control, H_2O_2 (1 mM) was applied for 1 h.

4.4. Western Blotting

For Western blotting, total protein extracts were obtained in cell lysis buffer containing 150 mM NaCl, 1 mM EDTA, 1% NP-40, 50 mM Tris (pH 8.0) as well as phosphatase and protease inhibitors. Protein concentrations were determined by BCA staining (#23225, Thermo Fisher Scientific, Hennigsdorf, Germany) as compared to BSA concentration standard. Following SDS polyacrylamide gel electrophoresis, proteins were blotted on nitrocellulose membranes, as described previously [55].

Several primary antibodies were derived from Cell Signaling Technology (Danvers, MA, USA): caspase-3 (9662, rabbit, 1:1000), caspase-8 (9746, mouse, 1:1000), caspase-9 (9502, rabbit, 1:1000), Mcl-1 (4572, rabbit, 1:1000), Bcl-w (2724, rabbit, 1:1000) and Bcl-2 (2872, rabbit, 1:1000). Other primary antibodies were derived from Santa Cruz Biotech (Dallas, TX, USA): Bcl-x_L (sc-8392, mouse, 1:1000) and β-actin (sc-47778, mouse, 1:1000). As secondary antibodies, peroxidase-labeled goat anti-rabbit and goat anti-mouse were used (Dako, Hamburg, Germany; 1:5000).

4.5. Statistical Analyses

All analyses were proven by two to five independent experiments. Each independent experiment itself consisted of triplicate values (three wells that were seeded, treated and analyzed individually). For determination of statistical significance by Student's *t*-test, only the mean values of the independent experiments were used (3–5 values). Statistical significance is indicated by asterisks in the presented figures (*, $p < 0.05$).

For Western blots, two experiments (caspases) or three experiments (Bcl-2 proteins) were performed, which derived from independent series of protein extracts. All signals were quantified by densitometric analysis and were normalized by the respective β-actin values. For the Bcl-2 proteins with three independent experiments, statistical evaluations were performed.

As concerning the identification of synergistic effects in combination treatments with S63845 and ABT-263, the program SyngeryFinder 3.0 was used [30]. In particular, the Bliss scoring method was applied, and delta scores (δ) $\geq$10 were considered as synergistic, whereas scores between −10 and 10 were considered as additive.

References

1. Dobos, G.; Assaf, C. Transcriptomic changes during stage progression of mycosis fungoides: From translational analyses to their potential clinical implications. *Br. J. Dermatol.* **2022**, *186*, 387–388. [CrossRef]
2. Willemze, R.; Cerroni, L.; Kempf, W.; Berti, E.; Facchetti, F.; Swerdlow, S.H.; Jaffe, E.S. The 2018 update of the WHO-EORTC classification for primary cutaneous lymphomas. *Blood* **2019**, *133*, 1703–1714. [CrossRef]
3. Agar, N.S.; Wedgeworth, E.; Crichton, S.; Mitchell, T.J.; Cox, M.; Ferreira, S.; Robson, A.; Calonje, E.; Stefanato, C.M.; Wain, E.M.; et al. Survival outcomes and prognostic factors in mycosis fungoides/Sézary syndrome: Validation of the revised International Society for Cutaneous Lymphomas/European Organisation for Research and Treatment of Cancer staging proposal. *J. Clin. Oncol.* **2010**, *28*, 4730–4739. [CrossRef]
4. Dummer, R.; Vermeer, M.H.; Scarisbrick, J.J.; Kim, Y.H.; Stonesifer, C.; Tensen, C.P.; Geskin, L.J.; Quaglino, P.; Ramelyte, E. Cutaneous T cell lymphoma. *Nat. Rev. Dis. Primers* **2021**, *7*, 61. [CrossRef]
5. Eberle, J. Countering TRAIL Resistance in Melanoma. *Cancers* **2019**, *11*, 656. [CrossRef]
6. Hanahan, D.; Weinberg, R.A. Hallmarks of cancer: The next generation. *Cell* **2011**, *144*, 646–674. [CrossRef]
7. Baron, E.D.; Stevens, S.R. Phototherapy for cutaneous T-cell lymphoma. *Dermatol. Ther.* **2003**, *16*, 303–310. [CrossRef]
8. Zhang, C.; Hazarika, P.; Ni, X.; Weidner, D.A.; Duvic, M. Induction of apoptosis by bexarotene in cutaneous T-cell lymphoma cells: Relevance to mechanism of therapeutic action. *Clin. Cancer Res.* **2002**, *8*, 1234–1240.
9. Al-Yacoub, N.; Fecker, L.F.; Möbs, M.; Plötz, M.; Braun, F.K.; Sterry, W.; Eberle, J. Apoptosis induction by SAHA in cutaneous T-cell lymphoma cells is related to downregulation of c-FLIP and enhanced TRAIL signaling. *J. Invest. Derm.* **2012**, *132*, 2263–2274. [CrossRef]
10. Bladon, J.; Taylor, P.C. Extracorporeal photopheresis: A focus on apoptosis and cytokines. *J. Derm. Sci.* **2006**, *43*, 85–94. [CrossRef]
11. Krammer, P.H.; Arnold, R.; Lavrik, I.N. Life and death in peripheral T cells. *Nat. Rev. Immunol.* **2007**, *7*, 532–542. [CrossRef]
12. Eberle, J.; Hossini, A.M. Expression and function of bcl-2 proteins in melanoma. *Curr. Genom.* **2008**, *9*, 409–419. [CrossRef]
13. Tait, S.W.G.; Green, D.R. Mitochondria and cell death: Outer membrane permeabilization and beyond. *Nat. Rev. Mol. Cell Biol.* **2010**, *11*, 621–632. [CrossRef]
14. Redza-Dutordoir, M.; Averill-Bates, D.A. Activation of apoptosis signalling pathways by reactive oxygen species. *Biochim. Et Biophys. Acta BBA Mol. Cell Res.* **2016**, *1863*, 2977–2992. [CrossRef]
15. Fischer, U.; Jänicke, R.U.; Schulze-Osthoff, K. Many cuts to ruin: A comprehensive update of caspase substrates. *Cell Death Differ.* **2003**, *10*, 76–100. [CrossRef]
16. Westphal, D.; Kluck, R.M.; Dewson, G. Building blocks of the apoptotic pore: How Bax and Bak are activated and oligomerize during apoptosis. *Cell Death Differ.* **2014**, *21*, 196–205. [CrossRef]
17. Beroukhim, R.; Mermel, C.H.; Porter, D.; Wei, G.; Raychaudhuri, S.; Donovan, J.; Barretina, J.; Boehm, J.S.; Dobson, J.; Urashima, M.; et al. The landscape of somatic copy-number alteration across human cancers. *Nature* **2010**, *463*, 899–905. [CrossRef]
18. Mojsa, B.; Lassot, I.; Desagher, S. Mcl-1 ubiquitination: Unique regulation of an essential survival protein. *Cells* **2014**, *3*, 418–437. [CrossRef]
19. Wenzel, S.S.; Grau, M.; Mavis, C.; Hailfinger, S.; Wolf, A.; Madle, H.; Deeb, G.; Dörken, B.; Thome, M.; Lenz, P.; et al. MCL1 is deregulated in subgroups of diffuse large B-cell lymphoma. *Leukemia* **2013**, *27*, 1381–1390. [CrossRef]
20. Quinn, B.A.; Dash, R.; Azab, B.; Sarkar, S.; Das, S.K.; Kumar, S.; Oyesanya, R.A.; Dasgupta, S.; Dent, P.; Grant, S.; et al. Targeting Mcl-1 for the therapy of cancer. *Expert Opin. Investig. Drugs* **2011**, *20*, 1397–1411. [CrossRef]

21. Townsend, P.A.; Kozhevnikova, M.V.; Cexus, O.N.F.; Zamyatnin, A.A.; Soond, S.M. BH3-mimetics: Recent developments in cancer therapy. *J. Exp. Clin. Cancer Res.* **2021**, *40*, 355. [CrossRef]
22. Tse, C.; Shoemaker, A.R.; Adickes, J.; Anderson, M.G.; Chen, J.; Jin, S.; Johnson, E.F.; Marsh, K.C.; Mitten, M.J.; Nimmer, P.; et al. ABT-263: A potent and orally bioavailable Bcl-2 family inhibitor. *Cancer Res.* **2008**, *68*, 3421–3428. [CrossRef]
23. Oltersdorf, T.; Elmore, S.W.; Shoemaker, A.R.; Armstrong, R.C.; Augeri, D.J.; Belli, B.A.; Bruncko, M.; Deckwerth, T.L.; Dinges, J.; Hajduk, P.J.; et al. An inhibitor of Bcl-2 family proteins induces regression of solid tumours. *Nature* **2005**, *435*, 677–681. [CrossRef]
24. Kotschy, A.; Szlavik, Z.; Murray, J.; Davidson, J.; Maragno, A.L.; Le Toumelin-Braizat, G.; Chanrion, M.; Kelly, G.L.; Gong, J.N.; Moujalled, D.M.; et al. The MCL1 inhibitor S63845 is tolerable and effective in diverse cancer models. *Nature* **2016**, *538*, 477–482. [CrossRef]
25. Senichkin, V.V.; Streletskaia, A.Y.; Gorbunova, A.S.; Zhivotovsky, B.; Kopeina, G.S. Saga of Mcl-1: Regulation from transcription to degradation. *Cell Death Differ.* **2020**, *27*, 405–419. [CrossRef]
26. Spinner, S.; Crispatzu, G.; Yi, J.H.; Munkhbaatar, E.; Mayer, P.; Höckendorf, U.; Müller, N.; Li, Z.; Schader, T.; Bendz, H.; et al. Re-activation of mitochondrial apoptosis inhibits T-cell lymphoma survival and treatment resistance. *Leukemia* **2016**, *30*, 1520–1530. [CrossRef]
27. Koch, R.; Christie, A.L.; Crombie, J.L.; Palmer, A.C.; Plana, D.; Shigemori, K.; Morrow, S.N.; Van Scoyk, A.; Wu, W.; Brem, E.A.; et al. Biomarker-driven strategy for MCL1 inhibition in T-cell lymphomas. *Blood* **2019**, *133*, 566–575. [CrossRef]
28. Zhang, C.L.; Kamarashev, J.; Qin, J.Z.; Burg, G.; Dummer, R.; Döbbeling, U. Expression of apoptosis regulators in cutaneous T-cell lymphoma (CTCL) cells. *J. Pathol.* **2003**, *200*, 249–254. [CrossRef]
29. Quast, S.A.; Berger, A.; Eberle, J. ROS-dependent phosphorylation of Bax by wortmannin sensitizes melanoma cells for TRAIL-induced apoptosis. *Cell Death Dis.* **2013**, *4*, e839. [CrossRef]
30. Ianevski, A.; Giri, A.K.; Aittokallio, T. SynergyFinder 3.0: An interactive analysis and consensus interpretation of multi-drug synergies across multiple samples. *Nucleic Acids Res.* **2022**, *50*, W739-43. [CrossRef]
31. Gong, J.-N.; Khong, T.; Segal, D.; Yao, Y.; Riffkin, C.D.; Garnier, J.-M.; Khaw, S.L.; Lessene, G.; Spencer, A.; Herold, M.J.; et al. Hierarchy for targeting prosurvival BCL2 family proteins in multiple myeloma: Pivotal role of MCL1. *Blood* **2016**, *128*, 1834–1844. [CrossRef]
32. Dengler, M.A.; Teh, C.E.; Thijssen, R.; Gangoda, L.; Lan, P.; Herold, M.J.; Gray, D.H.; Kelly, G.L.; Roberts, A.W.; Adams, J.M. Potent efficacy of MCL-1 inhibitor-based therapies in preclinical models of mantle cell lymphoma. *Oncogene* **2020**, *39*, 2009–2023. [CrossRef]
33. Klanova, M.; Kazantsev, D.; Pokorna, E.; Zikmund, T.; Karolova, J.; Behounek, M.; Renesova, N.; Sovilj, D.; Kelemen, C.D.; Helman, K.; et al. Anti-apoptotic MCL1 Protein Represents Critical Survival Molecule for Most Burkitt Lymphomas and BCL2-negative Diffuse Large B-cell Lymphomas. *Mol. Cancer Ther.* **2022**, *21*, 89–99. [CrossRef]
34. Manzano, M.; Patil, A.; Waldrop, A.; Dave, S.S.; Behdad, A.; Gottwein, E. Gene essentiality landscape and druggable oncogenic dependencies in herpesviral primary effusion lymphoma. *Nat. Commun.* **2018**, *9*, 3263. [CrossRef]
35. Ewald, L.; Dittmann, J.; Vogler, M.; Fulda, S. Side-by-side comparison of BH3-mimetics identifies MCL-1 as a key therapeutic target in AML. *Cell Death Dis.* **2019**, *10*, 917. [CrossRef]
36. Braun, F.K.; Al-Yacoub, N.; Plötz, M.; Möbs, M.; Sterry, W.; Eberle, J. Nonsteroidal anti-inflammatory drugs induce apoptosis in cutaneous T-cell lymphoma cells and enhance their sensitivity for TNF-related apoptosis-inducing ligand. *J. Invest. Derm.* **2012**, *132*, 429–439. [CrossRef]
37. Sumarni, U.; Reidel, U.; Eberle, J. Targeting Cutaneous T-Cell Lymphoma Cells by Ingenol Mebutate (PEP005) Correlates with PKCδ Activation, ROS Induction as Well as Downregulation of XIAP and c-FLIP. *Cells* **2021**, *10*, 987. [CrossRef]
38. Smith, V.M.; Dietz, A.; Henz, K.; Bruecher, D.; Jackson, R.; Kowald, L.; van Wijk, S.J.L.; Jayne, S.; Macip, S.; Fulda, S.; et al. Specific interactions of BCL-2 family proteins mediate sensitivity to BH3-mimetics in diffuse large B-cell lymphoma. *Haematologica* **2020**, *105*, 2150–2163. [CrossRef]
39. Valiuliene, G.; Vitkeviciene, A.; Skliute, G.; Borutinskaite, V.; Navakauskiene, R. Pharmaceutical Drug Metformin and MCL1 Inhibitor S63845 Exhibit Anticancer Activity in Myeloid Leukemia Cells via Redox Remodeling. *Molecules* **2021**, *26*, 2303. [CrossRef]
40. Paoluzzi, L.; Gonen, M.; Bhagat, G.; Furman, R.R.; Gardner, J.R.; Scotto, L.; Gueorguiev, V.D.; Heaney, M.L.; Manova, K.; O'Connor, O.A. The BH3-only mimetic ABT-737 synergizes the antineoplastic activity of proteasome inhibitors in lymphoid malignancies. *Blood* **2008**, *112*, 2906–2916. [CrossRef]
41. Del Gaizo Moore, V.; Schlis, K.D.; Sallan, S.E.; Armstrong, S.A.; Letai, A. BCL-2 dependence and ABT-737 sensitivity in acute lymphoblastic leukemia. *Blood* **2008**, *111*, 2300–2309. [CrossRef] [PubMed]
42. Touzeau, C.; Dousset, C.; Bodet, L.; Gomez-Bougie, P.; Bonnaud, S.; Moreau, A.; Moreau, P.; Pellat-Deceunynck, C.; Amiot, M.; Le Gouill, S. ABT-737 Induces Apoptosis in Mantle Cell Lymphoma Cells with a Bcl-2high/Mcl-1low Profile and Synergizes with Other Antineoplastic Agents. *Clin. Cancer Res.* **2011**, *17*, 5973–5981. [CrossRef]
43. Bodet, L.; Gomez-Bougie, P.; Touzeau, C.; Dousset, C.; Descamps, G.; Maïga, S.; Avet-Loiseau, H.; Bataille, R.; Moreau, P.; Le Gouill, S.; et al. ABT-737 is highly effective against molecular subgroups of multiple myeloma. *Blood* **2011**, *118*, 3901–3910. [CrossRef]
44. Adams, C.M.; Kim, A.S.; Mitra, R.; Choi, J.K.; Gong, J.Z.; Eischen, C.M. BCL-W has a fundamental role in B cell survival and lymphomagenesis. *J. Clin. Investig.* **2017**, *127*, 635–650. [CrossRef]

45. Diepstraten, S.T.; Chang, C.; Tai, L.; Gong, J.-n.; Lan, P.; Dowell, A.C.; Taylor, G.S.; Strasser, A.; Kelly, G.L. BCL-W is dispensable for the sustained survival of select Burkitt lymphoma and diffuse large B-cell lymphoma cell lines. *Blood Adv.* **2020**, *4*, 356–366. [CrossRef]
46. Wang, H.; Guo, M.; Wei, H.; Chen, Y. Targeting MCL-1 in cancer: Current status and perspectives. *J. Hematol. Oncol.* **2021**, *14*, 67. [CrossRef]
47. de Vos, S.; Leonard, J.P.; Friedberg, J.W.; Zain, J.; Dunleavy, K.; Humerickhouse, R.; Hayslip, J.; Pesko, J.; Wilson, W.H. Safety and efficacy of navitoclax, a BCL-2 and BCL-X(L) inhibitor, in patients with relapsed or refractory lymphoid malignancies: Results from a phase 2a study. *Leuk Lymphoma* **2021**, *62*, 810–818. [CrossRef]
48. Pullarkat, V.A.; Lacayo, N.J.; Jabbour, E.; Rubnitz, J.E.; Bajel, A.; Laetsch, T.W.; Leonard, J.; Colace, S.I.; Khaw, S.L.; Fleming, S.A.; et al. Venetoclax and Navitoclax in Combination with Chemotherapy in Patients with Relapsed or Refractory Acute Lymphoblastic Leukemia and Lymphoblastic Lymphoma. *Cancer Discov.* **2021**, *11*, 1440–1453. [CrossRef] [PubMed]
49. Prelude, T. A Study of PRT1419 Injection in Patients With Relapsed/Refractory Hematologic Malignancies. 2022. Available online: https://ClinicalTrials.gov/show/NCT04543305 (accessed on 1 June 2022).
50. Szlávik, Z.; Ondi, L.; Csékei, M.; Paczal, A.; Szabó, Z.B.; Radics, G.; Murray, J.; Davidson, J.; Chen, I.; Davis, B.; et al. Structure-Guided Discovery of a Selective Mcl-1 Inhibitor with Cellular Activity. *J. Med. Chem.* **2019**, *62*, 6913–6924. [CrossRef]
51. Kaltoft, K.; Bisballe, S.; Dyrberg, T.; Boel, E.; Rasmussen, P.B.; Thestrup-Pedersen, K. Establishment of two continuous T-cell strains from a single plaque of a patient with mycosis fungoides. *Vitr. Cell Dev. Biol.* **1992**, *28*, 161–167. [CrossRef]
52. Kaltoft, K.; Bisballe, S.; Rasmussen, H.F.; Thestrup-Pedersen, K.; Thomsen, K.; Sterry, W. A continuous T-cell line from a patient with Sézary syndrome. *Arch. Derm. Res.* **1987**, *279*, 293–298. [CrossRef] [PubMed]
53. Gazdar, A.F.; Carney, D.N.; Bunn, P.A.; Russell, E.K.; Jaffe, E.S.; Schechter, G.P.; Guccion, J.G. Mitogen Requirements for the In Vitro Propagation of Cutaneous T-Cell Lymphomas. *Blood* **1980**, *55*, 409–417. [CrossRef] [PubMed]
54. Starkebaum, G.; Loughran, T.P., Jr.; Waters, C.A.; Ruscetti, F.W. Establishment of an IL-2 independent, human T-cell line possessing only the p70 IL-2 receptor. *Int J. Cancer* **1991**, *49*, 246–253. [CrossRef] [PubMed]
55. Eberle, J.; Fecker, L.F.; Hossini, A.M.; Wieder, T.; Daniel, P.T.; Orfanos, C.E.; Geilen, C.C. CD95/Fas signaling in human melanoma cells: Conditional expression of CD95L/FasL overcomes the intrinsic apoptosis resistance of malignant melanoma and inhibits growth and progression of human melanoma xenotransplants. *Oncogene* **2003**, *22*, 9131–9141. [CrossRef] [PubMed]

cells

MDPI

Article

Targeting Cutaneous T-Cell Lymphoma Cells by Ingenol Mebutate (PEP005) Correlates with PKCδ Activation, ROS Induction as Well as Downregulation of XIAP and c-FLIP

Uly Sumarni, Ulrich Reidel and Jürgen Eberle *

Apoptosis Regulation in Skin Cancer, Skin Cancer Center Charité, Department of Dermatology Venerology und Allergology, Charité—Universitätsmedizin Berlin, corporate member of Freie Universität Berlin and Humboldt-Universität zu Berlin, 10117 Berlin, Germany; uly.sumarni@googlemail.com (U.S.); ulrich.reidel@charite.de (U.R.)

* Correspondence: juergen.eberle@charite.de; Tel.: +49-30-450-518-383

Abstract: New therapeutic strategies are needed for cutaneous T-cell lymphoma (CTCL), and the plant extract ingenol mebutate (PEP005) may be considered. PEP005 has been approved for actinic keratosis, and proapoptotic activities were described in different cancer cells. Here, we aimed to investigate its efficacy in four CTCL cell lines and its mode of action. While HuT-78 and HH responded with induced apoptosis as well as with loss of cell viability and cell proliferation, MyLa and SeAx remained resistant. Interestingly, both sensitive and resistant cells showed caspase-8 activation and enhanced levels of reactive oxygen species (ROS), while final caspase-3 activation was restricted to sensitive cells. Apoptosis induction was prevented by the caspase inhibitor QVD-Oph as well as by the antioxidant vitamin E. Caspase activation by PEP005 may be explained to some extent by the downregulation of the caspase antagonistic proteins c-FLIP and XIAP in sensitive cells, whereas both proteins were strongly expressed in resistant cells. Finally, PEP005 resulted in the activation of proapoptotic PKCδ, and the PKC inhibitor bisindolylmaleimide I reduced apoptosis, caspase-3 processing and ROS production, as well as restored cell viability. In conclusion, PKCδ appeared as a central player in apoptosis regulation in CTCL cells, also suggesting its therapeutic targeting.

Keywords: cutaneous T-cell lymphoma (CTCL); PEP005; PKC-delta; apoptosis; caspases; ROS; XIAP; c-FLIP

check for updates

1. Introduction

Cutaneous T-cell lymphomas (CTCL) form a heterogeneous group of extranodal non-Hodgkin's lymphomas and are characterized by primary cutaneous manifestation and clonal proliferation of skin-homing memory T-lymphocytes. In clinical appearance and prognosis, CTCL are clearly distinct from the histotypically cognate systemic lymphomas and their possible secondary cutaneous manifestations. The different characteristics of CTCL were acknowledged by the WHO/EORTC classification. The group of CTCL encloses Mycosis fungoides, Sézary syndrome and CD30(+) lymphoproliferative disorders [1,2]. The incidence of CTCL is at 3–4 cases per one million per year in Europe and at 10 cases per one million per year in the United States [3,4]. In its early stage, CTCL may show an often indolent clinical course, whereas in the later phase, it frequently transforms to a rapidly growing, malignant phenotype, significantly decreasing life expectancy [2,5]. New and alternative therapeutic options are needed for early and late disease.

The elimination of tumor cells by the induction of apoptosis represents a principal goal in cancer therapy, while therapy resistance is frequently explained by apoptosis deficiency [6,7]. Also several treatments of CTCL were related to apoptosis induction in tumor T-cells, e.g., phototherapy, photopheresis, the retinoid bexarotene and the histone deacetylase inhibitor vorinostat [8–11].

Two major pathways drive apoptosis induction. Thus, extrinsic proapoptotic pathways are initiated by death ligands, such as CD95L/FasL and TNF-related apoptosis-inducing ligand (TRAIL). Their binding to death receptors results in the formation of a death-inducing signaling complex and activation of initiator caspase-8 and caspase-10 [12]. Caspase-8 can cleave and activate the main effector caspase-3, which itself cleaves a large number of death substrates with the final result of DNA fragmentation and apoptosis induction [13]. While caspase-8 activation can be inhibited in a competitive mechanism by cellular FLICE-like inhibitory protein (c-FLIP) [14,15], caspase-3 is negatively regulated through the binding of chromosome X-linked inhibitor of apoptosis protein (XIAP) [16,17]. On the other hand, intrinsic apoptosis pathways are activated in response to cellular stress situations, e.g., by chemotherapy or DNA damage, and are critically regulated by the family of Bcl-2 proteins [18]. In particular, they rely on the loss of mitochondrial membrane potential and release of mitochondrial factors, such as cytochrome c, which triggers the activation of initiator caspase-9, which again can activate effector caspases [19].

In CTCL cells, activation of the extrinsic apoptosis pathways is of major importance. Thus, apoptosis resistance correlated with reduced expression of death receptor CD95/Fas as well as with high and constitutive expression of c-FLIP [20–22]. Additionally, activation of the prosurvival transcription factor NF-κB and of STAT3 was reported [23–26]. In particular, different therapeutic strategies, such as NSAIDs, suberoylanilide hydroxamic (SAHA) pentoxifylline and indirubin derivatives, resulted in the downregulation of c-FLIP and XIAP in CTCL cells [10,27–29]. Furthermore, reactive oxygen species (ROS) may contribute to the regulation of apoptosis, as shown in CTCL cells for an indirubin derivative [27]. ROS may derive from mitochondrial leakage or other sources [30], but their relation to described apoptosis pathways is less clear to date.

The protein kinase C (PKC) family of isoenzymes encloses several serine-threonine kinases, which are involved in the regulation of different cellular processes, including cell proliferation, cell differentiation and apoptosis [31]. While PKCα and PKCβ in particular support cell proliferation and cell invasion [32], PKCδ was reported as proapoptotic. Following possible phosphorylation and translocation steps, PKCδ can be activated through processing, which releases the active catalytic domain (41 kDa) from its 78 kDa proform. It was suggested that PKCδ can induce apoptosis through tyrosine phosphorylation and activation of caspase-3 [33,34].

Ingenol 3-angelate or ingenol mebutate (PEP005) is a hydrophobic diterpene ester isolated from the plant Euphorbia peplus. Its antineoplastic effects have been reported in different kinds of cancer cells, such as in leukemia, colon cancer and melanoma cells [31,35–38]. PEP005 has been approved by the FDA for the treatment of actinic keratosis in 2012. Here, we investigated its effects on cutaneous T-cell lymphoma cells and elucidated its mechanism of action. In this way, we aimed to identify strategies and additional molecular targets in CTCL cells for the induction of apoptosis.

2. Materials and Methods

2.1. Cell Culture and Treatment

For investigating the effects of PEP005 in CTCL cells, four representative CTCL cell lines were used. MyLa derived from a plaque biopsy of a patient with MF [39]; SeAx [40] and HuT-78 [41] derived from PBMCs of patients with Sézary syndrome; HH (ATCC, Manassas, VA, USA; CRL2105) derived from peripheral blood of a patient with aggressive CTCL [42]. Cells were maintained at 5% CO_2 in RPMI 1640 growth medium (Life Technologies, Darmstadt, Germany) supplemented with 10% FCS, 600 μM L-glutamine and antibiotics.

Most assays were performed in 24-well plates, and 5×10^4 cells were seeded per well. Cells were treated with 2–2000 nM ingenol mebutate (PEP005; AdipoGen Life Sciences, Liestal, Switzerland). Control cells received the solvent DMSO in the same concentrations as used for PEP005-treated cells (max. 0.2%). For caspase inhibition, cells received the pan-caspase inhibitor QVD-Oph (Abcam, Cambridge, UK; 10 μM) at 1 h before agonists

were applied. For ROS scavenging, cells were pre-treated for 1 h with 1 mM α-tocopherol (vitamin E, Fluka, Steinheim, Germany). For inhibition of PKCδ, bisindolylmaleimide I (Bis 1; Cayman Chemical, Ann Arbor, MI, USA) was used at 1 μM in HH and at 0.25 μM in HuT-78, respectively.

2.2. Determination of Apoptosis, Cytotoxicity, Cell Viability and Cell Proliferation

Quantification of apoptosis was performed by cell cycle analysis. Harvested cells were lysed in hypotonic buffer, and isolated nuclei were stained for 1 h with 40 mg/mL propidium iodide (Sigma-Aldrich, St. Louis, MO, USA). Cells in G1, G2 and S-phase as well as sub-G1 cells were quantified by flow cytometry at FL3A with a FACS Calibur (BD Bioscience, Bedford, MA, USA). Due to the washing out of small DNA fragments, nuclei with less DNA than G1 (sub-G1) correspond to apoptotic cells.

Cell viability was determined by staining cells with calcein-AM (PromoCell, Heidelberg, Germany), which is converted through intracellular esterase activity in viable cells to green-fluorescent calcein. Cells, grown and treated in 24-well plates, were harvested and stained for 1 h with 0.5 μM calcein-AM at 37 °C. After labeling, cells were washed with PBS and measured by flow cytometry (FL2H).

Cell proliferation was determined by WST-1 assay (Roche Diagnostics) following the protocol of the supplier. The assay depends on the cleavage of the water-soluble tetrazolium (WST) salt by mitochondrial dehydrogenases in metabolically active cells.

2.3. Mitochondrial Membrane Potential and Reactive Oxygen Species (ROS)

Mitochondrial membrane potential was determined by staining cells with the fluorescent dye $TMRM^+$ (Sigma-Aldrich). Cells, grown and treated in 24-well plates, were harvested and stained for 20 min at 37 °C in 1 μM $TMRM^+$. After washing twice with PBS, cell staining was quantified by flow cytometry (FL2H).

For the determination of intracellular ROS levels, cells grown in 24-well plates were pre-incubated for 1 h with the fluorescent dye H_2DCFDA (D-399, Thermo Fisher Scientific, Hennigsdorf, Germany, 10 μM), before starting treatment with effectors. After 2–24 h treatment, cells were harvested, washed several times with PBS and analyzed by flow cytometry (FL1H). As positive controls, cells were treated with H_2O_2 (1 mM, 1 h).

2.4. Western Blotting

For Western blotting, total protein extracts were obtained in cell lysis buffer containing 150 mM NaCl, 1 mM EDTA, 1% NP-40, 50 mM Tris (pH 8.0), as well as phosphatase and protease inhibitors. Following SDS polyacrylamide gel electrophoresis, proteins were blotted on nitrocellulose membranes.

Primary antibodies of Cell Signaling (Danvers, MA, USA): caspase-3 (9662, rabbit, 1:1000), cleaved caspase-3 (9664, rabbit, 1:1000), caspase-8 (9746, mouse, 1:1000), caspase-9 (9502, rabbit, 1:1000), XIAP (2042, rabbit, 1:1000). Primary antibodies of Santa Cruz Biotech (Dallas, TX, USA): c-FLIP (sc-5276, mouse, 1:500), p21 (sc-6246, mouse, 1:500), p53 (sc-126, mouse, 1:500), GAPDH (sc-32233, mouse, 1:1000). The antibody for PKCδ (PA587443, rabbit polyclonal, 1:1000) was from Thermo Fisher Scientific (Hennigsdorf, Germany). As secondary antibodies, peroxidase-labelled goat anti-rabbit and goat anti-mouse (Dako, Hamburg, Germany; 1:5000) were used.

2.5. Statistical Analyses

All assays were performed in triplicate determinations, and at least two independent experiments were performed. Presented Western blot data were verified by at least two independent series of cellular extracts. Statistical significance was proven by a Student's *t*-test (2-tailed, heteroscedastic) using all data of independent experiments (at least six individual measurements); *p*-values < 0.05 were considered as statistically significant.

3. Results

3.1. Effects of PEP005 on Apoptosis, Cell Viability and Cell Proliferation

Induction of apoptosis and loss of cell viability represent highly critical issues in cancer therapy. For investigating the potential therapeutic efficiency of PEP005 in cutaneous T-cell lymphoma, four CTCL cell lines (HH, HuT-78, MyLa and SeAx) were treated with increasing concentrations (2 nM–2 μM) for 48 h. Apoptosis was determined by cell cycle analysis and quantification of sub-G1 cells, while cell viability was monitored by calcein-AM staining. Apoptosis was significantly induced in HH and HuT-78, resulting in 19% and 42% apoptotic cells, respectively (50 nM PEP005). There was no further increase in apoptosis with higher concentrations; rather, 50 nM appeared as most efficient. In clear contrast, almost no apoptosis induction was observed in MyLa and SeAx (Figure 1a). In parallel with apoptosis, cell viability significantly decreased in sensitive cells, resulting in 88% of the control (HH, 50 nM) and 54% of the control (HuT-78, 50 nM), respectively. Again, effects were less pronounced in MyLa and SeAx (Figure 1b).
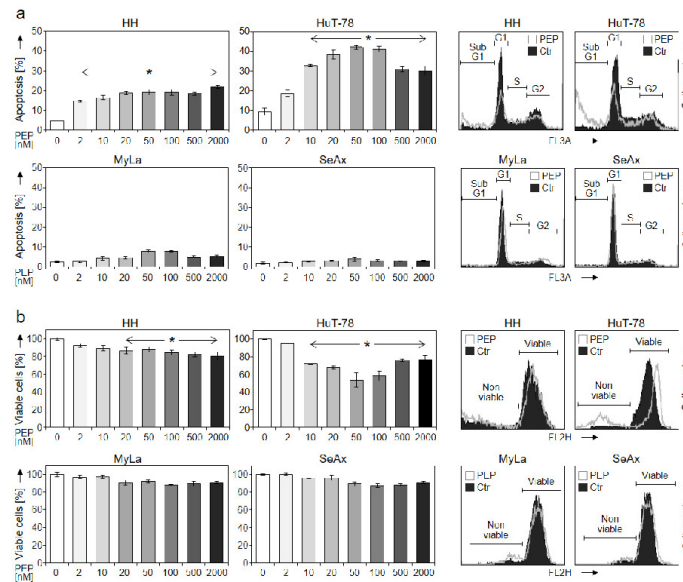

Figure 1. Dose dependency of induced apoptosis and decreased cell viability. Apoptotic rates (propidiumiodide staining, **a**) and cell viability (calcein staining, **b**) were determined in four CTCL cell lines (HH, HuT-78, MyLa and SeAx) treated for 48 h with increasing concentrations of PEP005 (2, 10, 20, 50, 100, 500, 2000 nM). Apoptotic rates correspond to percentages of cells with fragmented DNA, which were determined as sub-G1 cells. Cell viability values are shown in relation to non-treated controls, which were set to 100%. Characteristic histograms of cells treated with 50 nM PEP005 (PEP) are shown on the right side in overlays with control cells (Ctr). Cell populations in cell cycle phases G1, S, G2 and sub-G1 cells as well as viable and non-viable cells are indicated in (**a**,**b**), respectively. Mean values of triplicates ± SDs of representative experiments are shown. At least two independent experiments (each one with triplicates) revealed highly similar data. Statistical significance was calculated from all values (at least 6) and is shown for treated cells vs. controls (* $p < 0.05$).

Time dependency of apoptosis and cell viability were investigated at 24, 48 and 72 h (50 nM PEP005). The rate of apoptotic cells further increased with time resulting in 39% and 73% at 72 h in HH and HuT-78, respectively (Figure 2a). In parallel, cell viability further decreased with time, resulting in 52% and 50% viable cells at 72 h in HH and HuT-78, respectively, as compared to the controls (Figure 2b). Also some less pronounced effects were seen in resistant cells at 72 h. Thus, apoptosis was at 15% and 13%, and cell viability was at 75% and 76% in MyLa and SeAx, respectively (Figure 2a,b).
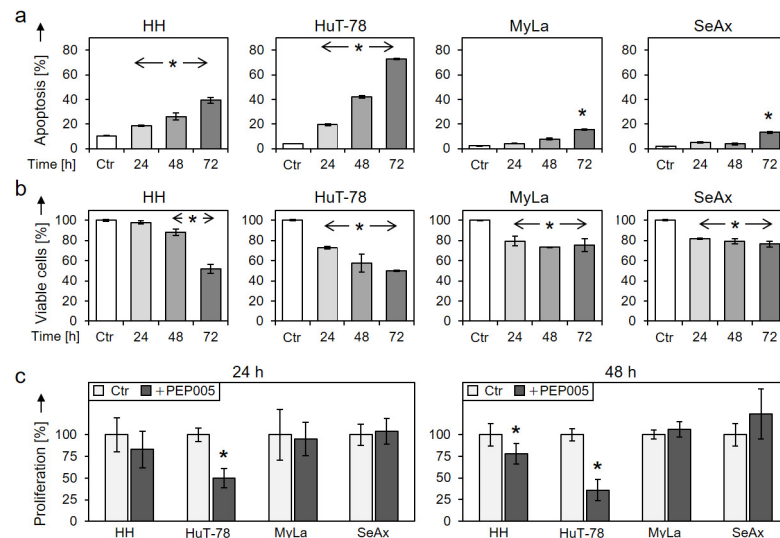
Figure 2. Time dependency and cell proliferation. Time dependency of (**a**) induced apoptosis and of (**b**) reduced cell viability were determined in four cell lines at 24, 48 and 72 h of treatment with 50 nM PEP005. For cell viability, non-treated controls were set to 100% (Ctr). (**c**) Cell proliferation rates of CTCL cell lines at 24 and 48 h in response to 50 nM PEP005 were determined by WST-1 assay. Values are given in relation to non-treated controls (Ctr), set to 100%. At least two independent experiments were performed, each one with triplicate values; statistical significance was calculated from all values (* $p < 0.05$).

In parallel, cell proliferation decreased in HH and HuT-78, as determined by WST-1 assay. Thus, at 48 h, cell proliferation in response to 50 nM PEP005 was at 78% and 36% in HH and HuT-78, respectively, whereas no antiproliferative effects were seen in MyLa and SeAx (Figure 2c).

3.2. Effects on Mitochondrial Membrane Potential (MMP) and ROS Levels

Loss of MMP, which is characteristic of the activation of intrinsic apoptosis pathways, was monitored at 24 h of treatment with 50 nM PEP005. In the most responsive cell line HuT-78, a significant loss of MMP was seen (36% of cells), while HH, MyLa and SeAx were not responsive (Figure 3a). Cell death pathways in cancer cells may be further induced by enhanced levels of reactive oxygen species (ROS). Indeed, increased ROS levels in response to PEP005 were seen in all four cell lines at 24 h of treatment, which, however, did not correlate with the apoptotic response nor with the concentration applied (Figure 3b).
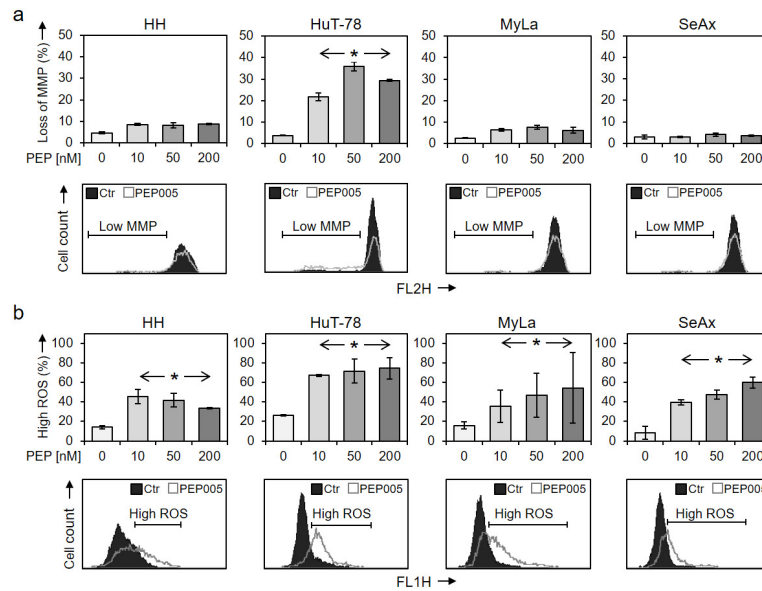
Figure 3. Loss of mitochondrial membrane potential and enhanced ROS levels. Changes of (**a**) mitochondrial membrane potential (MMP) and of (**b**) ROS levels were determined at 24 h of treatment with 10, 50 and 200 nM PEP005. Mean values of triplicates ± SDs are shown; a second independent series of experiments revealed highly comparable results. Representative histograms (overlays of treated cells vs. controls) are given below the bar charts, and cells with low MMP (**a**) or with high ROS (**b**) are indicated. Statistical significance was calculated from two independent experiments (at least six values) and is indicated for treated cells vs. controls (* $p < 0.05$).

3.3. Effects of PEP005 on Apoptosis-Related Proteins

To illuminate the mechanisms of PEP005-induced apoptosis in CTCL cells, apoptosis-related proteins were investigated by Western blotting. Processing of the initiator caspase of the extrinsic apoptosis pathway (caspase-8; 43, 41 kDa fragments) and of the initiator caspase of the intrinsic pathway (caspase-9, 35 kDa fragment) are indicative of an initiation of proapoptotic caspase cascades. Interestingly, strongest caspase-8 processing was seen in the two resistant cell lines MyLa and SeAx. Additionally, some caspase-9 processing was seen in HuT-78, MyLa and SeAx (Figure 4a). Initiator caspases thus appeared to be activated in response to PEP005 also in resistant CTCL cells, suggesting that apoptosis pathways may be blocked at subsequent steps.

The activation steps of effector caspases are different. As for caspase-3, an intermediate fragment of 21 kDa, which is due to processing by initiator caspases, does not yet represent an activated caspase-3. The mature caspase is rather represented by a 17 kDa fragment, which is due to caspase-3 autoprocessing. In line with caspase-8 activation in the resistant cells MyLa and SeAx, caspase-3 was also processed in these cells to its 21 kDa fragment; however, final processing to the active caspase-3 (17 kDa) was lacking in resistant cells at 24 and 48 h (Figure 4a,b). In clear contrast, the 17 kDa fragment of caspase-3 was strongly induced in HuT-78 at 24 h (Figure 4a) and in HH at 48 h (Figure 4b).

We thus looked for factors that can suppress caspase activity. Striking differences were observed for c-FLIP long and short isoforms (c-FLIP$_{L/S}$) and for XIAP, which serve as caspase-8 and caspase-3 antagonists, respectively. In resistant MyLa and SeAx, these proteins were strongly expressed, and c-FLIP$_{L/S}$ were even upregulated by PEP005. In contrast, c-FLIP$_{L/S}$ were only weakly expressed in HuT-78, and they were downregulated in HH by PEP005. Similarly, XIAP was weakly expressed in HH and downregulated by

PEP005 in HuT-78 (Figure 4a). These findings suggest a critical role of caspase antagonistic factors for limiting the sensitivity of CTCL cells to PEP005.
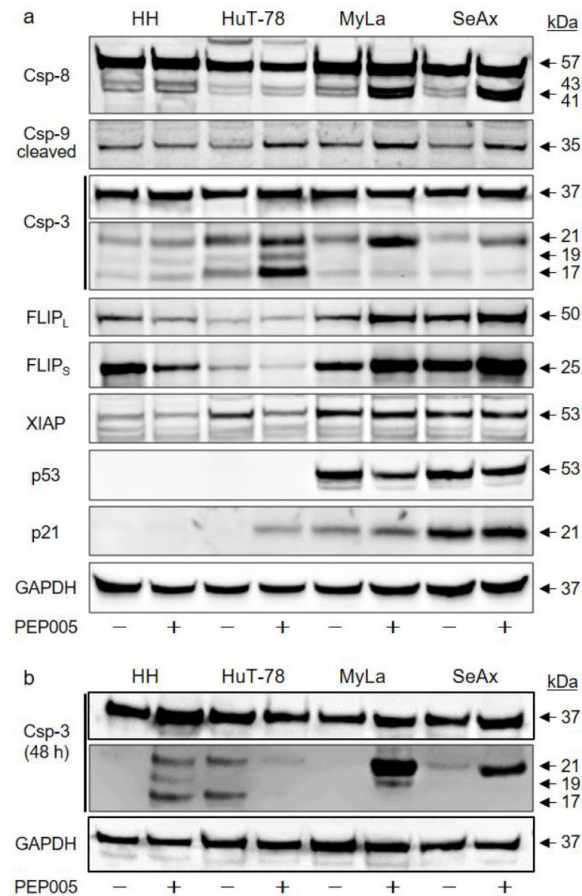

Figure 4. Effects on protein expression. (**a**) Effects of PEP005 (50 nM) on caspases and other apoptosis-related proteins were determined by Western blotting in four CTCL cell lines at 24 h of treatment. (**b**) For caspase-3, 48 h treatment was also investigated. (**a**, **b**) An amount of 30 μg of each protein extract was loaded per lane. Blots were probed with antibodies for caspase-8 (proform, 57 kDa; cleavage products, 43, 41 kDa), caspase-9 (cleavage product, 35 kDa), caspase-3 (proform, 35 kDa; cleavage products, 21, 19, 17 kDa), c-FLIP long/short isoforms (c-FLIP$_{L/S}$, 50/25 kDa), XIAP (53 kDa), p53 and p21 (53 and 21 kDa, respectively). The housekeeping protein GAPDH (37 kDa) was used as the loading control. Two independent series of protein extracts and Western blotting experiments revealed highly comparable results.

The expression of the tumor suppressor and proapoptotic transcription factor p53 negatively correlated with PEP005 sensitivity, as it was strongly expressed in resistant cells but completely lacking in HH and HuT-78. Similarly, the cell cycle inhibitor p21 was completely lacking in HH but strongly expressed in MyLa and SeAx. Only in HuT-78, p21 followed the expected regulation, namely, it was induced by PEP005 in parallel with inhibited cell proliferation (Figure 4a). Thus, p21 may contribute to the inhibition of cell proliferation in HuT-78 but not in other cell lines.

3.4. Inhibition of Apoptosis by QVD and by Vitamin E

We aimed to prove the caspase dependency of PEP005-induced apoptosis as well as its relation to ROS production. By using the pancaspase inhibitor QVD-Oph, apoptosis induction in HH and HuT-78 was almost completely prevented (Figure 5a), which was associated with the partial restoration of cell viability (Figure 5b). Western blotting revealed that caspase-3 processing in response to PEP005 was arrested by QVD-Oph at the level of the p21 intermediate cleavage product, clearly indicating the inhibition of the caspase-3 auto-processing step through QVD-Oph (Figure 5c).
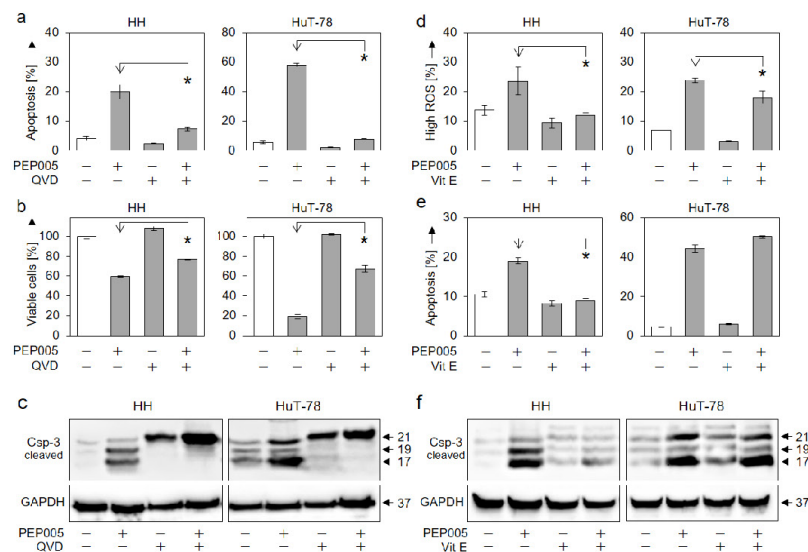
Figure 5. Inhibition of PEP005-mediated effects by QVD-Oph and vitamin E. Antagonistic effects of the pan-caspase inhibitor QVD-Oph (QVD, 5 µM, **a**–**c**) and of the antioxidant vitamin E (VitE, 1 mM, **d**–**f**) were determined in HH and HuT-78 cells. Assays included the determination of apoptosis (**a**,**e**, 48 h), cell viability (**b**, 48 h), ROS production (**d**, 24 h) and caspase-3 processing (**c**,**f**, Western blots, 24 h). (**a**,**b**,**d**,**e**) Mean values of triplicates ± SDs of representative experiments are shown. At least two independent experiments were performed. Statistical significance was calculated by using all values (at least 6) and is indicated for combination treatments vs. PEP005 alone (* $p < 0.05$). (**c**,**f**) Caspase-3 cleavage products (21, 19, 17 kDa) are indicated. Each 30 µg of protein extracts were loaded per lane. GAPDH (37 kDa) served as loading control. Two independent series of protein extracts and Western blots revealed highly comparable results.

Concerning the role of ROS, we show here that the antioxidant vitamin E can abolish ROS production in response to PEP005 in HH cells, while ROS could only be slightly decreased in HuT-78 (Figure 5d). In parallel, vitamin E prevented PEP005-induced apoptosis (Figure 5e) as well as the activation of caspase-3 in HH but not in HuT-78 (Figure 5f). We thus conclude that the antineoplastic effects of PEP005 in CTCL cells enclosed both caspase and ROS-mediated pathways.

3.5. Role of PKCδ in PEP005-Induced Apoptosis in CTCL

Proapoptotic activities have been attributed to protein kinase C delta (PKCδ), and previous studies have indicated that PEP005 functions as a PKCδ inhibitor. Here, we show significant activation of PKCδ in all four CTCL cell lines in response to 50 nM PEP005 (Figure 6a). Thus, in all cell lines, the 78 kDa proform was strongly reduced, indicating its processing, which was described to release the 41 kDa active catalytic domain [33,34]. PKCδ activation appeared to be upstream of both caspase-3 and ROS, as its processing could be inhibited neither by QVD-Oph nor by vitamin E (Figure 6b,c).
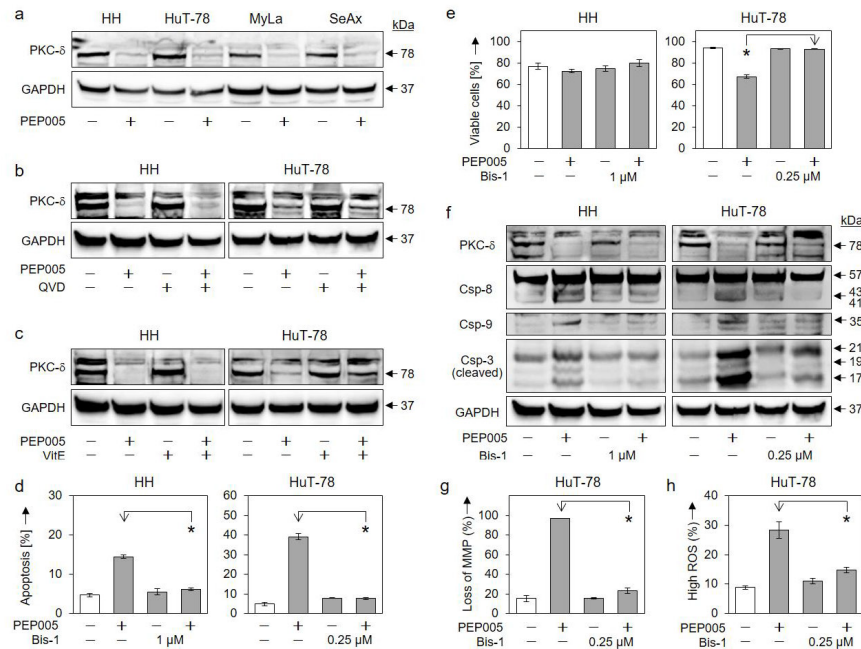
Figure 6. Role of PKCδ in PEP005-induced apoptosis. (**a**) Effects of PEP005 (50 nM, 24 h) on PKCδ proform (78 kDa) were investigated in four CTCL cell lines. (**b,c**) Lacking effects of QVD-Oph (QVD, 5 μM, b) and vitamin E (VitE, 1 mM, **c**) on PEP005-induced downregulation of PKCδ proform are shown (50 nM, 24 h). (**d,e**) Inhibition of PEP005-induced apoptosis (**d**) and restoration of cell viability (**e**) by Bis-1 in HH and HuT-78. Cells were treated for 24 h with PEP005 (50 nM) and/or Bis-1 (HH, 1 μM; HuT-78, 0.25 μM). (**f**) Inhibition of PEP005-mediated caspase-3, -8, and -9 processing through Bis-1, as investigated by Western blotting in HH and HuT-78. Cells were treated for 24 h with 50 nM PEP005; Bis-1 was used at 1 (HH) and 0.25 μM (HuT-78), respectively. (**g,h**) Antagonistic effects of Bis-1 on PEP005-mediated loss of MMP (**g**) and on PEP005-induced ROS production (**h**) in cell line HuT-78 (Time: 24 h; PEP005: 50 nM; Bis-1: 0.25 μM). (**a–c,f**) For Western blotting, 30 μg of each protein extract was loaded per lane, and blots were probed with antibodies for PKCδ proform (78 kDa), cleaved caspase-3 (21, 19, 17 kDa), caspase-8 (proform, 57 kDa; cleavage products, 43/41 kDa) and caspase-9 (cleavage product, 35 kDa). GAPDH (37 kDa) was used as loading control. For Western blots, two independent series of protein extracts revealed highly comparable results. (**d,e,g,h**) Mean values of triplicates ± SDs of representative experiments are shown. At least two independent experiments showed highly comparable results. Statistical significance was calculated from all values (at least 6) and is indicated for combination-treated cells vs. PEP005-treated cells (* $p < 0.05$).

The role of PKCδ in PEP005-mediated effects in CTCL cells was further investigated by the PKC inhibitor bisindolylmaleimide-1 (Bis-1). Underlining the critical role of PKCδ, PEP005-induced apoptosis was completely abolished by Bis-1 in HH and HuT-78, and cell viability was restored (Figure 6d,e). While Bis-1 did not affect PKCδ activation itself, it largely abolished PEP005-mediated processing of caspase-3, -8 and -9 (Figure 6f). Bis-1 also prevented PEP005-mediated loss of MMP (Figure 6g) and ROS production (Figure 6h) in HuT-78 cells. Thus, PKCδ appeared to be a master regulator in PEP005-induced effects in CTCL cells, and its activation appeared to be upstream of all other effects (Figure 7).
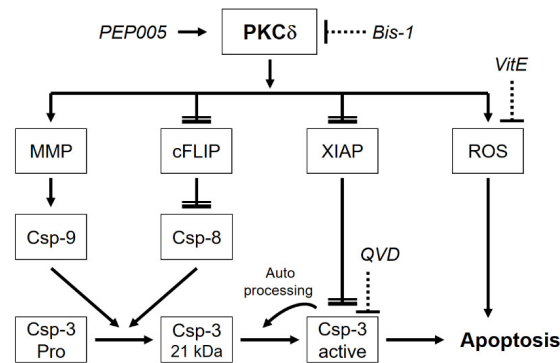
Figure 7. Molecular mechanisms of PKCδ-induced apoptosis in CTCL cells. In CTCL cells, PKCδ is induced by PEP005 and drives loss of mitochondrial membrane potential (MMP) related to caspase-9 activation, downregulation of c-FLIP related to caspase-8 activation, downregulation of XIAP related to caspase-3 activation as well as induction of reactive oxygen species (ROS) related to additional apoptosis promotion. The proform of caspase-3 (Pro) is cleaved by caspase-9 and caspase-8 to a 21 kDa intermediate product. Final processing to active caspase-3 is due to caspase-3 autocatalytic activity. For understanding the mechanisms, the PKC inhibitor bisindolylmaleimide I (Bis-1), the antioxidant vitamin E (VitE) and the pancaspase inhibitor QVD-Oph (QVD) were used. Further explanations are provided in the text.

4. Discussion

The plant extract ingenol mebutate PEP005 is considered for clinical development in blood and solid tumors. Its antineoplastic effects have been reported in cells of different cancer types, such as leukemia, colon cancer and melanoma [31,35–38,43]. In the present study, significant induction of apoptosis in response to PEP005 is reported in two of four CTCL cell lines, associated with reduced cell viability and cell proliferation. The sensitivity did not correlate to the cells' origin of either MF or Sézary patients [44]; rather, cell lines from both groups were either sensitive (HH, HuT-78) or resistant (MyLa, SeAx).

Deficient apoptosis programs are of particular importance for the pathogenesis of cancer, and thus induction of apoptosis and decrease in cell viability represent particular goals in cancer therapy [7]. Proapoptotic effects of PEP005 have also been reported previously in leukemia, colon cancer and melanoma cell lines [31,35,37,43]. A selective activity of PEP005 in cancer cells was suggested, as it did not inhibit the growth of human neonatal fibroblasts [38] and did not induce apoptosis in normal CD34(+) cord blood myeloblasts [35]. Despite several side effects reported for PEP005, the results of clinical trials and finally its FDA approval may largely rule out severe effects on normal human T-lymphocytes [45,46].

A major challenge in cancer therapy is to reach effective drug concentrations in target cells. For HH and HuT-78, relatively moderate concentrations of only 50 nM turned out to be highly effective, and apoptosis induction was not further increased by increasing the dose. Comparable effective concentrations (10–50 nM) were reported for sensitive myeloid leukemia cells and melanoma cells as well as for one of four tested colon cancer cell lines (Colo205). In contrast, several other melanoma and colon cancer cell lines were largely resistant or needed concentrations of 1–100 μM [31,35,37,38,43]. Also MyLa and SeAx remained resistant at 48 h up to 2 μM of PEP005. Thus, treatment with PEP005 may apply for a subset of CTCL patients, and there seems to be an optimal concentration range for obtaining the best response, which is low enough that it may also be achieved in clinical settings.

Apoptosis can be mediated by caspase-dependent or -independent pathways [47]. Activation of the main effector caspase-3 in response to PEP005 was reported in melanoma cells at a concentration of 500 nM [37], but the question, where in the pathway the caspase

cascade may be blocked in resistant cells has not been raised so far. Indicating the activation of caspase cascades, caspase-3 was processed in HuT-78 at 24 h and in HH at 48 h to its 17 kDa mature cleavage product, whereas its processing was arrested in resistant MyLa and SeAx at a 21 kDa intermediate, non-active cleavage product. The situation was different for initiator caspase-8, which appeared as strongly processed and activated in resistant cells. This can be explained by a described mechanism, according to which caspase-8 mediates the processing of procaspase-3 up to the 21 kDa intermediate product, whereas further processing from 21 to 17 kDa is due to caspase-3 auto-processing [48] (Figure 7). As caspase-3 activity was lacking in resistant cells, its processing was arrested at 21 kDa. The essential role of caspases was proven by a pan-caspase inhibitor, which almost completely abolished apoptosis in sensitive cells.

The interruption of the caspase cascade can be due to caspase-antagonistic proteins. While caspase-8 activation can be inhibited in a competitive way by the short and long c-FLIP isoforms [14,15], caspase-3 activity is inhibited by XIAP [16,17]. We report here characteristic correlations of PEP005 sensitivity with the expression and regulation of XIAP and c-FLIP. Thus, in the sensitive CTCL cell lines, both XIAP and c-FLIP were either weakly expressed, or they were downregulated by PEP005. In contrast, in resistant cells, they were strongly expressed and not downregulated. It is suggestive that the constitutively high expression of XIAP in resistant cells prevents caspase-3 activity and activation. The critical function of caspase antagonists in CTCL cells was also described in response to other treatments. Thus, c-FLIP was downregulated by SAHA and NSAIDs, while XIAP was downregulated by SAHA and pentoxifylline in CTCL cells [10,28,29].

Loss of mitochondrial membrane potential (MMP) is part of intrinsic apoptosis pathways activated in response to cellular stress situations [19]. Loss of MMP in response to PEP005 was reported both for sensitive and resistant melanoma cells, when using concentrations of >100 μM [43]. In CTCL cells, the loss of MMP was apparently not absolutely required for PEP005-mediated effects, as not seen in HH. However, the additional activation of intrinsic apoptosis pathways may have a contributory role and may explain the particularly high sensitivity of HuT-78.

An increasing body of evidence in recent years has shown that reactive oxygen species (ROS) may result in induction of apoptosis in cancer cells [27,47,49,50]. Indeed, ROS were induced by PEP005 in all four CTCL cell lines, and antioxidative treatment by vitamin E decreased ROS levels in HH, which was further associated with a reduction in apoptosis and restoration of cell viability. In this setting, ROS may serve as an additional promoter of apoptosis, but ROS alone were not sufficient for the induction of apoptosis in resistant cells.

Mutations in the tumor suppressor p53 were reported in CTCL and associated with advanced disease stage as well as poor prognosis [51]. P53 mutations were also reported in the cell lines used here, as in the coding region (HuT-78, SeAx), a splicing mutation (HH) and gene duplications (MyLa, HH) [44]. Only in MyLa cells, p53 appeared to be transcriptionally active [52]. Here, we saw a complete lack of basal p53 protein expression in HuT-78 and HH, as also reported previously [52]. In colon cancer cells, PEP005-mediated effects on cell cycle arrest and apoptosis induction were p53-independent [53]. This is in agreement with our results, as apoptosis was induced in HH and HuT-78, despite p53 mutation and lack of expression.

Induction of PEP005-induced apoptosis in sensitive CTCL cells was accompanied by a reciprocal loss of cell proliferation. The cyclin-dependent kinase inhibitor p21 can either be activated by p53 or p53-independent [54]. Here, we found significant upregulation of p21 in HuT-78 in response to PEP005, which may contribute to the high sensitivity of this cell line. Clearly, the regulation of p21 in these cells must be p53-independent.

PEP005 was described as an activator of PKCδ, and the dominant role of PKCδ in PEP005-mediated effects was demonstrated in leukemia, colon cancer and melanoma cells [31,35,38,43]. The proapoptotic function of PKCδ has also been shown in response to DNA damaging agents, UV radiation, phorbol 12-myristate-12-acetate and ROS. PKCδ is activated through the processing of its 78 kDa proform, which releases the active 41 kDa

catalytic domain [33,34]. Also in the CTCL cells reported here, activated PKCδ turned out to be the central player in PEP005-induced apoptosis. Its activation was shown here by the consistent loss of the 78 kDa proform, as antibodies did not detect the 41 kDa fragment.

In smooth muscle cells, it was suggested that PKCδ may act both upstream and downstream of caspase-3. Thus, PKCδ could also be processed and activated through caspase-3 [34]. This explanation was ruled out here for CTCL cells, as PKCδ was also activated by PEP005 in resistant MyLa and SeAx, while caspase-3 was not active, and, furthermore, PKCδ processing was not abolished by the pancaspase inhibitor QVD-Oph. Thus, other proteases must be involved in the processing of PKCδ in CTCL cells. PKCδ activation was also not controlled by induced ROS, as its activation was not impaired by the antioxidant vitamin E.

In conclusion, we show here in an in vitro approach the efficacy of PEP005 in a subset of CTCL cell lines, and we shed more light on its mode of action. To further approach a clinical development, the investigation of ex vivo patient samples and in vivo animal experiments may be the next steps. Providing a comparable situation in patients' tumor T-cells, a major challenge will be to identify patients that could profit from this strategy. Based on our in vitro data, resistant cell lines were characterized by distinct molecular characteristics, such as p53 and p21 expression, as well as by enhanced expression of c-FLIP and XIAP, which may serve as candidates for the stratification of patients.

Concerning the mode of action, PKCδ appeared to be an upstream player in PEP005-induced effects, as also proven by the PKC inhibitor Bis-1. An upstream and thus non-specific activity of this inhibitor was largely ruled out, as it remained without effect on PKCδ processing itself. Clearly proving the high-ranking role of PKCδ in PEP005-mediated effects in CTCL cells, Bis-1 prevented all downstream effects as apoptosis induction, caspase-3 activation, induction of ROS, loss of MMP and cell viability. These findings result in the perception that activated PKCδ represents a master regulator in apoptosis control in CTCL cells, triggering the loss of MMP; induction of ROS; downregulation of c-FLIP and XIAP; and the activation of caspase-9, caspase-8 and caspase-3, which may all be linked in a logical network, as suggested in Figure 7. PKCδ thus appears to be an additional molecular target in CTCL for the induction of apoptosis, which may further suggest its therapeutic targeting by PEP005 or by other related strategies.

References

1. Kempf, W.; Zimmermann, A.-K.; Mitteldorf, C. Cutaneous lymphomas—An update 2019. *Hematol. Oncol.* **2019**, *37* (Suppl. S1), 43–47. [CrossRef]
2. Willemze, R.; Cerroni, L.; Kempf, W.; Berti, E.; Facchetti, F.; Swerdlow, S.H.; Jaffe, E.S. The 2018 update of the WHO-EORTC classification for primary cutaneous lymphomas. *Blood* **2019**, *133*, 1703–1714. [CrossRef]
3. Korgavkar, K.; Xiong, M.; Weinstock, M. Changing incidence trends of cutaneous T-cell lymphoma. *JAMA Derm.* **2013**, *149*, 1295–1299. [CrossRef]

4.　Scarisbrick, J.J.; Prince, H.M.; Vermeer, M.H.; Quaglino, P.; Horwitz, S.; Porcu, P.; Stadler, R.; Wood, G.S.; Beylot-Barry, M.; Pham-Ledard, A.; et al. Cutaneous Lymphoma International Consortium Study of Outcome in Advanced Stages of Mycosis Fungoides and Sézary Syndrome: Effect of Specific Prognostic Markers on Survival and Development of a Prognostic Model. *J. Clin. Oncol.* **2015**, *33*, 3766–3773. [CrossRef]

5.　Jawed, S.I.; Myskowski, P.L.; Horwitz, S.; Moskowitz, A.; Querfeld, C. Primary cutaneous T-cell lymphoma (mycosis fungoides and Sézary syndrome): Part I. Diagnosis: Clinical and histopathologic features and new molecular and biologic markers. *J. Am. Acad. Derm.* **2014**, *70*, 205.e1–205.e16. [CrossRef]

6.　Eberle, J. Countering TRAIL Resistance in Melanoma. *Cancers* **2019**, *11*, 656. [CrossRef]

7.　Hanahan, D.; Weinberg, R.A. Hallmarks of cancer: The next generation. *Cell* **2011**, *144*, 646–674. [CrossRef] [PubMed]

8.　Baron, E.D.; Stevens, S.R. Phototherapy for cutaneous T-cell lymphoma. *Dermatol. Ther.* **2003**, *16*, 303–310. [CrossRef] [PubMed]

9.　Zhang, C.; Hazarika, P.; Ni, X.; Weidner, D.A.; Duvic, M. Induction of apoptosis by bexarotene in cutaneous T-cell lymphoma cells: Relevance to mechanism of therapeutic action. *Clin. Cancer Res.* **2002**, *8*, 1234–1240.

10.　Al-Yacoub, N.; Fecker, L.F.; Möbs, M.; Plötz, M.; Braun, F.K.; Sterry, W.; Eberle, J. Apoptosis induction by SAHA in cutaneous T-cell lymphoma cells is related to downregulation of c-FLIP and enhanced TRAIL signaling. *J. Investig. Derm.* **2012**, *132*, 2263–2274. [CrossRef] [PubMed]

11.　Bladon, J.; Taylor, P.C. Extracorporeal photopheresis: A focus on apoptosis and cytokines. *J. Derm. Sci.* **2006**, *43*, 85–94. [CrossRef]

12.　Krammer, P.H.; Arnold, R.; Lavrik, I.N. Life and death in peripheral T cells. *Nat. Rev. Immunol.* **2007**, *7*, 532–542. [CrossRef]

13.　Fischer, U.; Jänicke, R.U.; Schulze-Osthoff, K. Many cuts to ruin: A comprehensive update of caspase substrates. *Cell Death Differ.* **2003**, *10*, 76–100. [CrossRef]

14.　Irmler, M.; Thome, M.; Hahne, M.; Schneider, P.; Hofmann, K.; Steiner, V.; Bodmer, J.L.; Schröter, M.; Burns, K.; Mattmann, C.; et al. Inhibition of death receptor signals by cellular FLIP. *Nature* **1997**, *388*, 190–195. [CrossRef] [PubMed]

15.　Tummers, B.; Green, D.R. Caspase-8: Regulating life and death. *Immunol. Rev.* **2017**, *277*, 76–89. [CrossRef] [PubMed]

16.　Paulsen, M.; Ussat, S.; Jakob, M.; Scherer, G.; Lepenies, I.; Schütze, S.; Kabelitz, D.; Adam-Klages, S. Interaction with XIAP prevents full caspase-3/-7 activation in proliferating human T lymphocytes. *Eur. J. Immunol.* **2008**, *38*, 1979–1987. [CrossRef] [PubMed]

17.　Deveraux, Q.L.; Takahashi, R.; Salvesen, G.S.; Reed, J.C. X-linked IAP is a direct inhibitor of cell-death proteases. *Nature* **1997**, *388*, 300–304. [CrossRef] [PubMed]

18.　Fulda, S.; Debatin, K.M. Extrinsic versus intrinsic apoptosis pathways in anticancer chemotherapy. *Oncogene* **2006**, *25*, 4798–4811. [CrossRef] [PubMed]

19.　Chipuk, J.E.; Green, D.R. How do BCL-2 proteins induce mitochondrial outer membrane permeabilization? *Trends Cell Biol.* **2008**, *18*, 157–164. [CrossRef]

20.　Rezk Hassan, G.F.; Marey, K. Immunohistopathological Study of c-FLIP Protein in Mycosis Fungoides. *Asian Pac. J. Cancer Prev. APJCP* **2017**, *18*, 2493–2499. [PubMed]

21.　Wu, J.; Nihal, M.; Siddiqui, J.; Vonderheid, E.C.; Wood, G.S. Low FAS/CD95 expression by CTCL correlates with reduced sensitivity to apoptosis that can be restored by FAS upregulation. *J. Investig. Derm.* **2009**, *129*, 1165–1173. [CrossRef]

22.　Braun, F.K.; Fecker, L.F.; Schwarz, C.; Walden, P.; Assaf, C.; Dürkop, H.; Sterry, W.; Eberle, J. Blockade of death receptor-mediated pathways early in the signaling cascade coincides with distinct apoptosis resistance in cutaneous T-cell lymphoma cells. *J. Investig. Derm.* **2007**, *127*, 2425–2437. [CrossRef] [PubMed]

23.　Chang, T.-P.; Vancurova, I. NFκB function and regulation in cutaneous T-cell lymphoma. *Am. J. Cancer Res.* **2013**, *3*, 433–445. [PubMed]

24.　Sors, A.; Jean-Louis, F.; Pellet, C.; Laroche, L.; Dubertret, L.; Courtois, G.; Bachelez, H.; Michel, L. Down-regulating constitutive activation of the NF-kappaB canonical pathway overcomes the resistance of cutaneous T-cell lymphoma to apoptosis. *Blood* **2006**, *107*, 2354–2363. [CrossRef]

25.　Brouwer, I.J.; Out-Luiting, J.J.; Vermeer, M.H.; Tensen, C.P. Cucurbitacin E and I target the JAK/STAT pathway and induce apoptosis in Sézary cells. *Biochem. Biophys. Rep.* **2020**, *24*, 100832. [CrossRef]

26.　Eriksen, K.W.; Kaltoft, K.; Mikkelsen, G.; Nielsen, M.; Zhang, Q.; Geisler, C.; Nissen, M.H.; Röpke, C.; Wasik, M.A.; Odum, N. Constitutive STAT3-activation in Sezary syndrome: Tyrphostin AG490 inhibits STAT3-activation, interleukin-2 receptor expression and growth of leukemic Sezary cells. *Leukemia* **2001**, *15*, 787–793. [CrossRef]

27.　Soltan, M.Y.; Sumarni, U.; Assaf, C.; Langer, P.; Reidel, U.; Eberle, J. Key Role of Reactive Oxygen Species (ROS) in Indirubin Derivative-Induced Cell Death in Cutaneous T-Cell Lymphoma Cells. *Int. J. Mol. Sci.* **2019**, *20*, 1158. [CrossRef]

28.　Gahlot, S.; Khan, M.A.; Rishi, L.; Majumdar, S. Pentoxifylline augments TRAIL/Apo2L mediated apoptosis in cutaneous T cell lymphoma (HuT-78 and MyLa) by modulating the expression of antiapoptotic proteins and death receptors. *Biochem. Pharm.* **2010**, *80*, 1650–1661. [CrossRef]

29.　Braun, F.K.; Al-Yacoub, N.; Plötz, M.; Möbs, M.; Sterry, W.; Eberle, J. Nonsteroidal anti-inflammatory drugs induce apoptosis in cutaneous T-cell lymphoma cells and enhance their sensitivity for TNF-related apoptosis-inducing ligand. *J. Investig. Derm.* **2012**, *132*, 429–439. [CrossRef]

30.　Quast, S.A.; Berger, A.; Eberle, J. ROS-dependent phosphorylation of Bax by wortmannin sensitizes melanoma cells for TRAIL-induced apoptosis. *Cell Death Dis.* **2013**, *4*, e839. [CrossRef]

31. Benhadji, K.A.; Serova, M.; Ghoul, A.; Cvitkovic, E.; Le Tourneau, C.; Ogbourne, S.M.; Lokiec, F.; Calvo, F.; Hammel, P.; Faivre, S.; et al. Antiproliferative activity of PEP005, a novel ingenol angelate that modulates PKC functions, alone and in combination with cytotoxic agents in human colon cancer cells. *Br. J. Cancer* **2008**, *99*, 1808–1815. [CrossRef]

32. Zhang, J.; Anastasiadis, P.Z.; Liu, Y.; Thompson, E.A.; Fields, A.P. Protein kinase C (PKC) βII induces cell invasion through a Ras/Mek-, PKCι/Rac 1-dependent signaling pathway. *J. Biol. Chem.* **2004**, *279*, 22118–22123. [CrossRef]

33. Zhao, M.; Xia, L.; Chen, G.-Q. Protein Kinase Cδ in Apoptosis: A Brief Overview. *Arch. Immunol. Ther. Exp.* **2012**, *60*, 361–372. [CrossRef]

34. Kato, K.; Yamanouchi, D.; Esbona, K.; Kamiya, K.; Zhang, F.; Kent, K.C.; Liu, B. Caspase-mediated protein kinase C-delta cleavage is necessary for apoptosis of vascular smooth muscle cells. *Am. J. Physiol. Heart Circ. Physiol.* **2009**, *297*, H2253–H2261. [CrossRef]

35. Hampson, P.; Chahal, H.; Khanim, F.; Hayden, R.; Mulder, A.; Assi, L.K.; Bunce, C.M.; Lord, J.M. PEP005, a selective small-molecule activator of protein kinase C, has potent antileukemic activity mediated via the delta isoform of PKC. *Blood* **2005**, *106*, 1362–1368. [CrossRef]

36. Ogbourne, S.M.; Suhrbier, A.; Jones, B.; Cozzi, S.-J.; Boyle, G.M.; Morris, M.; McAlpine, D.; Johns, J.; Scott, T.M.; Sutherland, K.P.; et al. Antitumor Activity of 3-Ingenyl Angelate. *Plasma Membr. Mitochondrial Disrupt. Necrotic Cell Death* **2004**, *64*, 2833–2839.

37. Wang, D.; Liu, P. Ingenol-3-Angelate Suppresses Growth of Melanoma Cells and Skin Tumor Development by Downregulation of NF-κB-Cox2 Signaling. *Med. Sci. Monit.* **2018**, *24*, 486–502. [CrossRef] [PubMed]

38. Cozzi, S.-J.; Parsons, P.G.; Ogbourne, S.M.; Pedley, J.; Boyle, G.M. Induction of Senescence in Diterpene Ester–Treated Melanoma Cells via Protein Kinase C–Dependent Hyperactivation of the Mitogen-Activated Protein Kinase Pathway. *Cancer Res.* **2006**, *66*, 10083–10091. [CrossRef] [PubMed]

39. Kaltoft, K.; Bisballe, S.; Dyrberg, T.; Boel, E.; Rasmussen, P.B.; Thestrup-Pedersen, K. Establishment of two continuous T-cell strains from a single plaque of a patient with mycosis fungoides. *In Vitro Cell Dev. Biol.* **1992**, *28*, 161–167. [CrossRef] [PubMed]

40. Kaltoft, K.; Bisballe, S.; Rasmussen, H.F.; Thestrup-Pedersen, K.; Thomsen, K.; Sterry, W. A continuous T-cell line from a patient with Sézary syndrome. *Arch. Derm. Res.* **1987**, *279*, 293–298. [CrossRef]

41. Gootenberg, J.E.; Ruscetti, F.W.; Mier, J.W.; Gazdar, A.; Gallo, R.C. Human cutaneous T cell lymphoma and leukemia cell lines produce and respond to T cell growth factor. *J. Exp. Med.* **1981**, *154*, 1403–1418. [CrossRef]

42. Starkebaum, G.; Loughran, T.P., Jr.; Waters, C.A.; Ruscetti, F.W. Establishment of an IL-2 independent, human T-cell line possessing only the p70 IL-2 receptor. *Int. J. Cancer* **1991**, *49*, 246–253. [CrossRef]

43. Gillespie, S.K.; Zhang, X.D.; Hersey, P. Ingenol 3-angelate induces dual modes of cell death and differentially regulates tumor necrosis factor–related apoptosis-inducing ligand–induced apoptosis in melanoma cells. *Mol. Cancer Ther.* **2004**, *3*, 1651–1658.

44. Netchiporouk, E.; Gantchev, J.; Tsang, M.; Thibault, P.; Watters, A.K.; Hughes, J.M.; Ghazawi, F.M.; Woetmann, A.; Odum, N.; Sasseville, D.; et al. Analysis of CTCL cell lines reveals important differences between mycosis fungoides/Sezary syndrome vs. HTLV-1(+) leukemic cell lines. *Oncotarget* **2017**, *8*, 95981–95998. [CrossRef]

45. Lebwohl, M.; Swanson, N.; Anderson, L.L.; Melgaard, A.; Xu, Z.; Berman, B. Ingenol mebutate gel for actinic keratosis. *N. Engl. J. Med.* **2012**, *366*, 1010–1019. [CrossRef]

46. Bucko, A.D.; Jarratt, M.; Stough, D.B.; Kyhl, L.; Villumsen, J.; Hall, A. Pharmacokinetics of ingenol mebutate gel under maximum use conditions in large treatment areas. *J. Dermatol. Treat.* **2018**, *29*, 74–79. [CrossRef] [PubMed]

47. Franke, J.C.; Plötz, M.; Prokop, A.; Geilen, C.C.; Schmalz, H.G.; Eberle, J. New caspase-independent but ROS-dependent apoptosis pathways are targeted in melanoma cells by an iron-containing cytosine analogue. *Biochem. Pharm.* **2010**, *79*, 575–586. [CrossRef]

48. Liu, H.; Chang, D.W.; Yang, X. Interdimer processing and linearity of procaspase-3 activation. A unifying mechanism for the activation of initiator and effector caspases. *J. Biol. Chem.* **2005**, *280*, 11578–11582. [CrossRef]

49. Bauer, D.; Werth, F.; Nguyen, H.A.; Kiecker, F.; Eberle, J. Critical role of reactive oxygen species (ROS) for synergistic enhancement of apoptosis by vemurafenib and the potassium channel inhibitor TRAM-34 in melanoma cells. *Cell Death Dis.* **2017**, *8*, e2594. [CrossRef] [PubMed]

50. Zhivkova, V.; Kiecker, F.; Langer, P.; Eberle, J. Crucial role of reactive oxygen species (ROS) for the proapoptotic effects of indirubin derivative DKP-073 in melanoma cells. *Mol. Carcinog.* **2019**, *58*, 258–269. [CrossRef]

51. Wooler, G.; Melchior, L.; Ralfkiaer, E.; Rahbek Gjerdrum, L.M.; Gniadecki, R. TP53 Gene Status Affects Survival in Advanced Mycosis Fungoides. *Front. Med.* **2016**, *3*, 51. [CrossRef]

52. Lamprecht, B.; Kreher, S.; Möbs, M.; Sterry, W.; Dörken, B.; Janz, M.; Assaf, C.; Mathas, S. The tumour suppressor p53 is frequently nonfunctional in Sézary syndrome. *Br. J. Derm.* **2012**, *167*, 240–246. [CrossRef] [PubMed]

53. Serova, M.; Ghoul, A.; Benhadji, K.A.; Faivre, S.; Le Tourneau, C.; Cvitkovic, E.; Lokiec, F.; Lord, J.; Ogbourne, S.M.; Calvo, F. Effects of protein kinase C modulation by PEP005, a novel ingenol angelate, on mitogen-activated protein kinase and phosphatidylinositol 3-kinase signaling in cancer cells. *Mol. Cancer Ther.* **2008**, *7*, 915–922. [CrossRef]

54. Huo, J.X.; Metz, S.A.; Li, G.D. p53-independent induction of p21waf1/cip1 contributes to the activation of caspases in GTP-depletion-induced apoptosis of insulin-secreting cells. *Cell Death Differ.* **2004**, *11*, 99–109. [CrossRef] [PubMed]

International Journal of
Molecular Sciences

MDPI

Article

Key Role of Reactive Oxygen Species (ROS) in Indirubin Derivative-Induced Cell Death in Cutaneous T-Cell Lymphoma Cells

Marwa Y. Soltan [1,2], Uly Sumarni [1], Chalid Assaf [1,3], Peter Langer [4,5], Ulrich Reidel [1] and Jürgen Eberle [1,*]

[1] Skin Cancer Centre Charité, Department of Dermatology and Allergy, Charité—Universitätsmedizin Berlin, Charitéplatz 1, 10117 Berlin, Germany; Marwayassin@med.asu.edu.eg (M.Y.S.); uly.sumarni@googlemail.com (U.S.); chalid.assaf@helios-gesundheit.de (C.A.); ulrich.reidel@charite.de (U.R.)
[2] Department of Dermatology and Venereology, Faculty of Medicine, Ain Shams University, Cairo 11591, Egypt
[3] Clinic for Dermatology and Venereology, Helios Klinikum Krefeld, Lutherplatz 40, 47805 Krefeld, Germany
[4] Institute of Chemistry, University of Rostock, Albert-Einstein-Str. 3a, 18059 Rostock, Germany; peter.langer@uni-rostock.de
[5] Leibniz Institute of Catalysis at the University of Rostock e.V., Albert-Einstein-Str. 29a, 18059 Rostock, Germany
* Correspondence: juergen.eberle@charite.de; Tel.: +49-30-450-518-383

check for updates

Abstract: Cutaneous T-cell lymphoma (CTCL) may develop a highly malignant phenotype in its late phase, and patients may profit from innovative therapies. The plant extract indirubin and its chemical derivatives represent new and promising antitumor strategies. This first report on the effects of an indirubin derivative in CTCL cells shows a strong decrease of cell proliferation and cell viability as well as an induction of apoptosis, suggesting indirubin derivatives for therapy of CTCL. As concerning the mode of activity, the indirubin derivative DKP-071 activated the extrinsic apoptosis cascade via caspase-8 and caspase-3 through downregulation of the caspase antagonistic proteins c-FLIP and XIAP. Importantly, a strong increase of reactive oxygen species (ROS) was observed as an immediate early effect in response to DKP-071 treatment. The use of antioxidative pre-treatment proved the decisive role of ROS, which turned out upstream of all other proapoptotic effects monitored. Thus, reactive oxygen species appear as a highly active proapoptotic pathway in CTCL, which may be promising for therapeutic intervention. This pathway can be efficiently activated by an indirubin derivative.

Keywords: CTCL; apoptosis; cell viability; c-FLIP; XIAP

1. Introduction

Reactive oxygen species (ROS) play important roles in tissue damage and aging, as also addressed in this special issue. On the other hand, an increasing number of scientific studies in recent years indicated a particular role of ROS in apoptosis regulation in cancer cells. The mechanism(s) are still under discussion. Here, we give an example of cutaneous T-cell lymphoma (CTCL), where ROS is induced by the drug candidate indirubin.

Non-Hodgkin's lymphomas (NHL) have shown increasing incidence in the last decades. About 5% of NHL are characterized by primary cutaneous manifestation through clonal proliferation of skin-homing memory T cells. This group of cutaneous T-cell lymphomas (CTCL) encloses Mycosis

fungoides, Sézary syndrome and CD30(+) lymphoproliferative disorders. Cutaneous T-cell lymphomas represent a clinically and biologically distinct group of NHL without evidence for systemic disease at the time of first diagnosis. In clinical appearance and prognosis, they are clearly different from the histotypically cognate systemic lymphomas and their possible secondary cutaneous manifestations. Typically, they have the immunophenotype of CD3+ CD4+ CD45RO+ memory T-lymphocytes. While in its early stage CTCL may show an also indolent clinical course, it frequently transforms to a rapidly growing, malignant phenotype in later phases [1,2]. New treatments are needed particularly for these patients.

The elimination of tumor cells through the induction of apoptosis represents a principle goal in cancer treatment, and therapy resistance can thus be frequently explained by apoptosis deficiency [3]. Also, established therapies for CTCL as UV radiation or extracorporal photopheresis aim at an induction of apoptosis in tumor cells [4]. Extrinsic proapoptotic pathways are initiated by death ligands as CD95L/FasL or TRAIL (TNF-related apoptosis-inducing ligand), which also contribute to self-control of lymphocytes. Their binding to death receptors results in the formation of a death-inducing signaling complex, where initiator caspase-8 is activated [5]. Caspase-8 activation can be prevented by the competitive inhibitor protein c-FLIP (cellular FLICE-inhibitory protein) [6]. Initiator caspase-8 may cleave and activate the main effector caspase-3, which itself cleaves a large number of death substrates with the final result of DNA fragmentation [7]. Caspase-3 is negatively regulated through the binding of XIAP (chromosome X-linked inhibitor of apoptosis protein) [8].

In CTCL cells, the activation of the extrinsic caspase cascade plays a decisive role in controlling apoptosis. Thus, apoptosis resistance is correlated with reduced expression of the death receptor CD95/FAS [9] as well as with high and constitutive expression of c-FLIP [10]. Also, activation of the pro-survival transcription factors NF-κB [11] and STAT3 [12] were reported. In particular, different therapeutic strategies as NSAIDs, SAHA (suberoylanilide hydroxamic) and pentoxifylline resulted in downregulation of c-FLIP and XIAP in CTCL cells [13–15]. Finally, reactive oxygen species (ROS) may contribute to the regulation of apoptosis [16,17]. This is also suggested by enhanced levels of singlet oxygen ($^1O_2$) in the course of photodynamic therapy (PDT), used for the treatment of actinic keratosis [18,19] and also considered for CTCL [20]. However, the relation of ROS with described apoptosis pathways is still largely elusive.

The natural compound indirubin and a number of reported chemical derivatives are considered as candidates for cancer therapy. Indirubin was identified as an active component in a traditional Chinese medicine remedy (Danggui Longhui Wan), also applied for chronic myeloid leukemia. In clinical trials, indirubin has shown significant antitumor activity in chronic myeloid and chronic granulocytic leukemia [21,22]. Explaining the mode of action, a large number of intracellular targets have been described for indirubin derivatives, including cyclin-dependent kinases (CDK1, CDK2, CDK4 and CDK5), pRb, glycogen synthase kinase 3 (GSK-3), STAT3 (Signal transducer and activator of transcription), EGFR (Epidermal growth factor receptor), c-Jun, and JNK2 [23–26]. The activation of extrinsic apoptosis pathways by indirubin derivatives was found in melanoma cells [27,28]. To improve the anti-cancer activity of indirubin, we have previously introduced a series of chemical modifications [29–31]. Here, we investigated the direct effects of the indirubin derivative DKP-071 in CTCL cells. We furthermore unraveled its mode of action, which is based on caspase activation, downregulation of the caspase antagonists c-FLIP and XIAP and, in particular, on early production of ROS.

2. Results

2.1. Decreased Cell Proliferation and Viability Along with Induced Apoptosis by DKP-071

Synthesis and structural aspects of the indirubin derivative DKP-071/substance 9d (Figure 1a) have been reported previously [31]. Here, its effects in three CTCL cell lines MyLa, HuT-78 and HH were investigated. These cell lines are characterized by the formation of cell clusters, a typical

lymphocyte differentiation step [32,33]. In a first approach, we observed reduced cell cluster size in response to DKP-071, likely indicating reduced T-cell activity (Figure 1b). In line with this, cell proliferation was significantly reduced at 24 h, as determined by WST-1 assay (Figure 1c). Reduced cell numbers were however not due to direct cytotoxicity, as lactate dehydrogenase (LDH) release assays at 24 h did not show a significant increase in MyLa or in HH cells (Figure 1d).
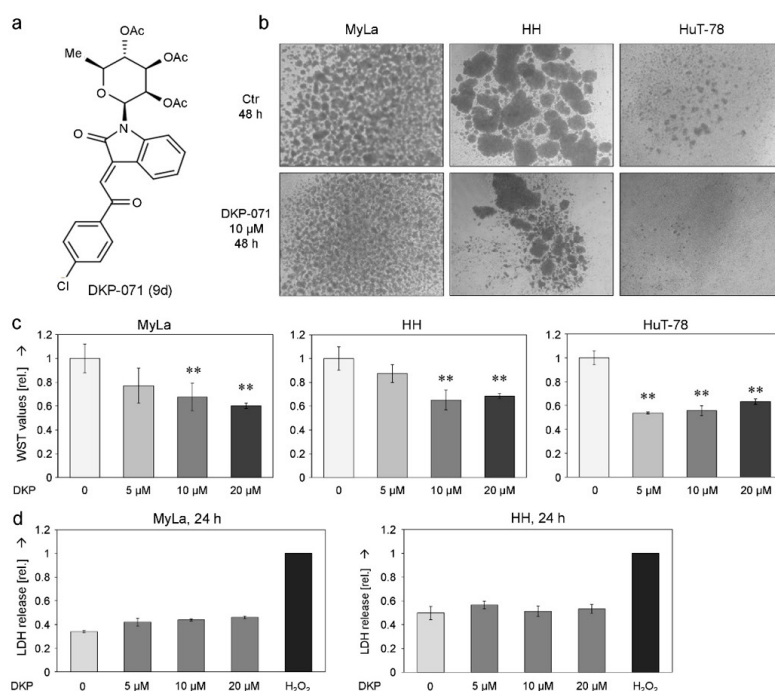

Figure 1. Decreased cell proliferation of CTCL cells by DKP-071. (**a**) Chemical structure of the indirubin derivative DKP-071 (termed substance 9d in [31]). (**b**) Cell cluster formation in CTCL cell lines MyLa, HuT-78 and HH. Control cells (Ctr) are shown vs. cells treated for 48 h with 10 µM DKP-071 (magnification: 1:40). Many independent experiments showed the same result. (**c**) Cell proliferation of MyLa, HuT-78 and HH, at 24 h in response to treatment with 5, 10 and 20 µM DKP-071 (DKP). Cell proliferation data were determined by WST-1 assay, and values are shown in relation (rel) to negative controls (0), which were set to "1". Statistical significance is indicated (** $p < 0.01$). (**d**) Cytotoxicity was determined at 24 h in MyLa and in HH cells by LDH release assay. Values are shown in relation (rel) to H_2O_2-treated positive controls, which were set to "1".

Cell viability, as determined by calcein staining, was strongly decreased. A dose dependency (5–20 µM) was shown for MyLa and HH cells. At 48 h of treatment, 10 µM DKP-071 reduced the numbers of viable cells to 23% (MyLa), 9% (HuT-78) and 38% (HH), respectively (Figure 2a). Based on cell viability data, we calculated IC50 values of 7 µM DKP-071 for Myla and 11 µM for HH. For HuT-78, we used the WST data of Figure 1c, which resulted in an IC50 value of 8 µM for HuT-78. Loss of cell viability went along with an induction of apoptosis, which was determined by counting sub-G1 cells in cell cycle analyses. Induction of apoptosis showed a comparable dose dependency. At 48 h of treatment, 10 µM DKP-071 induced apoptosis in 17% (MyLa), 24% (HuT-78) and 22% of HH cells, respectively (Figure 2b). The concentration of 10 µM was selected for subsequent experiments.

2.2. Changes of Mitochondrial Membrane Potential and ROS Production

Questioning the mechanisms that mediate the antineoplastic effects of DKP-071 in CTCL cells, we determined the relative changes in the mitochondrial membrane potential (MMP) as well as relative levels of reactive oxygen species (ROS) in response to treatment. Loss of MMP, indicative for an activation of mitochondrial apoptosis pathways, already started in the three cell lines at 5 h (31–49%) but was much more evident at later time (24 h, 90% cells with low MMP; Figure 3a).

Reactive oxygen species (ROS) may mediate independent cell death pathways in cancer cells which are not yet completely understood [16]. Earlier than the loss of MMP, ROS levels were already strongly enhanced after 2 h. Thus, 87%, 83% and 57% of MyLa, HuT-78 and HH cells, respectively, showed high ROS levels at 2 h of DKP-071 treatment (Figure 3b).
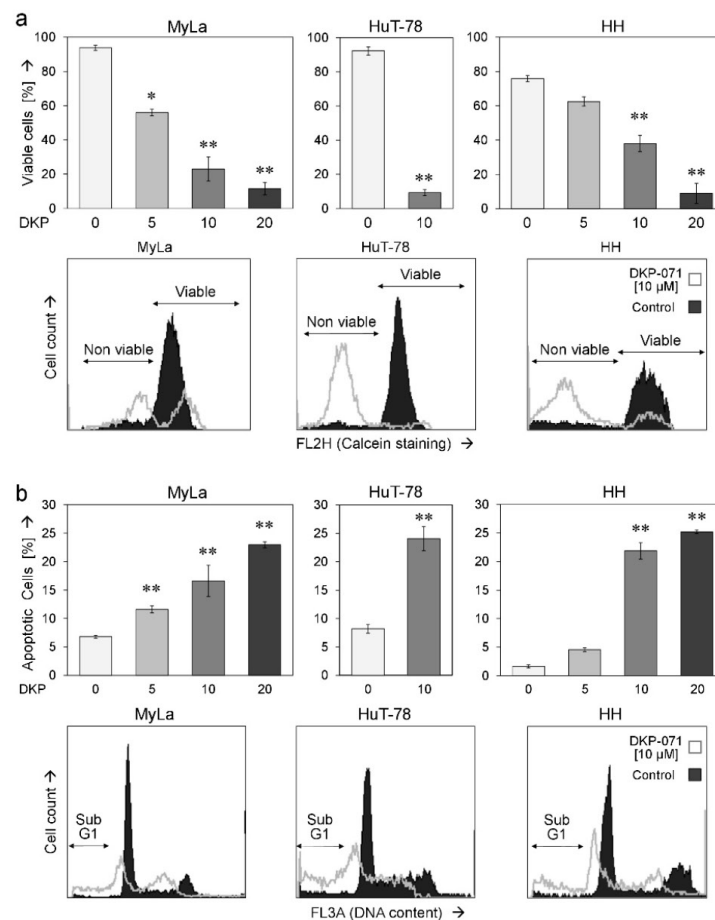

Figure 2. Reduced cell viability and induction of apoptosis. (**a**) Cell viability and (**b**) apoptosis were determined in three cell lines, in response to 48 h treatment with DKP-071 (5, 10 and 20 μM for MyLa and HH as well as 10 μM for HuT-78). Values were determined by calcein staining (**a**) and propidiumiodide staining (**b**), respectively. Characteristic histograms are shown for each cell line (10 μM treatment, overlays with controls); fractions of non-viable and viable as well as of apoptotic cells (sub-G1) are indicated. Mean values of triplicates +/− SDs of a representative experiment are shown. Statistical significance is indicated (treated cells vs. controls; * $p < 0.05$; ** $p < 0.01$).
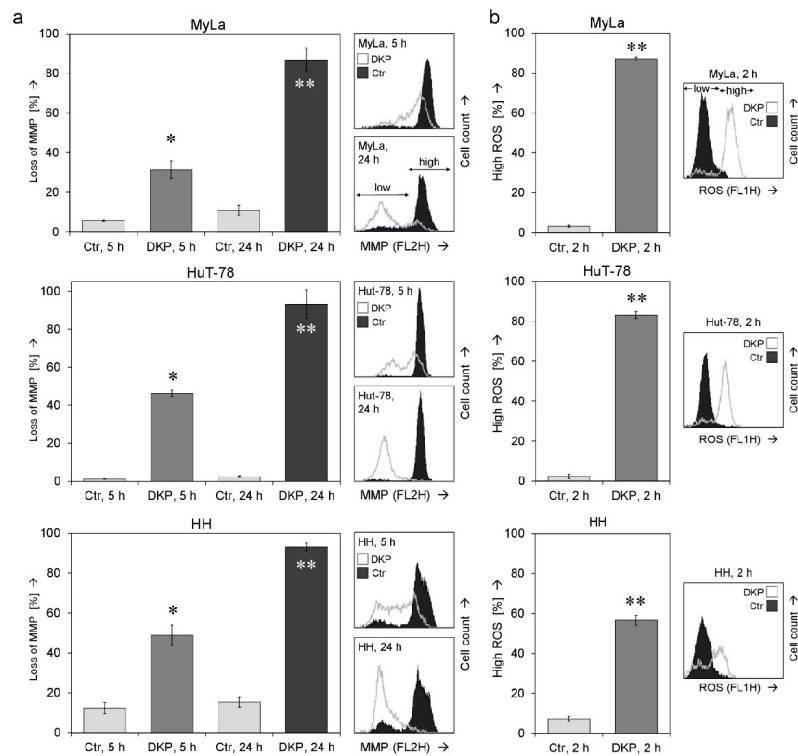
Figure 3. Effects on mitochondrial membrane potential and on ROS levels. (**a**) Relative changes in mitochondrial membrane potential (MMP) were determined at 5 h and 24 h in three CTCL cell lines in response to treatment with DKP-071 (10 µM). Mean values of triplicates +/− SD are shown; a second independent experiment series of MyLa revealed highly comparable results. Representative histograms (overlays of treated cells vs. controls) are given on the right side. (**b**) ROS levels were determined at 2 h of treatment. Mean values of triplicates +/− SD are shown; for MyLa, three independent experiments, each one with triplicates, revealed highly comparable results. Representative histograms (overlays of treated cells vs. controls) are given on the right side. Statistical significance is indicated (treated cells vs. controls; * $p < 0.05$; ** $p < 0.01$).

2.3. Critical role of ROS for Proapoptotic Effects of DKP-071

To prove the significance of ROS as well as of caspase activation for the antineoplastic effects, the antioxidants tocopherol (vitamin E, VE) and N-acetyl cysteine (NAC) as well as the pan-caspase inhibitor QVD-Oph were applied. ROS production in response to DKP-071 was slightly reduced by VE and was strongly reduced by NAC, as shown in MyLa at 2 h. Most effective was a combination of VE and NAC (both at 2 mM, VE/NAC), which completely abolished ROS production after DKP-071 treatment in the three cell lines. QVD-Oph remained without effect on ROS, indicating that ROS was independent of caspase activity (Figure 4).

ROS scavenging by VE/NAC proved the significant and upstream role of ROS for DKP-071-mediated effects. Thus, cell proliferation, which was decreased by DKP-071 at 24 h, was restored in three cell lines by VE/NAC (Figure 5a). Similarly, the effects of DKP-071 on cell viability were strongly diminished by VE/NAC as shown in MyLa at 48 h (from 4% to 78% viable cells, Figure 5b). Finally, the induction of apoptosis, induced by DKP-071 in MyLa at 48 h (35%), was completely prevented by VE/NAC (3%, Figure 5c). Caspase inhibition through QVD-Oph

also diminished apoptosis and loss of cell viability, which was, however, less effective than the antioxydative treatment (Figure 4b,c). These findings support the explanation that ROS production was an upstream step.
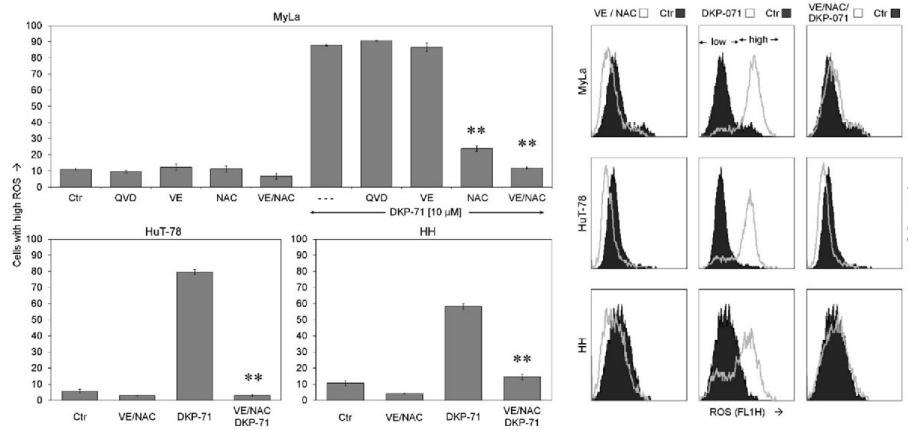

Figure 4. ROS suppression by antioxidative treatment. ROS levels are shown in MyLa in response to DKP-071 (10 μM). In addition, antagonists as vitamin E (VE, 1 mM), N-acetyl cysteine (NAC, 1 mM), the pancaspase inhibitor QVD-Oph (QVD, 10 μM), as well as combined NAC and VE (each 2 mM) were applied 1 h before DKP-071 treatment was started. Cells which received only DKP-071 but no antagonist are indicated by (- - -). The antioxidative effect was also shown in HuT-78 and in HH by the use of VE/NAC. Mean values of triplicates +/− SD of a representative experiment are shown; for MyLa, three independent experiments, each one with triplicates, revealed highly comparable results. Examples of flow cytometry measurement are shown on the right side as overlays versus control. Statistical significance of the differences of DKP-071/NAC-treated cells as well as DKP-071/VE/NAC-treated cells is indicated, each compared to the cells that received only DKP-071 (** $p < 0.01$).
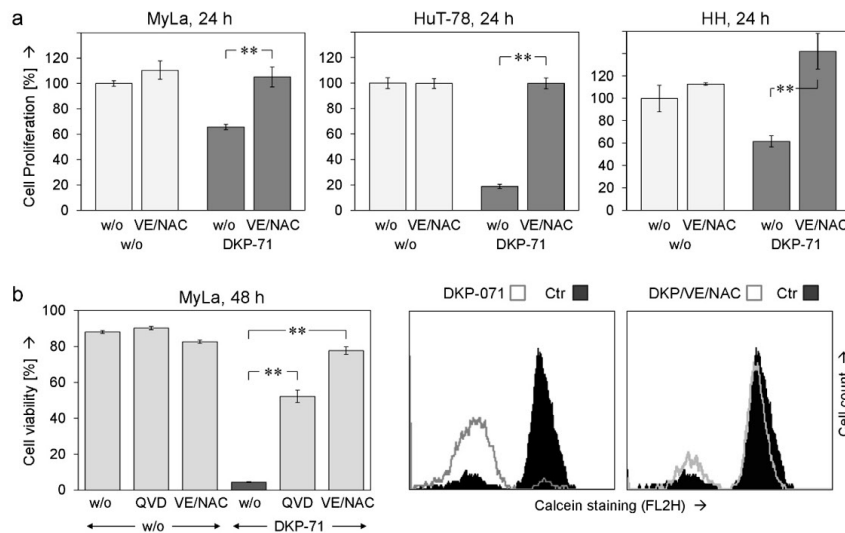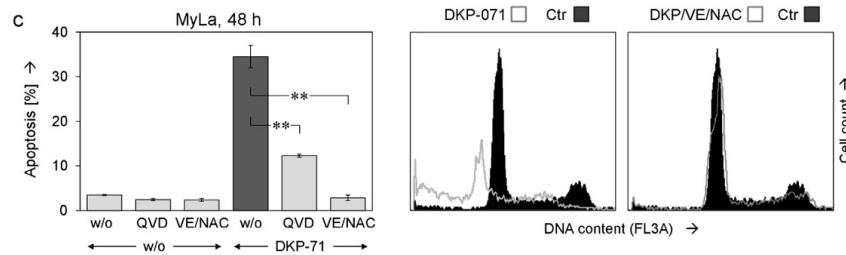

Figure 5. *Cont.*

Figure 5. ROS suppression prevents apoptosis and restores cell viability. (**a**) Cell proliferation was determined at 24 h in response to DKP-071 as well as in response to the combination of NAC and VitE (2 mM; VE/NAC). Values were normalized to non-treated controls (100%). (**b,c**) Effects of agonists and antagonists on apoptosis induction (**b**) and cell viability (**c**), both at 48 h, are shown for MyLa cells. Examples of flow cytometry measurement are shown on the right side as overlays of treated cells versus controls. Mean values of triplicates +/− SD of representative experiments are shown; at least two independent experiments, each one with triplicates, revealed highly comparable results. Statistical significance of the differences between DKP-071/VE/NAC-treated cells to cells that received only DKP-071 is indicated (** $p < 0.01$).

2.4. Role of Caspases and Caspase Antagonistic Proteins

ROS also appeared upstream of MMP loss. Thus, VE/NAC almost completely prevented the loss of MMP in MyLa at 5 h (24% to 7%) whereas caspase inhibition was less effective here (18%, Figure 6a). Extrinsic caspase pathways are of major importance for apoptosis regulation in lymphoma cells, also including CTCL [10]. Thus, we investigated by Western blotting the activation/processing of initiator caspase-8 and the main effector caspase-3 as well as the expression of the caspase-3 antagonist XIAP and the caspase-8 antagonist c-FLIP.

In response to 40 h treatment with DKP-071, the proform of caspase-8 (53/55 kD) disappeared, indicating its complete processing. In parallel, Caspase-3 was processed to its mature, active cleavage product of 15 kDa. Importantly, VE/NAC strongly reduced the processing both of caspase-8 and caspase-3. In particular, no active cleavage product of caspase-3 (15 kDa) was detected, but the processing was stopped at an intermediate product of 19 kDa. In clear contrast, QVD-Oph remained without effect on caspase-8. It, however, prevented caspase-3 autoprocessing and halted the cascade at the 19 and 17 kDa intermediate cleavage products (Figure 6b, top). These findings clearly showed that ROS was upstream of any caspase regulation, while QVD-Oph acts downstream as a caspase-3 antagonist.

Explaining the activation of caspases, DKP-071 strongly reduced the expression of two most characteristic caspase antagonists, namely XIAP (51 kDa) and c-FLIP (long isoform, 52 kDa and short isoform, 25 kDa). Of particular note, this downregulation was completely prevented by antioxidants (VE/NAC), while caspase-3 inhibition through QVD-Oph remained without effect on c-FLIP and XIAP (Figure 6b, bottom). Thus, ROS was also upstream of the downregulation of c-FLIP and XIAP. These findings suggest a cascade in CTCL cells, leading from ROS production in response to DKP-071 treatment to c-FLIP and XIAP downregulation and further to caspase activation and apoptosis (Figure 6c).
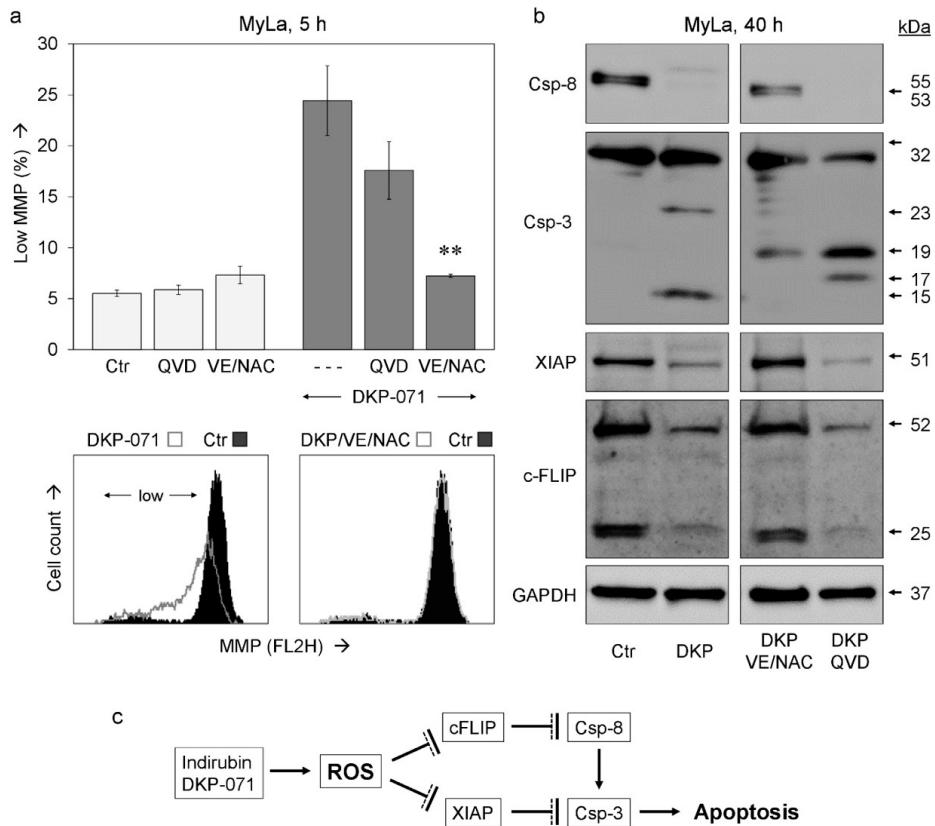
Figure 6. Effects on MMP and caspase cascade. (**a**) Effects of antioxidative treatment (VE/NAC, 2 mM) as well as of QVD-Oph (QVD, 10 μM) on mitochondrial membrane potential (MMP) are shown for MyLa cells at 5 h of DKP-071 treatment. Cells, which received only DKP-071 but no antagonist are indicated by (- - -). Mean values of triplicates +/− SD of a representative experiment are shown; two independent experiments, each one with triplicates, revealed highly comparable results. Statistical significance of the differences between DKP-071/VE/NAC-treated cells to cells that received only DKP-071 is indicated (** $p < 0.01$). Examples of flow cytometry measurement are shown below as overlays versus control. The cell population with low MMP is indicated. (**b**) Effects of DKP-071 and antioxidative pre-treatment on the expression of characteristic regulatory proteins of the extrinsic apoptosis caspase cascade were investigated by Western blotting. Each 30 μg of protein was loaded per lane, and blots were probed with antibodies for extrinsic initiator caspase-8 (proform, 53/55 kDa), main effector caspase-3 (proform, 32 kDa; cleavage products, 23, 19, 17, 15 kDa), caspase-3 antagonist XIAP (51 kDa) and caspase-8 antagonist c-FLIP (FLIP$_L$, long, 52 kDa; FLIP$_S$, short, 25 kDa). The housekeeping protein glyceraldehyde 3-phosphate dehydrogenase (GAPDH, 37 kDa) was used as loading control. Three independent series of protein extracts and Western blotting experiments revealed highly comparable results. (**c**) The pathway suggested for indirubin DKP-071-mediated apoptosis. Arrows indicate activation; blunt end lines indicate inhibition.

3. Discussion

Many new therapies established in recent decades for most tumors have sometimes dramatically enhanced patients' survival. Also for CTCL, present therapeutic options as topical steroids, bexarotene, phototherapy, interferon or some forms of targeted therapy have strongly improved the clinical

outcome and often allow long-term survival. Nevertheless, in its late phase, CTCL may transform to a rapidly growing and ulcerating phenotype, characterized also by pronounced therapy resistance [1,2]. As apoptosis deficiency represents an in principal decisive issue in therapy resistance, the specific targeting of apoptosis pathways appears as a promising strategy [3].

Indirubin has been identified as the major component of a traditional Chinese medicine remedy, also applied for leukemia. In clinical trials for chronic myeloid and chronic granulocytic leukemia, it revealed significant antitumor activity, resulting in partial or complete remissions [21,22]. Chemical modifications of indirubin may further enhance its activity. Thus, we have recently reported the synthesis of new indirubin derivatives characterized by N-glycosylated 3-alkylideneoxindol structures [31]. This first report on the effects of an indirubin derivative in CTCL cells shows a particular high activity resulting in decreased cell proliferation and cell viability as well as induction of apoptosis. There is no cutaneous non-tumorigenic T-cell line, which could be used for investigations in vitro and prove the tumor-specificity of the effects. However, due to the only moderate side effects reported for indirubin in clinical trials [21,22], the here investigated indirubin derivative may be suggested as a potential new therapeutic option for CTCL. A proapoptotic strategy, as by DKP-071, may also apply for early CTCL, characterized by an indolent clinical course and apoptosis susceptibility.

As concerning the pathways, by which indirubins may exert their effects, multiple targets have been suggested including CDKs, GSK-3β, pRb, c-Src, FGF-R1, VEGFR, STAT3, c-Jun and JNK2 [23–26]. In melanoma cells, we have previously shown that indurubin derivatives enhance extrinsic apoptosis pathways as induced by TRAIL (TNF-related apoptosis-inducing ligand [27,28]. Extrinsic apoptosis pathways via caspase-8/caspase-3 are of particular importance for apoptosis regulation in CTCL cells [10,34]. Also in CTCL, DKP-071 mediated its proapoptotic effects via activation of the extrinsic caspase cascade, as shown by caspase-8 and caspase-3 processing as well as by the inhibition of the effects of indirubin through the caspase-3 antagonist QVD-Oph. Caspase activity is controlled by several antiapoptotic proteins such as the competitive caspase-8 antagonist c-FLIP and the protein family of cIAPs (cellular inhibitor of apoptosis proteins), e.g., the caspase-3 antagonist XIAP (chromosome X-linked) [6,8]. These two antagonists appeared as essentially involved in the present setting, as strongly downregulated by DKP-071 in CTCL cells. Downregulation of these two factors in CTCL has also been reported by other treatments. Thus, c-FLIP was downregulated in response to SAHA (suberoylanilide hydroxamic) and NSAIDs, while XIAP was downregulated in response to SAHA and pentoxifylline [13–15].

Reactive oxygen species (ROS) play important roles in tissue damage and aging, and antioxidative strategies were established to prevent these negative effects. Besides this, ROS may also be involved in proapoptotic signaling in cancer cells [16,28,35,36]. As an example from the clinic, photodynamic therapy (PDT), used for the treatment of actinic keratosis, results in the production of high amounts of singlet oxygen. However, the role of ROS in PDT is still controversially discussed [18–20]. ROS may act as a signaling molecule e.g., by affecting the mitochondrial membrane and thus activating intrinsic, mitochondrial apoptosis pathways, or it may provoke cellular damage e.g., by oxidizing membrane lipids resulting in necrosis or activation of a damage response.

Here, we show even another alternative. In CTCL, ROS acts in cellular signaling clearly upstream of the extrinsic apoptosis pathway. It is induced already at 2 h in response to indirubin treatment and resides upstream of the downregulation of XIAP and c-FLIP as well as upstream of the loss of MMP, suggesting a signaling cascade as shown in Figure 6c. Also for other treatments in CTCL cells, relations of ROS and apoptosis induction have been reported, such as for an inhibitor of the antioxidative protein mucin 1 [37], for silencing of the enhancer of zeste homolog 2 (EZH2) [38] and for doxycycline [39]. Thus, ROS production appears to be an important cellular signaling step related to the induction of apoptosis. The new proapoptotic pathways behind this may be useful for targeted cancer therapy. In CTCL, our data suggest a strong relation between ROS, caspase antagonists and the activation of the extrinsic apoptosis pathway. This signaling cascade is efficiently triggered by the indirubin derivative DKP-071, suggesting it as a therapeutic strategy for CTCL.

4. Materials and Methods

4.1. Cell Culture and Treatments

Three CTCL cell lines have been used here, which derive from patients with Mycosis fungoides and Sézary syndrome, respectively: Cell line MyLa was kindly supplied by Prof. K. Kaltoft, Århus University, Århus, DK. It derived from a plaque biopsy of a patient with MF [40]; HuT-78 was kindly supplied by Prof. R.C. Gallo, University of Maryland, Baltimore, MD, USA. [41] It derived from PBMCs of a patient with Sézary syndrome; and HH (CRL-2105, ATCC, Manassas, VA, USA) derived from peripheral blood of a patient with aggressive CTCL [42]. Cells were grown at 37 °C, 5% CO_2 in RPMI 1640 medium supplemented with L-glutamine, 10% FCS and antibiotics (Biochrom, Berlin, Germany). Under these applied conditions, the cell lines revealed a similar growth behavior and proliferation rate; only the formation of cell clusters, typical for T-cells, varied considerably (Figure 1a).

For assays, cells were seeded in 24-well culture plates (100,000 cells and 500 µL per well) or in 96-well pates (40,000 cells and 200 µL per well). For protein extraction, cells were seeded in 6-well plates (400,000 per well, 2 mL). Treatments started at 24 h after seeding.

The indirubin derivative DKP-071 (termed substance 9d in [31]; Figure 1a) was used in concentrations of 5–20 µM. For caspase inhibition, cells were pre-incubated for 1 h with the pan-caspase inhibitor QVD-Oph (Sigma-Aldrich, Taufkirchen, Germany, 10 µM). For ROS scavenging, cells were pre-treated for 1 h with 1 mM α-tocopherol (vitamin E, Fluka, Steinheim, Germany), with N-acetylcysteine (NAC; Sigma-Aldrich, Taufkirchen, Germany; 1 mM) or with a combination of vitamin E and NAC (VE/NAC; each 2 mM).

4.2. Assays for Apoptosis, Cytotoxicity, Cell Viability and Cell Proliferation

Apoptotic cells were quantified as sub-G1 cells (less DNA than G1 cells) in cell cycle analyses. The assay reveals less DNA in apoptotic cells, because small DNA fragments are washed out from isolated nuclei [43]. Cells were harvested by centrifugation, lysed and stained for at least 1 h in hypotonic PI solution (40 µg/mL propidium iodide, Sigma-Aldrich, in 0.1% sodium citrate, 0.1% Triton X-100). Stained isolated nuclei were analyzed by flow cytometry at FL3A with a FACS Calibur (BD Bioscience, Bedford, MA, USA). Cells in G1, G2 and S-phase as well as sub-G1 cells were determined.

Cell cytotoxicity was determined by the analysis of cell supernatants for the activity of lactate dehydrogenase (LDH), which is released from cytotoxic cells in culture. Aliquots of cell supernatants were collected at 24 h, and LDH activity was quantified with a LDH activity assay (Cytotoxicity detection assay; Roche Diagnostics, Penzberg, Germany), following the protocol of the supplier. As positive controls, Triton X-100 (0.7%)-treated cells were used. Relative values were determined in an ELISA reader. The increased LDH activity in treated wells traces back to damaged, cytotoxic cells.

Cell viability was determined by staining cells with calcein-AM (PromoCell, Heidelberg, Germany), which is a cell-permeant non-fluorescent substance that is converted to green-fluorescent calcein in live cells by the activity of intracellular esterases. Cells, grown and treated in 24-well plates, were harvested after 24 h or 48 h by centrifugation. After washing 1× with PBS, they were resuspended in 200 µL of 2.5 µg/mL calcein-AM in PBS. Staining was done at 37 °C for 1 h. Labeled cells were washed again with 1 mL of PBS and were resuspended in 200 µL PBS. The percentage of viable cells was determined by flow cytometry (FL2H). In the calcein assay, the total cell number does not contribute to the results, only the percentage of active cells in the remaining cell population is determined.

Cell proliferation was determined by WST-1 assay (Roche Diagnostics). It depends on the cleavage of the water-soluble tetrazolium salt by mitochondrial dehydrogenases in metabolically active cells. CTCL cells were seeded in 96-well plates, and treatments were started after 24 h. At the time of analysis (24–48 h), WST-1 reagent was added for 1–2 h, and the absorbance at 450 nm was determined in an ELISA reader. Data were reported as the percentage of non-treated controls. The WST-1 assay gives an overview of all the antiproliferative effects of a given drug, which includes a lack of cells due to

decreased cell proliferation as well as a lack of cells due to the induction of apoptosis or induction of cytotoxicity. Furthermore, the cell activity of the remaining cells contributes to the results.

4.3. Mitochondrial Membrane Potential (MMP) and Reactive Oxygen Species (ROS)

Changes to MMP over time or in response to drug treatment can be assessed by staining cells with the fluorescent dye $TMRM^+$ (Tetramethylrhodamin-methylester, Sigma-Aldrich). Due to its positive charge, $TMRM^+$ accumulates in negatively charged mitochondria. In the course of depolarisation of the mitochondria, (e.g., at the beginning of apoptosis), anions are released and $TMRM^+$ concentrations decrease. This staining may also be used to determine the effectiveness of therapeutic compounds [44]. Cells grown and treated in 24-well plates were harvested and stained for 20 min at 37 °C with 1 μM $TMRM^+$. After two-times washing with PBS, cells were analyzed by flow cytometry (FL2H).

Intracellular ROS levels were determined by the cell-permeable substance H_2DCFDA ($2',7'$-dichlorodihydrofluorescein diacetate; Thermo Fisher Scientific, Hennigsdorf, Germany). In cells with high ROS, the non-fluorescent H_2DCFDA is oxidized and thus converted in the strongly fluorescent DCF ($2',7'$-Dichlorfluorescein). Cells grown in 24-well plates were pre-treated for 1 h with H_2DCFDA (10 μM), before starting treatment with effectors. After treatment, cells were harvested by centrifugation, washed with 1 mL PBS, resuspended in PBS, and analyzed by flow cytometry (FL1H). As positive controls, cells were treated with H_2O_2 (1 mM, 1 h).

4.4. Western Blotting

For Western blotting, total protein extracts were obtained by cell lysis in 150 mM NaCl, 1 mM EDTA, 2 mM PMSF, 1 mM leupeptin, 1 mM pepstatin, 0.5% SDS, 0.5% NP-40 and 10 mM Tris-HCl, pH 7.5. Western blotting on nitrocellulose membranes was performed as described previously [45]. Primary antibodies: Cleaved caspase-3 (9664, rabbit, 1:1000, Cell Signaling, Danvers, MA, USA); XIAP (#2042, rabbit, 1:1000, Cell Signaling); caspase-8 (#9746; mouse, 1:1000, Cell Signaling); c-FLIP (G-11, sc-5276; Santa Cruz, Heidelberg, Germany; 1:50); and GAPDH (sc-32233, mouse, 1:1000, Santa Cruz Biotech). Secondary antibodies: peroxidase-labelled goat anti-rabbit and goat anti-mouse (Dako, Hamburg, Germany; 1:5000).

4.5. Statistics

Assays described above were performed in triplicate determinations, and usually at least two completely independent series were performed for each experiment. For the determination of statistical significance, the values of all individual experiments were given together, after normalizing according to the controls. A Student's *t*-test (two-tailed, heteroscedastic) was applied, and *p*-values of <0.05 were considered as statistically significant, while *p*-values of <0.01 were considered as highly significant. When applicable, significance is indicated in the bar charts (* for $p < 0.05$; ** for $p < 0.01$). The results of Western blots were reproduced in three independent series of experiments.

5. Conclusions

In summary, cutaneous T-cell lymphoma cells can be targeted by the induction of ROS. This results in an activation of the extrinsic apoptosis pathway via downregulation of c-FLIP and XIAP. This pathway is efficiently activated by an indirubin derivative, which thus represents an interesting candidate for therapy of cutaneous T-cell lymphoma.

References

1. Willemze, R.; Jaffe, E.S.; Burg, G.; Cerroni, L.; Berti, E.; Swerdlow, S.H.; Ralfkiaer, E.; Chimenti, S.; Diaz-Perez, J.L.; Duncan, L.M.; et al. WHO-EORTC classification for cutaneous lymphomas. *Blood* **2005**, *105*, 3768–3785. [CrossRef] [PubMed]
2. Jawed, S.I.; Myskowski, P.L.; Horwitz, S.; Moskowitz, A.; Querfeld, C. Primary cutaneous T-cell lymphoma (mycosis fungoides and Sezary syndrome): Part II. Prognosis, management, and future directions. *J. Am. Acad. Dermatol.* **2014**, *70*, 223.e1–223.e17. [CrossRef] [PubMed]
3. Eberle, J.; Kurbanov, B.M.; Hossini, A.M.; Trefzer, U.; Fecker, L.F. Overcoming apoptosis deficiency of melanoma-hope for new therapeutic approaches. *Drug Resist. Updates* **2007**, *10*, 218–234. [CrossRef] [PubMed]
4. Bladon, J.; Taylor, P.C. Extracorporeal photopheresis induces apoptosis in the lymphocytes of cutaneous T-cell lymphoma and graft-versus-host disease patients. *Br. J. Haematol.* **1999**, *107*, 707–711. [CrossRef] [PubMed]
5. Krammer, P.H.; Arnold, R.; Lavrik, I.N. Life and death in peripheral T cells. *Nat. Rev. Immunol.* **2007**, *7*, 532–542. [CrossRef] [PubMed]
6. Irmler, M.; Thome, M.; Hahne, M.; Schneider, P.; Hofmann, K.; Steiner, V.; Bodmer, J.L.; Schroter, M.; Burns, K.; Mattmann, C.; et al. Inhibition of death receptor signals by cellular FLIP. *Nature* **1997**, *388*, 190–195. [CrossRef] [PubMed]
7. Fischer, U.; Janicke, R.U.; Schulze-Osthoff, K. Many cuts to ruin: A comprehensive update of caspase substrates. *Cell Death Differ.* **2003**, *10*, 76–100. [CrossRef] [PubMed]
8. Deveraux, Q.L.; Takahashi, R.; Salvesen, G.S.; Reed, J.C. X-linked IAP is a direct inhibitor of cell-death proteases. *Nature* **1997**, *388*, 300–304. [CrossRef] [PubMed]
9. Wu, J.; Nihal, M.; Siddiqui, J.; Vonderheid, E.C.; Wood, G.S. Low FAS/CD95 expression by CTCL correlates with reduced sensitivity to apoptosis that can be restored by FAS upregulation. *J. Investig. Dermatol.* **2009**, *129*, 1165–1173. [CrossRef] [PubMed]
10. Braun, F.K.; Fecker, L.F.; Schwarz, C.; Walden, P.; Assaf, C.; Durkop, H.; Sterry, W.; Eberle, J. Blockade of death receptor-mediated pathways early in the signaling cascade coincides with distinct apoptosis resistance in cutaneous T-cell lymphoma cells. *J. Investig. Dermatol.* **2007**, *127*, 2425–2437. [CrossRef] [PubMed]
11. Sors, A.; Jean-Louis, F.; Pellet, C.; Laroche, L.; Dubertret, L.; Courtois, G.; Bachelez, H.; Michel, L. Down-regulating constitutive activation of the NF-kappaB canonical pathway overcomes the resistance of cutaneous T-cell lymphoma to apoptosis. *Blood* **2006**, *107*, 2354–2363. [CrossRef] [PubMed]
12. Eriksen, K.W.; Kaltoft, K.; Mikkelsen, G.; Nielsen, M.; Zhang, Q.; Geisler, C.; Nissen, M.H.; Ropke, C.; Wasik, M.A.; Odum, N. Constitutive STAT3-activation in Sezary syndrome: Tyrphostin AG490 inhibits STAT3-activation, interleukin-2 receptor expression and growth of leukemic Sezary cells. *Leukemia* **2001**, *15*, 787–793. [CrossRef] [PubMed]
13. Braun, F.K.; Al-Yacoub, N.; Plotz, M.; Mobs, M.; Sterry, W.; Eberle, J. Nonsteroidal anti-inflammatory drugs induce apoptosis in cutaneous T-cell lymphoma cells and enhance their sensitivity for TNF-related apoptosis-inducing ligand. *J. Investig. Dermatol.* **2012**, *132*, 429–439. [CrossRef] [PubMed]
14. Al-Yacoub, N.; Fecker, L.F.; Mobs, M.; Plotz, M.; Braun, F.K.; Sterry, W.; Eberle, J. Apoptosis induction by SAHA in cutaneous T-cell lymphoma cells is related to downregulation of c-FLIP and enhanced TRAIL signaling. *J. Investig. Dermatol.* **2012**, *132*, 2263–2274. [CrossRef] [PubMed]
15. Gahlot, S.; Khan, M.A.; Rishi, L.; Majumdar, S. Pentoxifylline augments TRAIL/Apo2L mediated apoptosis in cutaneous T cell lymphoma (HuT-78 and MyLa) by modulating the expression of antiapoptotic proteins and death receptors. *Biochem. Pharmacol.* **2010**, *80*, 1650–1661. [CrossRef] [PubMed]
16. Quast, S.A.; Berger, A.; Eberle, J. ROS-dependent phosphorylation of Bax by wortmannin sensitizes melanoma cells for TRAIL-induced apoptosis. *Cell Death Dis.* **2013**, *4*, e839. [CrossRef] [PubMed]
17. Bauer, D.; Werth, F.; Nguyen, H.A.; Kiecker, F.; Eberle, J. Critical role of reactive oxygen species (ROS) for synergistic enhancement of apoptosis by vemurafenib and the potassium channel inhibitor TRAM-34 in melanoma cells. *Cell Death Dis.* **2017**, *8*, e2594. [CrossRef] [PubMed]
18. Zou, Z.; Chang, H.; Li, H.; Wang, S. Induction of reactive oxygen species: An emerging approach for cancer therapy. *Apoptosis* **2017**, *22*, 1321–1335. [CrossRef] [PubMed]

19. Salmeron, M.L.; Quintana-Aguiar, J.; De La Rosa, J.V.; Lopez-Blanco, F.; Castrillo, A.; Gallardo, G.; Tabraue, C. Phenalenone-photodynamic therapy induces apoptosis on human tumor cells mediated by caspase-8 and p38-MAPK activation. *Mol. Carcinog.* **2018**, *57*, 1525–1539. [CrossRef] [PubMed]

20. Salva, K.A.; Kim, Y.H.; Rahbar, Z.; Wood, G.S. Epigenetically Enhanced PDT Induces Significantly Higher Levels of Multiple Extrinsic Pathway Apoptotic Factors than Standard PDT, Resulting in Greater Extrinsic and Overall Apoptosis of Cutaneous T-cell Lymphoma. *Photochem. Photobiol.* **2018**, *94*, 1058–1065. [CrossRef] [PubMed]

21. Xiao, Z.; Hao, Y.; Liu, B.; Qian, L. Indirubin and meisoindigo in the treatment of chronic myelogenous leukemia in China. *Leuk. Lymphoma* **2002**, *43*, 1763–1768. [CrossRef] [PubMed]

22. Blazevic, T.; Heiss, E.H.; Atanasov, A.G.; Breuss, J.M.; Dirsch, V.M.; Uhrin, P. Indirubin and Indirubin Derivatives for Counteracting Proliferative Diseases. *Evid. Based Complement. Altern. Med.* **2015**, *2015*, 654098. [CrossRef] [PubMed]

23. Perabo, F.G.; Frossler, C.; Landwehrs, G.; Schmidt, D.H.; von Rucker, A.; Wirger, A.; Muller, S.C. Indirubin-3′-monoxime, a CDK inhibitor induces growth inhibition and apoptosis-independent up-regulation of survivin in transitional cell cancer. *Anticancer Res.* **2006**, *26*, 2129–2135. [PubMed]

24. Meijer, L.; Skaltsounis, A.L.; Magiatis, P.; Polychronopoulos, P.; Knockaert, M.; Leost, M.; Ryan, X.P.; Vonica, C.A.; Brivanlou, A.; Dajani, R.; et al. GSK-3-selective inhibitors derived from Tyrian purple indirubins. *Chem. Biol.* **2003**, *10*, 1255–1266. [CrossRef] [PubMed]

25. Zhen, Y.; Sorensen, V.; Jin, Y.; Suo, Z.; Wiedlocha, A. Indirubin-3′-monoxime inhibits autophosphorylation of FGFR1 and stimulates ERK1/2 activity via p38 MAPK. *Oncogene* **2007**, *26*, 6372–6385. [CrossRef] [PubMed]

26. Zhang, Y.; Du, Z.; Zhuang, Z.; Wang, Y.; Wang, F.; Liu, S.; Wang, H.; Feng, H.; Li, H.; Wang, L.; et al. E804 induces growth arrest, differentiation and apoptosis of glioblastoma cells by blocking Stat3 signaling. *J. Neurooncol.* **2015**, *125*, 265–275. [CrossRef] [PubMed]

27. Berger, A.; Quast, S.A.; Plotz, M.; Hein, M.; Kunz, M.; Langer, P.; Eberle, J. Sensitization of melanoma cells for death ligand-induced apoptosis by an indirubin derivative—Enhancement of both extrinsic and intrinsic apoptosis pathways. *Biochem. Pharmacol.* **2011**, *81*, 71–81. [CrossRef] [PubMed]

28. Zhivkova, V.; Kiecker, F.; Langer, P.; Eberle, J. Crucial role of reactive oxygen species (ROS) for the proapoptotic effects of indirubin derivative DKP-073 in melanoma cells. *Mol. Carcinog.* **2019**, *58*, 258–269. [CrossRef] [PubMed]

29. Libnow, S.; Methling, K.; Hein, M.; Michalik, D.; Harms, M.; Wende, K.; Flemming, A.; Kockerling, M.; Reinke, H.; Bednarski, P.J.; et al. Synthesis of indirubin-N′-glycosides and their anti-proliferative activity against human cancer cell lines. *Bioorg. Med. Chem.* **2008**, *16*, 5570–5583. [CrossRef] [PubMed]

30. Kunz, M.; Driller, K.M.; Hein, M.; Libnow, S.; Hohensee, I.; Ramer, R.; Hinz, B.; Berger, A.; Eberle, J.; Langer, P. Synthesis of thia-analogous indirubin N-Glycosides and their influence on melanoma cell growth and apoptosis. *ChemMedChem* **2010**, *5*, 534–539. [CrossRef] [PubMed]

31. Kleeblatt, D.; Becker, M.; Plötz, M.; Schonherr, M.; Villinger, A.; Hein, M.; Eberle, J.; Kunz, M.; Rahman, Q.; Langer, P. Synthesis and Bioactivity of N-glycosylated 3-(2-Oxo-2- arylethylidene)-indolin-2-ones. *RSC Adv.* **2015**, *5*, 20623–20633. [CrossRef]

32. Bang, K.; Lund, M.; Mogensen, S.C.; Thestrup-Pedersen, K. In vitro culture of skin-homing T lymphocytes from inflammatory skin diseases. *Exp. Dermatol.* **2005**, *14*, 391–397. [CrossRef] [PubMed]

33. Drexler, H.G.; Pommerenke, C.; Eberth, S.; Nagel, S. Hodgkin lymphoma cell lines: To separate the wheat from the chaff. *Biol. Chem.* **2018**, *399*, 511–523. [CrossRef] [PubMed]

34. Braun, F.K.; Hirsch, B.; Al-Yacoub, N.; Durkop, H.; Assaf, C.; Kadin, M.E.; Sterry, W.; Eberle, J. Resistance of cutaneous anaplastic large-cell lymphoma cells to apoptosis by death ligands is enhanced by CD30-mediated overexpression of c-FLIP. *J. Investig. Dermatol.* **2010**, *130*, 826–840. [CrossRef] [PubMed]

35. Chen, J.C.; Zhang, Y.; Jie, X.M.; She, J.; Dongye, G.Z.; Zhong, Y.; Deng, Y.Y.; Wang, J.; Guo, B.Y.; Chen, L.M. Ruthenium(II) salicylate complexes inducing ROS-mediated apoptosis by targeting thioredoxin reductase. *J. Inorg. Biochem.* **2019**, *193*, 112–123. [CrossRef] [PubMed]

36. Takasaki, T.; Hagihara, K.; Satoh, R.; Sugiura, R. More than Just an Immunosuppressant: The Emerging Role of FTY720 as a Novel Inducer of ROS and Apoptosis. *Oxid. Med. Cell. Longev.* **2018**, *2018*, 4397159. [CrossRef] [PubMed]

37. Jain, S.; Washington, A.; Leaf, R.K.; Bhargava, P.; Clark, R.A.; Kupper, T.S.; Stroopinsky, D.; Pyzer, A.; Cole, L.; Nahas, M.; et al. Decitabine Priming Enhances Mucin 1 Inhibition Mediated Disruption of Redox Homeostasis in Cutaneous T-Cell Lymphoma. *Mol. Cancer Ther.* **2017**, *16*, 2304–2314. [CrossRef] [PubMed]

38. Yi, S.; Sun, J.; Qiu, L.; Fu, W.; Wang, A.; Liu, X.; Yang, Y.; Kadin, M.E.; Tu, P.; Wang, Y. Dual Role of EZH2 in Cutaneous Anaplastic Large Cell Lymphoma: Promoting Tumor Cell Survival and Regulating Tumor Microenvironment. *J. Investig. Dermatol.* **2017**, *138*, 1126–1136. [CrossRef] [PubMed]

39. Alexander-Savino, C.V.; Hayden, M.S.; Richardson, C.; Zhao, J.; Poligone, B. Doxycycline is an NF-kappaB inhibitor that induces apoptotic cell death in malignant T-cells. *Oncotarget* **2016**, *7*, 75954–75967. [CrossRef] [PubMed]

40. Kaltoft, K.; Bisballe, S.; Dyrberg, T.; Boel, E.; Rasmussen, P.B.; Thestrup-Pedersen, K. Establishment of two continuous T-cell strains from a single plaque of a patient with mycosis fungoides. *In Vitro Cell. Dev. Biol.* **1992**, *28A*, 161–167. [CrossRef] [PubMed]

41. Gootenberg, J.E.; Ruscetti, F.W.; Mier, J.W.; Gazdar, A.; Gallo, R.C. Human cutaneous T cell lymphoma and leukemia cell lines produce and respond to T cell growth factor. *J. Exp. Med.* **1981**, *154*, 1403–1418. [CrossRef] [PubMed]

42. Starkebaum, G.; Loughran, T.P., Jr.; Waters, C.A.; Ruscetti, F.W. Establishment of an IL-2 independent, human T-cell line possessing only the p70 IL-2 receptor. *Int. J. Cancer* **1991**, *49*, 246–253. [CrossRef] [PubMed]

43. Riccardi, C.; Nicoletti, I. Analysis of apoptosis by propidium iodide staining and flow cytometry. *Nat. Protoc.* **2006**, *1*, 1458–1461. [CrossRef] [PubMed]

44. Creed, S.; McKenzie, M. Measurement of Mitochondrial Membrane Potential with the Fluorescent Dye Tetramethylrhodamine Methyl Ester (TMRM). *Methods Mol. Biol.* **2019**, *1928*, 69–76. [PubMed]

45. Eberle, J.; Fecker, L.F.; Hossini, A.M.; Wieder, T.; Daniel, P.T.; Orfanos, C.E.; Geilen, C.C. CD95/Fas signaling in human melanoma cells: Conditional expression of CD95L/FasL overcomes the intrinsic apoptosis resistance of malignant melanoma and inhibits growth and progression of human melanoma xenotransplants. *Oncogene* **2003**, *22*, 9131–9141. [CrossRef] [PubMed]

Lebenslauf

Mein Lebenslauf wird aus datenschutzrechtlichen Gründen in der elektronischen Version meiner Arbeit nicht veröffentlicht.

Komplette Publikationsliste

Aus dieser Arbeit sind folgende Publikationen hervorgegangen:

- Sumarni U, Zhu J, Sinnberg T, Eberle J. Sensitivity of Cutaneous T-Cell Lymphoma Cells to the Mcl-1 Inhibitor S63845 Correlates with the Lack of Bcl-w Expression. Int J Mol Sci. 2022 Oct 18;23(20):12471. doi: 10.3390/ijms232012471. PMID: 36293331; PMCID: PMC9604298.

- Sumarni, U.; Reidel, U.; Eberle, J. Targeting Cutaneous T-Cell Lymphoma Cells by Ingenol Mebutate (PEP005) Correlates with PKCδ Activation, ROS Induction as Well as Downregulation of XIAP and c-FLIP. *Cells* 2021, *10*, 987. https://doi.org/10.3390/cells10050987.

- Soltan MY, Sumarni U, Assaf C, Langer P, Reidel U, Eberle J. Key Role of Reactive Oxygen Species (ROS) in Indirubin Derivative-Induced Cell Death in Cutaneous T-Cell Lymphoma Cells. Int J Mol Sci. 2019 Mar 7;20(5):1158. doi: 10.3390/ijms20051158. PMID: 30866411; PMCID: PMC6429192.

Aus dieser Arbeit sind folgende Kongressbeiträge hervorgegangen:

- 49. Jahrestagung Arbeitsgemeinschaft Dermatologische Forschung (ADF), 2023, Innsbruck, Österreich

- 48. Jahrestagung Arbeitsgemeinschaft Dermatologische Forschung (ADF), 2022, virtuell

- 47. Jahrestagung Arbeitsgemeinschaft Dermatologische Forschung (ADF), 2021, virtuell

- 34. Deutscher Krebskongress, 2020, Berlin

Danksagung

Ich möchte mich bei PD Dr. Jürgen Eberle, meinem Doktorvater, für seine kontinuierliche Ermutigung während der gesamten Zeit meiner Promotion und dafür, dass er mir die Möglichkeit gab, in seinem Labor zu arbeiten, bedanken. Mein besonderer Dank gilt Stefanie Mai für ihre Betreuung während der ersten Zeit meiner Doktorarbeit. Außerdem möchte ich Zina Sarif und Jiaqi Zhu für die produktiven Gespräche meinen Dank aussprechen. Ich danke den Studenten der Gruppe von Prof. Dr. rer. nat. Peter Walden, die mich während der ersten Zeit meiner Doktorarbeit mit produktiven Gesprächen begleitet hat. Ebenfalls möchte ich der gesamten Forschungsgruppe der Klinik für Dermatologie, Venerologie und Allergologie für den inspirierenden Meinungsaustausch während der wöchentlichen Research-Seminare bedanken.

Schließlich möchte ich mich bei den wichtigsten Menschen in meinem Leben bedanken, meiner Mutter Hani Noer Indah, meinem Vater Mintono Chandra, meinen Schwestern Tjan Juliartik und Mei Liana Esti, meinem Bruder Liliek Kusnadi, meiner Nichte Cherryl Arletta Kusnadi, meinen Onkeln Andreas Aan und Bingreddy Wangsatimur-Neumann die mir geholfen haben, diesen Traum zu verwirklichen. Ich widme diese Arbeit meiner Familie.